DOCTORAL DISSERTATION

博士論文

STUDY ON SHALLOW TUNNEL EXCAVATION IN UNSATURATED GROUND THROUGH TRAPDOOR TEST

落とし戸実験による不飽和地盤中の浅層トンネル掘削に関する研究

Yokohama National University

Graduate School of Urban Innovation

国立大学法人横浜国立大学大学院都市イノベーション学府

FANG XU

ファン　スウ

September 2022

2022 年 9 月

STUDY ON SHALLOW TUNNEL EXCAVATION IN UNSATURATED GROUND THROUGH TRAPDOOR TEST

落とし戸実験による不飽和地盤中の浅層トンネル掘削に関する研究

by

FANG XU

ファン　スウ

A Dissertation Submitted to the Graduate School of Urban Innovation, Yokohama National University in Partial Fulfillment of the Requirement for the Degree of

Doctor of Engineering

Yokohama National University, Graduate School of Urban Innovation

国立大学法人横浜国立大学大学院都市イノベーション学府

Examination Committee

Professor, Dr. Mamoru KIKUMOTO (Chair)

Professor, Dr. Kimitoshi HAYANO

Professor, Dr. Takayuki SUZUKI

Professor, Dr. Koichi MAEKAWA

Associate Professor, Dr. Ying CUI

September 2022

2022 年 9 月

ABSTRACT

The earth pressure acting on the crown of a tunnel after excavation is less than overburden pressure (static earth pressure) due to soil arching effect, which can be evaluated theoretically by Terzaghi's theory (1943). Furthermore, trapdoor test developed by Terzaghi (1936) is usually used to simulate tunnel excavation (e.g., Tanaka and Sakai, 1987; Kikumoto, 2004). However, the ground in Terzaghi's theory and trapdoor tests is usually assumed to be fully-dried. Actually, the ground in nature is almost unsaturated, and studies on loosening earth pressure (earth pressure after tunnel excavation or trapdoor being lowered) in unsaturated ground are hardly to be found. Therefore, the mechanism of a shallow tunnel excavation in unsaturated ground was explored in this study.

To simulate a shallow tunnel excavation, a series of trapdoor tests in saturated and unsaturated ground were carried out to explore soil mechanic, failure mechanism and surface settlement. It is shown that the loosening earth pressure is smaller than initial pressure, and gradually decreases from the center to the end of trapdoor. At stationary zone, the earth pressure is larger than initial pressure, and gradually decreases to initial pressure as the distance to the end of trapdoor is larger. Meanwhile, total loosening earth pressure is smaller as the depth of groundwater level is deeper, because the confining pressure and shear stress is smaller due to the smaller suction. Contrarily, the corresponding effective loosening earth pressure is slightly larger. The experiment result also shows that shear bands in unsaturated ground is more oblique as the depth of groundwater level is deeper, and multiple shear bands are observed. Moreover, maximum surface settlement in unsaturated ground is smaller when the depth of groundwater level is deeper.

Then a simple and rational theory to evaluate loosening pressure in unsaturated ground is proposed based on Soil-water characteristic curve (van Genuchten, 1980), Bishop's effective stress (1959), Mohr-Coulomb failure criteria and limit equilibrium theory. The proposed theory is applied to predict the vertical distribution of loosening earth pressure in unsaturated ground, which shows a significant difference from that in saturated ground. The remarkable effects of groundwater depth, soil type and scale of overburden height and trapdoor width on loosening earth pressure were also revealed. This is because suction primarily contributes to the increase in effective loosening earth pressure and shear resistance. Based on soil-water characteristic curve, the degree of saturation decreases, which causes wet density to decrease and the total and effective loosening earth pressures to have contrary tendencies. Moreover, effective loosening earth pressures vary with soil type as the degree of saturation varies. The total loosening earth pressures are, however, very similar regardless of soil type, because wet density and shear resistance have the similar tendencies.

Furthermore, the scale effect in saturated ground is not observed, and the proposed theory also verified there is no scale effect. However, the proposed theory can identify the scale effect in unsaturated ground is existed, the scale effect cannot be observed in experiment because the limitation of scale size of width of trapdoor. Meanwhile, the observed loosening earth pressure is consistent with that predicted by the proposed theory, which means the proposed theory is a valid model to predict loosening earth pressure after a shallow tunnel excavation in unsaturated ground.

Based on the proposed theory and assumptions proposed by Tamura (2001) and Kikumoto et al. (2004), theory I and II is developed to predict the distribution of loosening earth pressure across a trapdoor and stress

redistribution around the trapdoor respectively. It is revealed that the observed stress redistribution could be captured by the theory II. The theory I could somewhat capture the observed distribution of loosening earth pressure, however, as the ratio of the depth of groundwater level to overburden height is larger than 0.5, the distribution of loosening earth pressure at the boundary of trapdoor has some negative pressure, which mean the theory I still has some limitation.

In 2005, the Ushikagi tunnel was collapsed due to the raise of groundwater level due to agriculture irrigation. Therefore, some tests are carried out to explore the changing in loosening earth pressure as the groundwater level is raised. It is revealed that loosening earth pressure is larger as the groundwater level is raise to ground surface. Because the soil arching effect is weaker since the confining pressure and shear strength is smaller caused by the smaller suction. Meanwhile, the loosening earth pressure due to the raise of groundwater level is consistent with that due to trapdoor being lowered under the same depth of groundwater level. Moreover, the changing of loosening earth pressure due to the raise of groundwater level can be predicted by the proposed theory, which means that the proposed theory can consider the behavior of unsaturated soils.

Table of Contents

LIST OF FIGURES

LIST OF TABLES

CHAPTER 1 INTRODUCTION

1.1 Research background

The landform of Japan is mostly mountainous and hilly, the need to effectively use underground space has increased, especially in urban, various tunnels were built for Metro, gas and water supply, flood drainage and mountain railway construction. The ground above a tunnel is usually assumed to be in a fully-dried or fully-saturated state in practical designs so that classical theories (e.g., Terzaghi, 1943) can be applied to evaluate loosening earth pressures (vertical earth pressure after excavation) acting on a tunnel (e.g., Zhang et al., 2016; Chen and Peng, 2018). However, the soil mechanics of tunnel excavation in unsaturated soils is still unknown.

To simulate tunnel excavation, trapdoor test (e.g., Terzaghi, 1936) is usually used to explore the process of it. Many researchers conducted trapdoor tests to investigate tunnel excavation (e.g., Atkinson et al., 1977; Nakai et al., 1997), sinkhole (e.g., Möller, 2020) and cavity (e.g., Jacobsz, 2016), retaining wall (e.g., Rui, et al., 2020) and pile-supported embankment (e.g., Hong et al., 2007). Some researchers conducted more advanced trapdoor tests under single gravity or centrifuge condition to investigate the effect of surface footing loading on stability of soil arching (e.g., Mahdi et al., 2017), soil arching (e.g., Sadrekarimi and Abbasnejad, 2010; Britton and Naughton, 2011; Guo and Zhou, 2013; Ahmadi and Hosseininia, 2018; Xu et al., 2019), the contact force between each model particle by using digital RGB photoealstic analysis (e.g., Park et al., 2020), failure mechanisms (e.g., Costa et al., 2009; Dewoolkar et al., 2007; Iglesia et al., 2014; Liang et al., 2020), loosening earth pressure acting on a trapdoor (e.g., Ladanyi and Hoyaux, 1969; Tanaka and Sakai, 1987, 1993; Adachi et al., 2003; Chevalier et al., 2012). Song (2018) investigated the effect of groundwater level on soil arching and loosening pressure by trapdoor test in sand ground, however, the shear bands and the distribution of earth pressures around a trapdoor were not known. Overall, the mechanics of trapdoor test and the failure mechanisms in unsaturated soils have not been investigated. Moreover, numerical methods, as a famous method, can be used to investigate the detailed behavior of ground during tunneling (e.g., Koutsabeloulis and Griffiths, 1989; Dang and Meguid, 2008; Chevalier and Otani, 2011; Shahin et al., 2011; Kong et al., 2018), they require lots of parameters and those based on the mechanics of unsaturated soils have not yet to be applied to tunneling issues. However, the stability of a shallow tunnel may be affected by variations in pressure that result from a rise in the groundwater level, for example, the Ushikagi tunnel collapsed as shown in Fig. 1.1. Hence, a rational method for evaluating loosening earth pressure on a tunnel in unsaturated ground is needed.

Theories for unsaturated soils have been gradually established over the past few decades, which includes suction, volume change, shear resistance, flow laws and so on (e.g., Fredlund and Rahardjo, 1993a). According to the theories of saturated soils, effective stress is an extremely important role because the deformation of soils and shear resistance are influenced by it. In realistic, the ground is mostly in unsaturated state, the void of unsaturated soils includes water and air which is different with saturated soils, suction affect the mechanics of unsaturated

soils. By extension of effective stress of saturated soils (e.g., Terzaghi, 1936), the effective stress tensor for unsaturated soils proposed by Bishop (1959) has also been applied widely to model the stress–strain behavior of unsaturated soils (e.g., Komolvilas and Kikumoto, 2017). This tensor can uniquely describe the critical state stress ratio regardless of the degree of saturation (Sivakumar, 1993). And the parameter χ in Bishop's effective stress is usually assumed to be a function of the degree of saturation, S_r (e.g., Schrefler, 1984; Öberg and Sällfors, 1997).

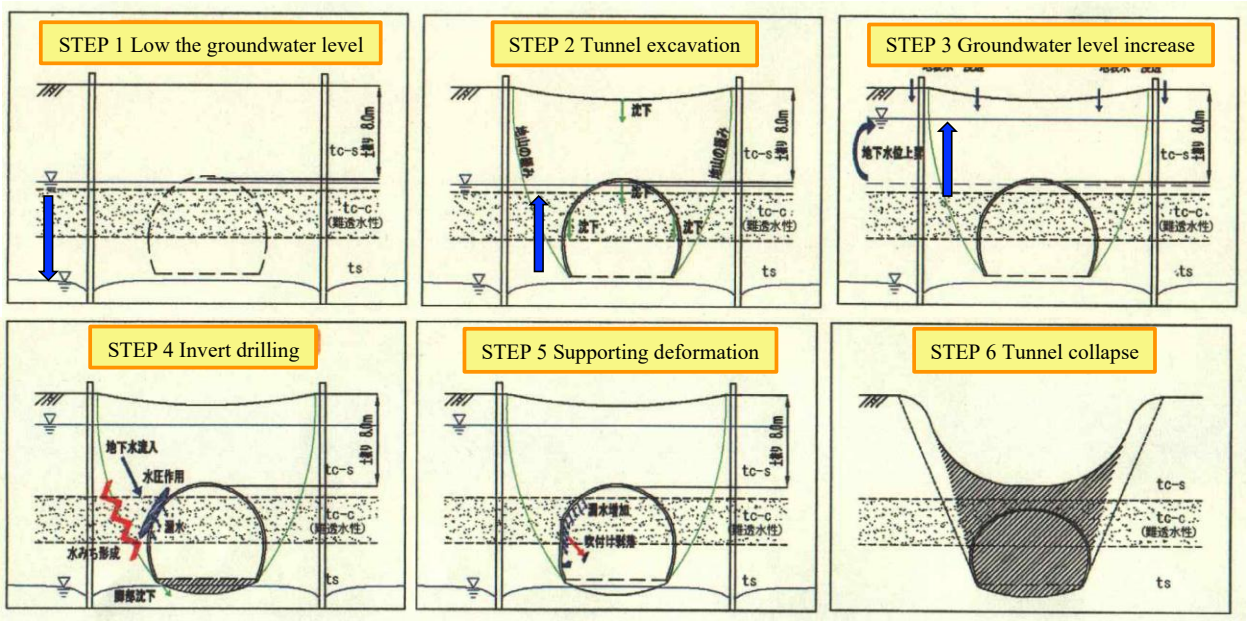

Fig. 1.1 The Ushikagi tunnel collapse (http://www.ktr.mlit.go.jp/gaikan/pi_kouhou/09/ss3/ss3_1.pdf).

The degree of saturation and suction has a relationship, which is usually called soil-water characteristic curve (swcc). Laboratory studies have been shown that there is a relationship between the swcc and the unsaturated soil properties (Fredlund and Rahardjo, 1993b). Since the swcc is an essential information for estimation of unsaturated soils mechanics in geotechnical engineering practice, it is important to precisely predict the swcc. Therefore, various soil-water characteristic curve models have been proposed to describe the relationship between suction and the degree of saturation (e.g., Brooks and Corey, 1964; van Genuchten, 1980; Fredlund and Xing, 1994).

Based on the swcc, the shear strength could be predicted by it (e.g., Fredlund et al., 1995). The shear strength of unsaturated soils is usually evaluated using two independent stress state variables such as net normal stress ($\sigma - u_a$) and suction ($u_a - u_w$), an extended Mohr-Coulomb failure envelope was proposed to predict the shear strength of unsaturated soils (e.g., Fredlund et al., 1978; Pufahl et al., 1983; Gan et al., 1988).

In this dissertation, to explore shallow tunnel excavation in unsaturated ground, a series of trapdoor test was carried out to explore soil mechanics, failure mechanism and surface settlement. Then a rational model was proposed to evaluate loosening earth pressures acting on a trapdoor based on limit equilibrium theory, combining

soil-water characteristic curves, Mohr-Coulomb failure criteria and effective stress for unsaturated soils. The proposed theory was applied to evaluate vertical distribution of loosening earth pressure. Furthermore, effect of the depth of groundwater level and soil types on loosening earth pressure was investigated. Meanwhile, scale effect in saturated and unsaturated ground observed in trapdoor test was compared with that predicted by the proposed theory. Based on the proposed theory and assumptions proposed by Tamura (2001) and Kikumoto et al. (2004), theories were proposed to evaluate the distribution of loosening earth pressure across a trapdoor and stress redistribution around the trapdoor, which were applied to compare with the observed distribution of earth pressure. Finally, the changing in loosening earth pressure due to the raise of groundwater level was explored to investigate tunnel stability due to the raise of groundwater level. Moreover, as depth of groundwater level were identical, loosening earth pressure due to the raise of groundwater level was compared with that due to trapdoor being lowered and that predicted by the proposed theory.

1.2 Objectives of the thesis

The mechanism of shallow tunnel excavation in unsaturated ground was explored through trapdoor test in this study. The objectives of this thesis are summarized as following:

1. Series of trapdoor test in saturated and unsaturated ground. (Chapter 3)
   - To explore the distribution of earth pressure and the changing in loosening earth pressure with displacement of trapdoor.
   - shear bands and evolution of shear bands with displacement of trapdoor.
   - surface settlement profile and maximum surface settlement with displacement of trapdoor.
   - Effect of depth of groundwater level on loosening earth pressure.
2. A rational theory to evaluate loosening earth pressure in unsaturated ground. (Chapter 4)
   - Evaluation of loosening earth pressure in unsaturated ground.
   - Effect of depth of groundwater level and soil types on loosening earth pressure.
   - Scale effect on vertical distribution of loosening earth pressure
   - Scale effect in saturated and unsaturated ground observed by trapdoor test and that predicted by the proposed theory.
   - The comparison of the observed loosening earth pressure and the predicted loosening earth pressure.
3. Theories were developed to predict the distribution of loosening pressure acting on a trapdoor and stress redistribution around the trapdoor. And the theories were applied to investigate the consistency with the observed distribution of earth pressure. (Chapter 5)
4. Tunnel stability due to the raise of groundwater level. (Chapter 6)
   - The changing in loosening earth pressure after trapdoor test due to the raise of groundwater level.
   - The loosening earth pressure due to the raise of groundwater level was compared with that due to trapdoor being lowered and that predicted by the proposed theory.

1.3 Thesis structure

The structure of this thesis is given as follows:

Chapter 1 Introduction

The description of research background is to identify what have been done and what haven't been done on this research topic. Also, the objectives of this research and the structure of this thesis were stated.

Chapter 2 Literature review

Firstly, trapdoor test (e.g., Evans, 1984; Nakai et al., 1997; Kikumoto, 2004; Costa et al., 2009) and numerical simulation (e.g., Stone and Wood, 1992; Murakami et al., 1997) on soil mechanics, failure mechanism and surface settlement was reviewed. Then theoretical solutions for evaluating loosening earth pressure were reviewed (e.g., Terzaghi, 1943; Kikumoto, 2004). However, research on trapdoor test in unsaturated ground was difficult to be found (Song et al., 2018). Since shallow tunnel excavation in unsaturated ground was explored in this thesis, behavior of unsaturated soils included soil water characteristic curve (e.g., van Genuchten, 1980), effective stress (e.g., Bishop, 1959) and shear stress (e.g., Bishop and Blight, 1963) were reviewed. Finally, the novelty of this study was summarized.

Chapter 3 Trapdoor test in saturated and unsaturated ground

Series of trapdoor test in saturated and unsaturated ground were carried out to explore the distribution of earth pressure and the changing in loosening earth pressure with displacement of trapdoor. Then shear bands and evolution of shear bands with displacement of trapdoor were investigated. Effect of overburden ratio on shear bands in saturated ground and effect of depth of groundwater level on shear bands in unsaturated were discussed. Furthermore, surface settlement profile and maximum surface settlement with displacement of trapdoor was also explored. Effect of depth of groundwater level on loosening earth pressure was estimated.

Chapter 4 A theory to predict loosening earth pressure in unsaturated ground

A simple theory was proposed to evaluate loosening earth pressure in unsaturated ground based on the mechanics of unsaturated soils. The aim is to model vertical earth pressure in unsaturated ground above a shallow tunnel after excavation. For this, a trapdoor problem is used (e.g., Terzaghi, 1936; Murayama and Matsuoka, 1971; Adachi et al., 2003; Costa et al., 2009), in which tunnel excavation is directly modeled by stress release triggered by the lowering of a trapdoor (a part of the bottom boundary of the ground). The earth pressure acting on the trapdoor corresponds to the vertical earth pressure that acts on the crown of the tunnel after excavation. The theory were verified through the comparison with a classical theory for loosening earth pressure in fully-dried or fully-saturated ground (Terzaghi, 1943). Through a series of simulations using the proposed theory, differences in loosening earth pressures in different soil types such as sand, loam and silty clay were investigated. The effects of groundwater level, the scale of overburden height, and trapdoor width on loosening earth pressure

were also evaluated. Scale effect in saturated and unsaturated ground observed in trapdoor test and predicted by the proposed theory was explored. Moreover, the observed loosening earth pressure was compared with that predicted by the proposed theory.

Chapter 5 Theories to predict the distribution of earth pressure

Theory I and II was proposed to evaluate the distribution of loosening earth pressure and stress redistribution based on the proposed theory, limit equilibrium theory and assumptions proposed by Tamura (2001) and Kikumoto et al. (2004). Then the theories were applied to capture the observed the distribution of loosening earth pressure and stress redistribution. However, the theory I for evaluating the distribution of loosening earth pressure had some limitation because the distribution of loosening earth pressure had some negative pressure.

Chapter 6 Effect of the groundwater level raise on loosening earth pressure after trapdoor test

To explore tunnel stability due to the raise of groundwater level, some tests were carried out to explore the changing in loosening earth pressure as the groundwater level was raised. Loosening earth pressure was smaller as the depth of groundwater level was raised. Then as the depth of groundwater level was identical, the loosening earth pressure due to the raise of groundwater level was compared with that due to trapdoor being lowered and that predicted by the proposed theory. The consistent comparison result meant the proposed theory could consider behavior of unsaturated soils.

Chapter 7 Conclusions

In this chapter, a series of conclusions on mechanism of shallow tunnel excavation in unsaturated ground was summarized, meanwhile, the research prospects in future were also provided.

CHAPTER 2 LITERATURE REVIEW

This chapter is to review the previous studies on the soil mechanics and failure mechanism during trapdoor test, and the behavior of unsaturated soils relevant to this research.

2.1 Tunnel excavation through trapdoor test

For a shallow tunnel excavation, trapdoor test (e.g., Terzaghi, 1936) is usually used to simulate the process of it. It is revealed that the loosening pressure is smaller than overburden pressure due to soil arching (e.g., Terzaghi, 1943). "*Arching is one of the most universal phenomena encountered in soils both in the field and in the laboratory"* (e.g., Terzaghi, 1943).

However, soil arching was firstly recognized and investigated in non-geotechnical context. In early 1800's, French military engineer was asked to design a magazine silo (e.g., Feld, 1948; Tien, 1996). An interesting phenomenon they found was that the load acting on the base of silo only was a portion of total weight of material above the base, and the reduction of load was transferred to the side walls. According to Experiments, an arch was formed above the active base. Subsequently, soil arch above a tunnel was also recognized in the 1920's and 1930's. Engineers found that the loads on the crown of a tunnel was significant less than overburden pressure, especially in the ground with good condition. So many researchers (e.g., Evans, 1984; Atkinson et al., 1977; Nakai et al., 1997; Kikumoto, 2004) focused on the behavior and theory of soil arch to predict the loads acting on a tunnel, which could achieve the considerable saving for construction.

2.1.1 Experimental findings by trapdoor test

After trapdoor test being conducted by Terzaghi (1936), many researchers carry out advanced trapdoor tests under single gravity or centrifuge condition to investigate failure mechanism, loosening pressure, stress redistribution around a trapdoor and settlement of ground surface.

Loosening pressure and stress redistribution

Evans (1984) carried out trapdoor test in sand ground to explore loosening pressure across a trapdoor. The test apparatus is shown in Fig. 2.1, the unit of measurement of apparatus is inch. Herein, width of trapdoor is denoted with B. The typical behavior of loosening pressure after trapdoor has a downward displacement δ is shown in Fig. 2.2. At the beginning of displacement of trapdoor, the normalized loosening pressure decreases rapidly to a minimum value, the point of it is usually termed as that of 'maximum arching'. Meanwhile, the normalized displacement of trapdoor δ/B necessary to mobilize 'maximum arching' is approximately 1.8 % which is coincide with Dewoolkar's observation (2007). As trapdoor continue to move downward, the normalized loosening pressure increases somewhat and a relatively constant value is obtained. This is generally termed as 'ultimate arching'. The requirement of the normalized displacement of trapdoor δ/B to reach 'ultimate arching' is 10 %.

To explore the distribution of earth pressure across a trapdoor, Evans conducted a series of active and passive trapdoor tests under various overburden ratios. For active mode as shown in Fig. 2.3 (a), the loosening pressure is largest at the center of trapdoor, and then gradually decrease to a minimum value at the end of trapdoor. The shape of the distribution of loosening pressure is a symmetric parabola. However, for passive mode as shown in Fig. 2.3 (b), loosening pressure acquires a minimum value at the center of trapdoor, and slightly increases to a larger value at the end of trapdoor. The shape of stress distribution on a trapdoor is almost uniform. The observation of the distribution of earth pressure for both active and passive mode is consistent with Harris test result (1974).

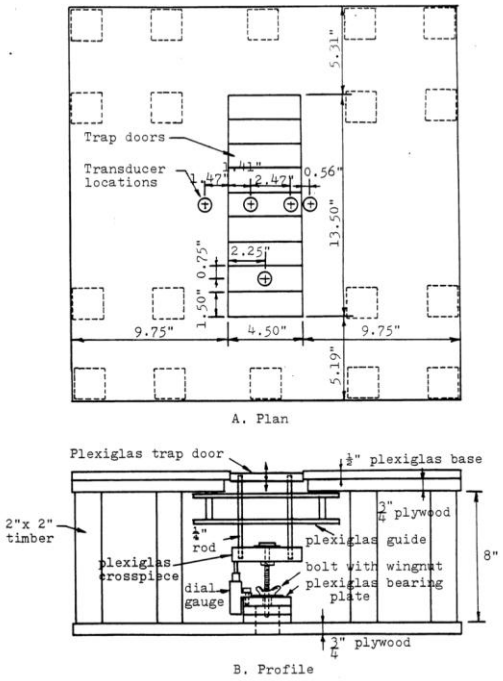

Fig. 2.1 The apparatus of trapdoor test, unit is inch (from Evans, 1984).

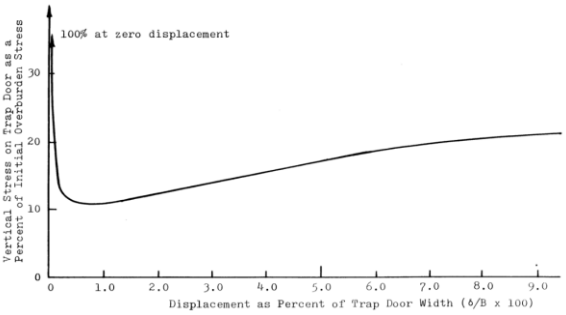

Fig. 2.2 The typical behavior of stress across a trapdoor as the trapdoor move downward (from Evans, 1984).

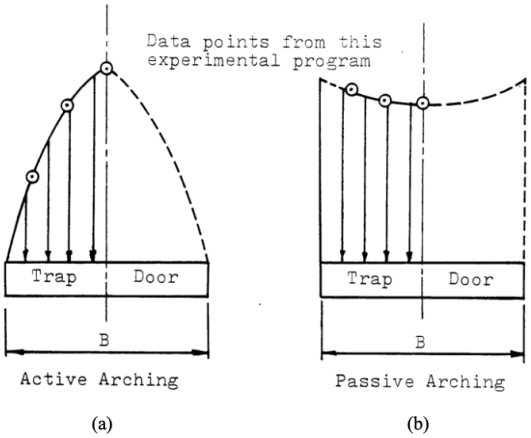

Fig. 2.3 The distribution of earth pressure across a trapdoor after (a) downward movement; (b) upward movement (from Evans, 1984).

A series of trapdoor tests were carried out by Kikumoto (2004) under 2-Dimension (2D) and 3-Dimension (3D) condition to explore the loosening pressure across a trapdoor and stress redistribution around the trapdoor. The apparatus for 2D and 3D tests is shown in Fig. 2.4 (a) and (b) respectively. For the 2D trapdoor test, the ground is modeled with aluminum bar, however, Toyoura sand is used to generate the model ground for 3D trapdoor test. As shown in Fig. 2.5 (a) and (b), tests result under various overburden height H of constant width of trapdoor D is compared with that calculated by Terzaghi's theory (1943). According to tests results, the lateral earth pressure coefficient K_h for 2D (The value of K_h is the same as Terzaghi's recommendation) and 3D trapdoor test is appropriate to be one. However, Adachi (2003) conducted 3D trapdoor test in Silica sand ground, in which he found that the lateral earth pressure coefficient K_h was approximately to be 2.0 to capture experiment result.

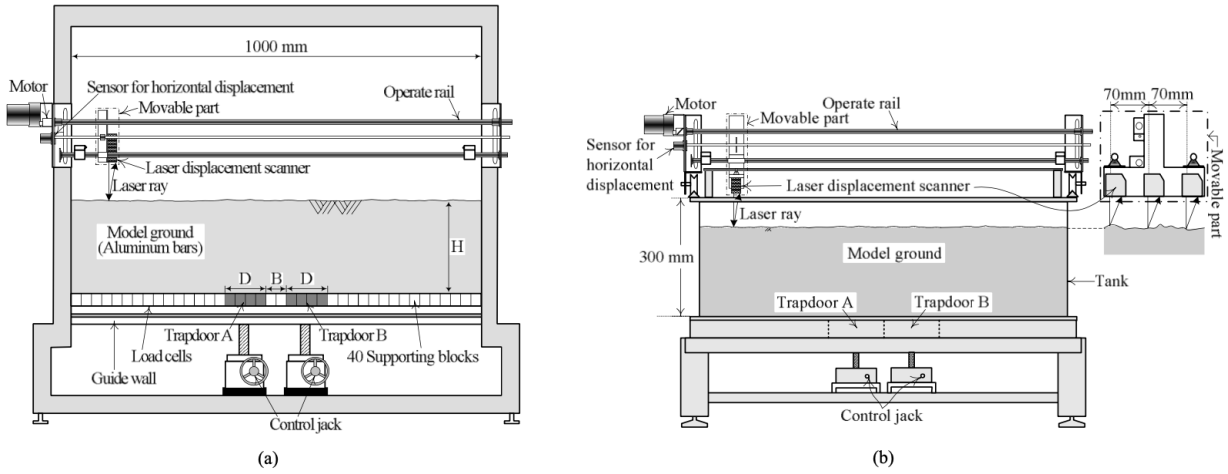

Fig. 2.4 The apparatus for (a) 2D trapdoor test; (b) 3D trapdoor test (from Kikumoto, 2004).

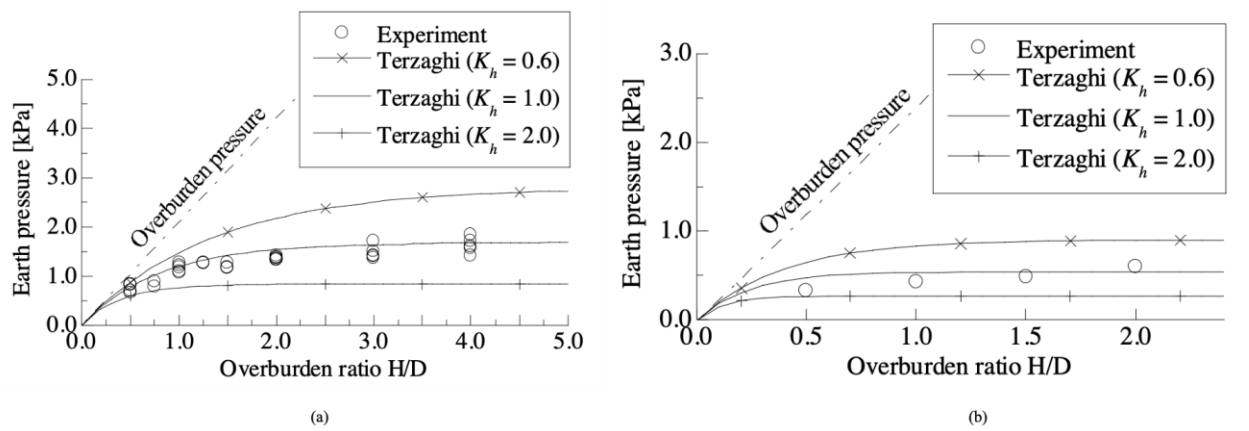

Fig. 2.5 Comparison of test results under different overburden height H of constant width of trapdoor D and that calculated by Terzaghi's theory (a) for 2D trapdoor test; (b) for 3D trapdoor test (from Kikumoto, 2004).

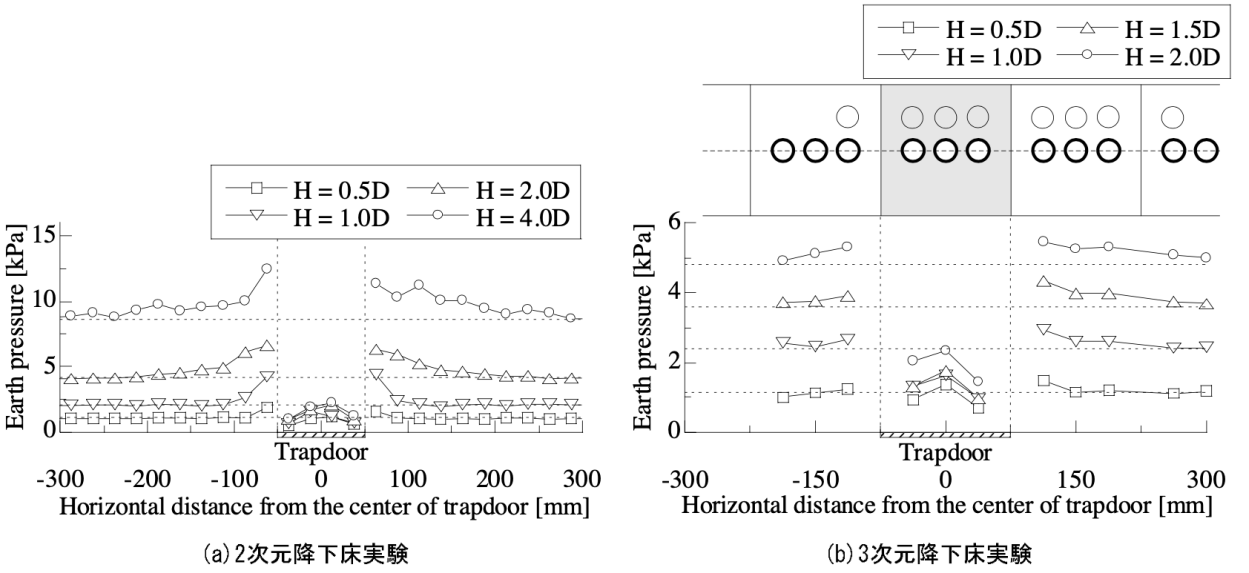

Fig. 2.6 The test result under various overburden ratio as the displacement of trapdoor is 2 mm. (a) for 2D trapdoor test; (b) for 3D trapdoor test (from Kikumoto, 2004).

The loosening pressure acting on a trapdoor and stress redistribution around the trapdoor for 2D and 3D trapdoor tests under various overburden ratio when the displacement of the trapdoor is 2 mm are shown in Fig. 2.6 (a) and (b). According to the experiment results, the loosening pressure is gradually decreased from the center line of trapdoor to the edge of that, which is consistent with Evans's report (1984). At the stationary zone, the earth pressure is larger than initial pressure, and gradually decreases to initial pressure as the distance to the end of trapdoor increases.

Moreover, trapdoor test in unsaturated ground (Song et al., 2018) was carried out to explore loosening earth pressure acting on a trapdoor and displacement of sands. However, the ground was disturbed as trapdoor was moved downwards because the trapdoor was suspended by two steel cables. Meanwhile, the distribution of earth pressure and failure mechanism was not shown in their study.

Stress chain in trapdoor test

Traditional stress measurement methods are difficult to investigate the stress chain of interparticle. A new technology of photoelasticity methods is developed to explore the stress chain. Currently, photoelasticity methods include circular polariscope and reflection polariscope. To apply circular polariscope shown in Fig. 2.7 (a), transparent material (such as polymer or glass) is necessary to be used to model ground, which limits its utilization. Reflection polariscope is easier to be used to explore stress chain of interparticle which is shown in Fig. 2.7 (b). The theory of photoelasticity methods is that a unpolarized light passed through a polariscope to generate the polarized light, the polarized light is reflected by the photoelasticity material and is accepted by an analyzer, then optical fringe is emerged on the photoelasticity images, the intensity of which is depended on the magnitude of external force acting on the photoelasticity material, finally, the stress can be measured because there is a relationship between intensity of light and magnitude of external force (e.g., Daniels et al., 2017; Park and Jung, 2020). Park and Jung (2020) used digital RGB photoelasticity analysis to explore the color intensity of the photoelasticity images decomposed by red (R), green (G) and blue (B), respectively. They found that RGB color intensity showed segmented liner relationship with particle force. Park et al. (2020) applied photoelasticity methods to investigate the arching phenomenon during trapdoor test in granular ground modeled by PTFE cylindrical particle on the end of which was coated by a photoelasticity sheet. The soil arching was successfully observed as trapdoor moved downward, and he concluded that the formation of arching was because of the movement of the stress chain of interparticle rather than a change of the magnitude of it. However, photoelasticity methods cannot be applied to explore the stress chain of interparticle for actual soil, otherwise it will be a powerful tool to examine soil arching and stress chain of interparticle.

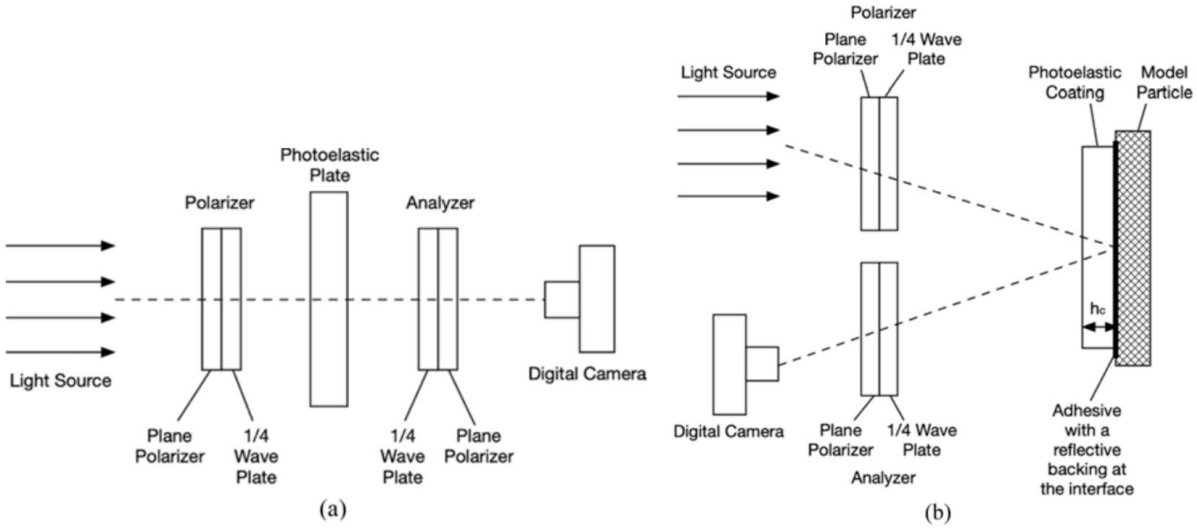

Fig. 2.7 Arrangement of optical element in: (a) A circular polariscope; (b) A reflection polariscope (from Park and Jung, 2020).

Failure mechanism

The failure mechanism in a shallow trapdoor test and deep trapdoor test is totally different. Multiple failure surfaces as shown in Fig. 2.8 are observed in a shallow trapdoor test under single gravity (e.g., Vardoulakis et al., 1981; Stone and Wood, 1992; Rui et al., 2019b) or centrifuge (e.g., Stone and Wood, 1992; Tanaka and Sakai, 1993; Iglesia et al., 2014). A curved soil arching OA occurred initially as the trapdoor has a small displacement, however, as increase of the displacement of trapdoor, the soil arching OC becomes to be vertical.

Vardoulakis (1981) carried out single trapdoor test with dry sand under the condition of 1 *g*, the schematic view of apparatus is shown as Fig. 2.9. The failure surfaces of a shallow active trapdoor test (overburden ratio *H*/*D* is 1.65) are shown as Fig. 2.10. It is clearly observed that two inclined sliding surfaces emerge and converge to the center line of trapdoor at the beginning of the trapdoor displacement, and then two vertical sliding surfaces are formed and reach the ground surface as the trapdoor has a large displacement. Dewoolkar (2007) carried out active circular trapdoor tests under single gravity or centrifuge and observed the similar failure mechanism.

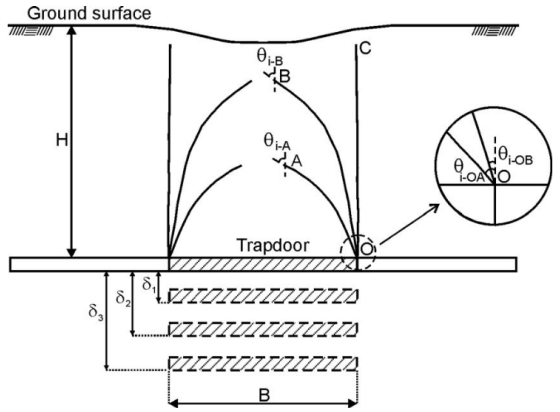

Fig. 2.8 Schematic view of the propagation of failure surfaces due to an active trapdoor under shallow conditions (from Costa et al., 2009).

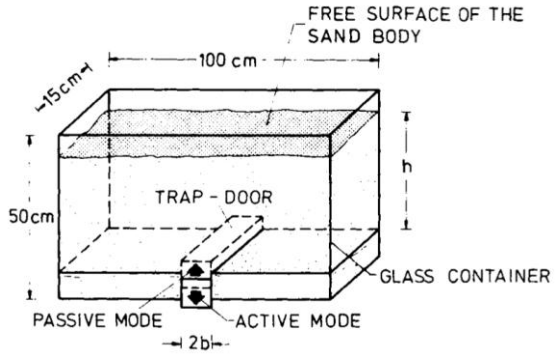

Fig. 2.9 Schematic view of apparatus for trapdoor test (from Vardoulakis et al., 1981).

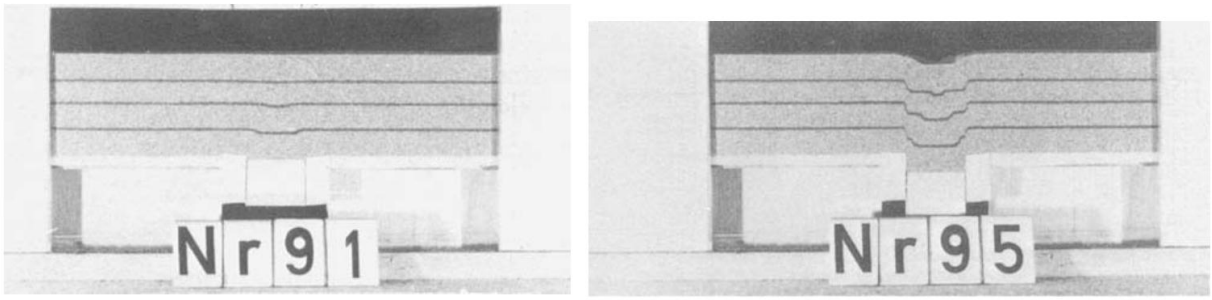

(a) (b)

Fig. 2.10 Failure surfaces of active trapdoor test after (a) a small displacement of trapdoor; (b) a large displacement of trapdoor (from Vardoulakis et al., 1981).

However, for the deep trapdoor test, there is only a single failure surface. Active trapdoor model tests under 1 *g* or 45 *g* condition were carried out by Costa (2009) with Ottawa sand. As shown in Fig. 2.11, the rigid aluminum strong box is in length of 419 mm, width of 203 mm and height of 300 mm. For all tests, the overburden height H is 159 mm with constant overburden ratio H/D of 4.5. The failure surfaces are shown in Fig. 2.12 as the normalized displacement of trapdoor δ/D is equal to 0.14, 0.29 and 0.57 respectively. It is revealed that a single failure surface progressively develops from the edge of trapdoor and extends upwards for both 1 *g* and 45 *g* trapdoor test. However, the slope of failure surface under 1 *g* test is smaller than that under 45 *g*.

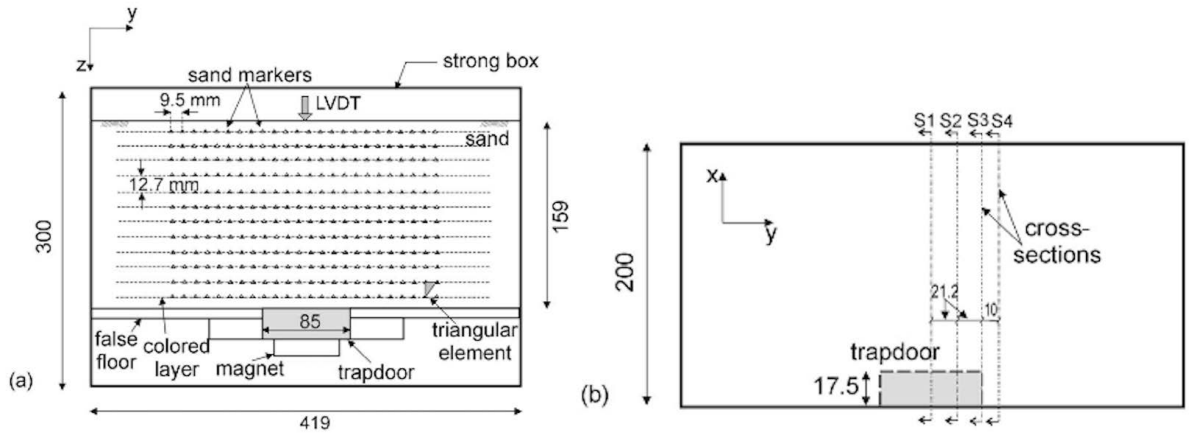

Fig. 2.11 Model configuration: (a) elevation view showing sand markers; (b) plan view showing position of the transverse sections within the backfill (from Costa et al., 2009).

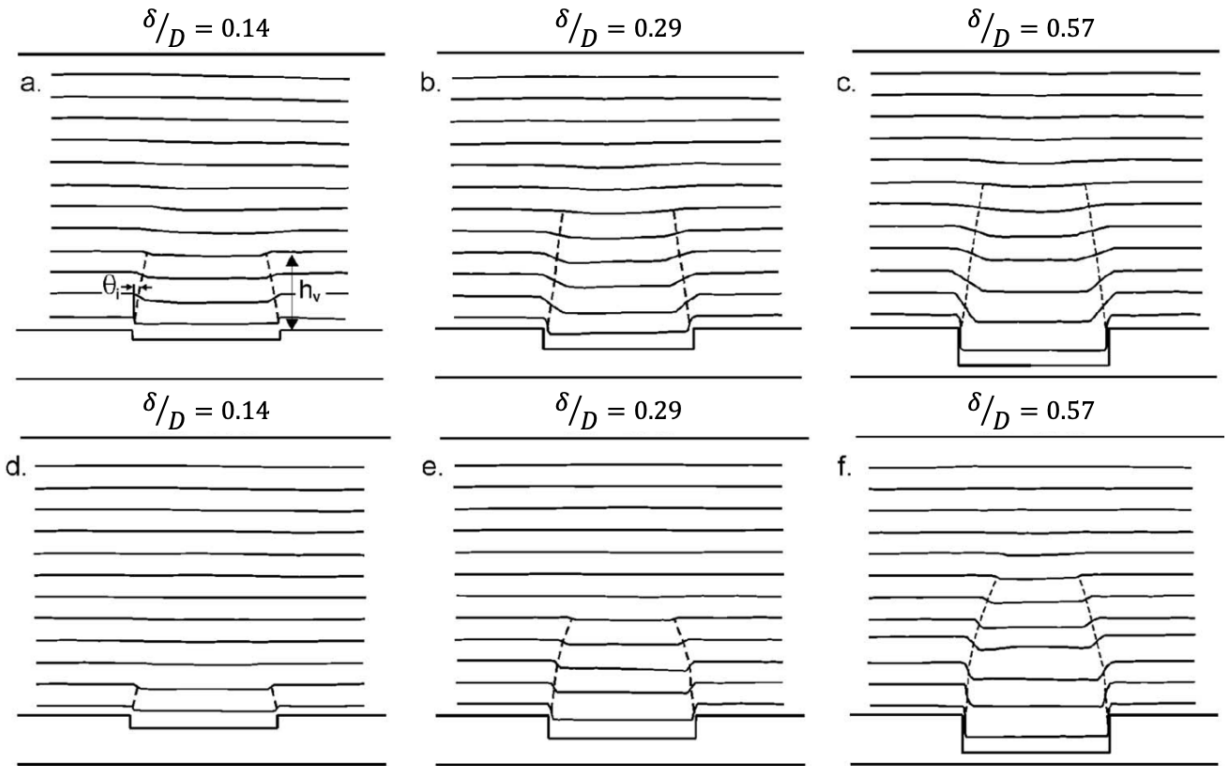

Fig. 2.12 Failure surface in the longitudinal section of models with dense backfill ($D_r = 85\%$). Models tested under 45 g: (a) $\delta/D = 0.14$ ($\theta_i = 9^\circ$); (b) $\delta/D = 0.29$ ($\theta_i = 7^\circ$); (c) $\delta/D = 0.57$ ($\theta_i = 7^\circ$). Models tested under 1 g: (d) $\delta/D = 0.14$ ($\theta_i = 13^\circ$); (e) $\delta/D = 0.29$ ($\theta_i = 7^\circ$); (f) $\delta/D = 0.57$ ($\theta_i = 4^\circ$) (Improved from Costa et al., 2009).

Surface settlement

Nakai (1997) carried out 2D and 3D trapdoor test to investigate the settlement of ground surface, meanwhile, the effect of soil type, test condition and overburden ratio on it was also explored. The experiment result is shown in Fig. 2.13. We can see that the settlement of ground surface become to be smaller as overburden ratio increase from 1.0 to 2.0 because the soil arching is emerged to support the soil above arch. For the effect of soil type, the settlement in Toyoura sand ground is smaller than that in Kaolin clay, because the friction angle of sand is larger than that of clay, the larger of friction angle cause the larger of shear resistance (e.g., Chevalier et al., 2012; Guo and Zhou, 2013; Ahmadi and Hosseininia, 2018). The settlement of ground surface in 3D trapdoor test is larger than that in 2D trapdoor test for clay, which is independent with overburden ratio. For sand, the same tendency is observed as overburden ratio is 1.0, but the difference of settlement from 2D and 3D tests is smaller than that of clay. However, when overburden ratio is 2.0, the contrary tendency is observed. The possible reason I thought is boundary condition, the width of apparatus for 2D test is smaller than that for 3D test, so the friction between ground and walls of apparatus for 2D test is more significant than that for 3D test. For clay, the same tendency is observed from 2D and 3D test because the effect of overburden ratio on soil arching is insignificant. However,

the effect of overburden ratio on soil arching of sand is significant, for higher overburden ratio, fully arch is generated to support the upper soil, in this case, the boundary condition is insignificant.

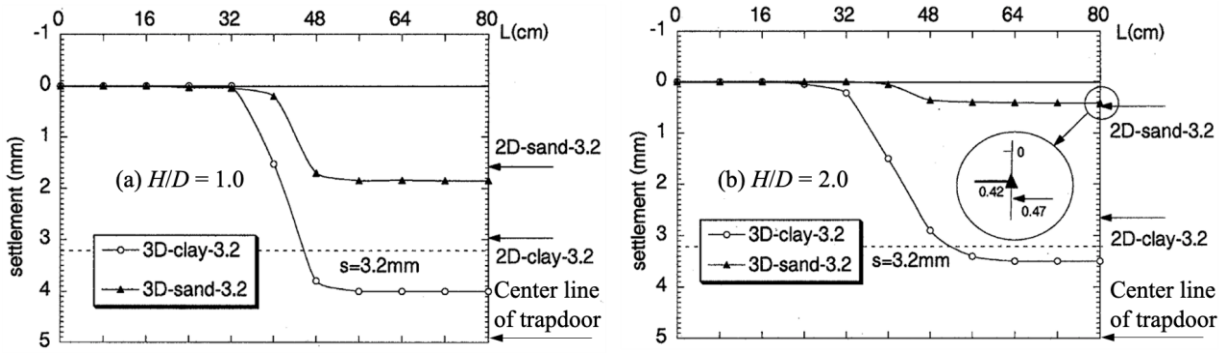

Fig. 2.13 Observed surface settlement from 2D and 3D tests under (a) overburden ratio H/D = 1.0; (b) overburden ratio H/D = 2.0 (improved from Nakai et al., 1997).

2.1.2 Numerical simulation for trapdoor test

Numerical methods included Finite Element Method (FEM) and Discrete Element Method (DEM) is a much more comprehensive, prevalent and available way to do research on trapdoor test (e.g., Tanaka and Sakai, 1987 1993; Dang and Meguid, 2008; Chevalier et al., 2012; Jiang et al., 2018). However, the drawback of numerical methods is also obvious. First, a lot of parameters are needed to be determined, and the good results sometimes depend on the chosen parameters. Second, the analysis for simulation of trapdoor test or tunnel excavation, especially for large scale domain, is usually time-consuming, supercomputer is necessary.

Koutsabeloulis and Griffiths (1989) performed an analysis with FEM on plane strain trapdoor test for active and passive mode. The influence of density of mesh, friction angle ϕ and overburden ratio H/D on normalized loosening pressure was investigated. Density of mesh has insignificant effect on normalized loosening pressure, meanwhile, the FEM result is consistent with that calculated by Davis's upper bound solution (Davis, 1968). The larger of friction angle and overburden ratio cause the smaller normalized loosening pressure, which is coincide with the prediction of Terzaghi's theory (Terzaghi, 1943).

Murakami et al. (1997) conducted DEM analysis to study the evolution of shear bands of active and passive trapdoor test taking into account rolling friction. Dislocation lines due to sliding, roiling and separating the particles in contact was defined to visualize the deformation process as trapdoor moved upward or downward. The distribution of dislocation lines in a zone was usually called "sliding zone". In the vicinity of the zone, some vortices in diameter of 10-20 times the grain particle were emerged and vanished during the generating of the shear bands. A couple stress developed in the shearing process was presumed to be the main factor to cause the vortices. This is an explanation on the evolution of discontinuum shear bands (e.g., Stone and Wood, 1992).

Liang and Xu (2019) used DEM to explore the average loosening pressure versus displacement of the trapdoor and the effect of overburden ratio on it, which are similar as other researchers' report (e.g., Terzaghi, 1943;

Evans, 1984; Kikumoto, 2004; Iglesia et al., 2014). The distribution of loosening pressure across a trapdoor was also investigated, it was revealed that the loosening pressure at the edge of the trapdoor was larger than that at center line of trapdoor. However, the distribution of loosening pressure is contrary to that observed from trapdoor tests (e.g., Harris, 1974; Evans, 1984; Kikumoto, 2004).

Park and Adachi (2002) carried out model tests and FEM analysis to explore the loosening pressure acting on a trapdoor and stress redistribution around the trapdoor and surface settlement profile in trapdoor test considering inclined layers. The distribution of earth pressure is shown in Fig. 2.14. The distribution tendency of loosening pressure and stress redistribution under different inclined angle of the inclined layer to horizontal line is similar to the usual trapdoor tests (e.g., Evans, 1984; Kikumoto, 2014). However, the distribution of earth pressure is significant nonsymmetrical particularly as inclined angle is 60 degree. For the surface settlement profile shown in Fig. 2.15, it is also nonsymmetrical, and the point of maximum surface settlement move to different side of centerline of trapdoor when the inclined angle equal to 30° and 60° respectively.

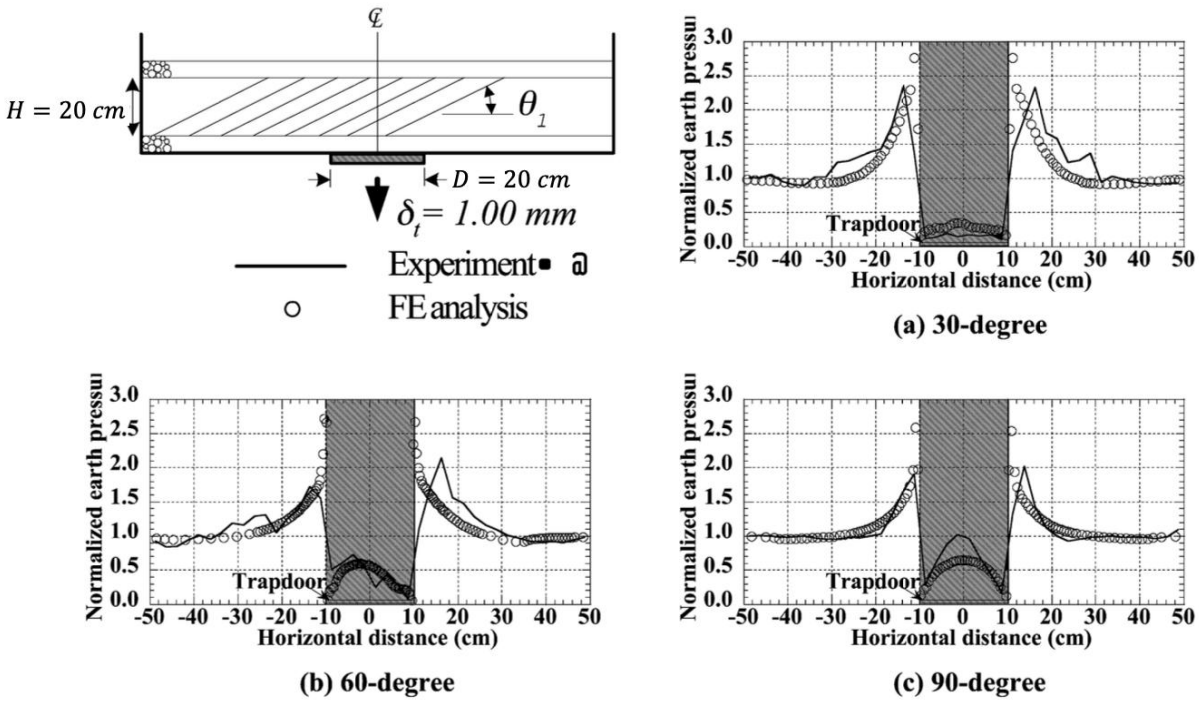

Fig. 2.14 Distribution of earth pressure at $\delta_t = 1.00\ mm$ and $H = 20\ cm$, $D = 20\ cm$ (a) $\theta_1 = 30^{\circ}$; (b) $\theta_1 = 60^{\circ}$; (c) $\theta_1 = 90^{\circ}$ (improved from Park and Adachi, 2002).

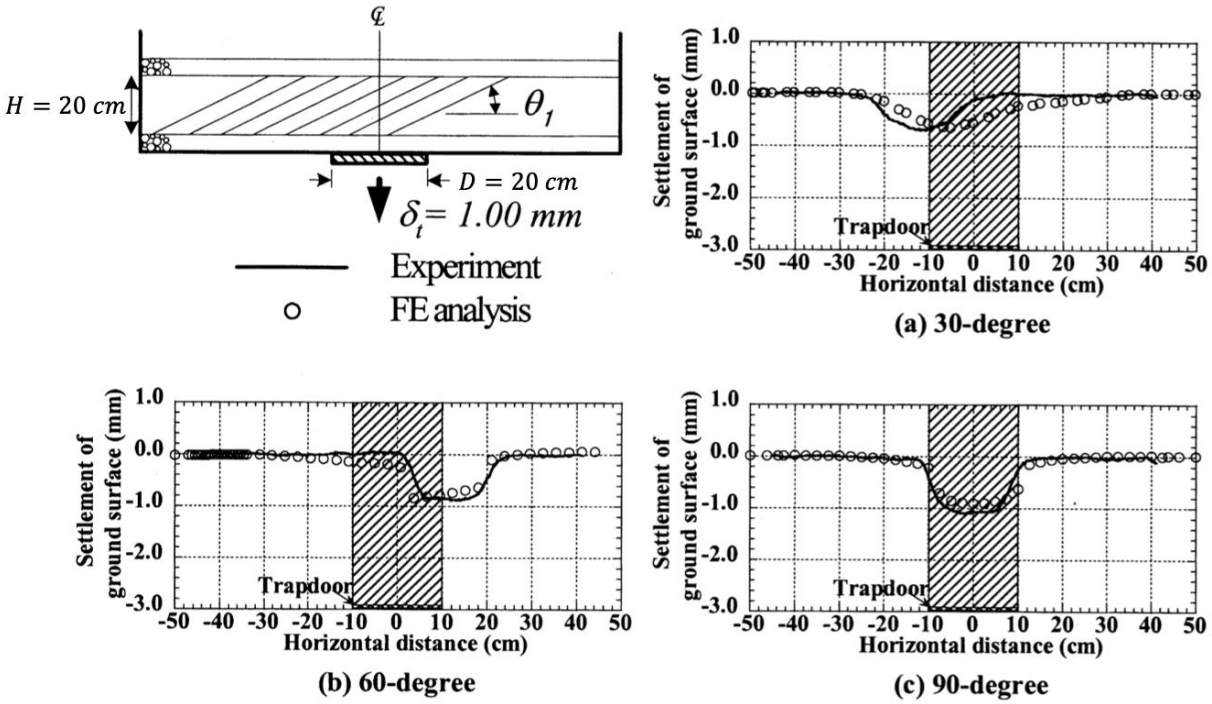

Fig. 2.15 Surface settlement profile at $\delta_t = 1.00\ mm$ and $H = 20\ cm$, $D = 20\ cm$ (a) $\theta_1 = 30^{\circ}$; (b) $\theta_1 = 60^{\circ}$; (c) $\theta_1 = 90^{\circ}$ (improved from Park and Adachi, 2002).

2.2 Theoretical solution for trapdoor test

Trapdoor test was firstly developed by Terzaghi to simulate tunnel excavation and investigate soil arching in granular material under strip condition in 1936 (e.g., Terzaghi, 1936). Furthermore, a theory was proposed by Terzaghi to evaluate the loosening pressure acting on a trapdoor (e.g., Terzaghi, 1943). Until now, his theory and recommendations are still widely used. As shown in Fig. 2.16 (a), as the trapdoor moves downwards, the shear resistances are emerged along the sliding surface ac and bd between yielding zone and stationary zone and tend to prevent the downwards movement of the yielding zone. The shear resistances significantly reduce the earth pressure (loosening pressure) acting on the trapdoor and transfer the reduction of loosening pressure onto the adjoining stationary zone, which is usually called the arching effect. Meanwhile, the total reduction of the load acting on the trapdoor should be equal to the total increase of the load in adjoining stationary zone. To simplify the model, Terzaghi assumed the two vertical sliding surfaces ae and bd to develop the theory. A small element of yielding zone was illustrated as shown Fig. 2.16 (b). According to the limit equilibrium theory, a simple formula was generated by Terzaghi as follows

$$\sigma_z = \frac{\rho_d g D - 2c'}{2K_h tan\phi}\left(1 - e^{\frac{-2K_h tan\phi \cdot z}{D}}\right) + qe^{\frac{-2K_h tan\phi \cdot z}{D}} \tag{2.1}$$

where σ_z is total loosening pressure; z is the distance to ground surface; D is width of trapdoor; ρ_d is dry density; K_h (Terzaghi described K_h as an empirical constant and recommended that it be taken to equal 1.0 for analysis purposes.) is lateral earth pressure coefficient; ϕ is internal friction angle; q is surcharge; c' is cohesion.

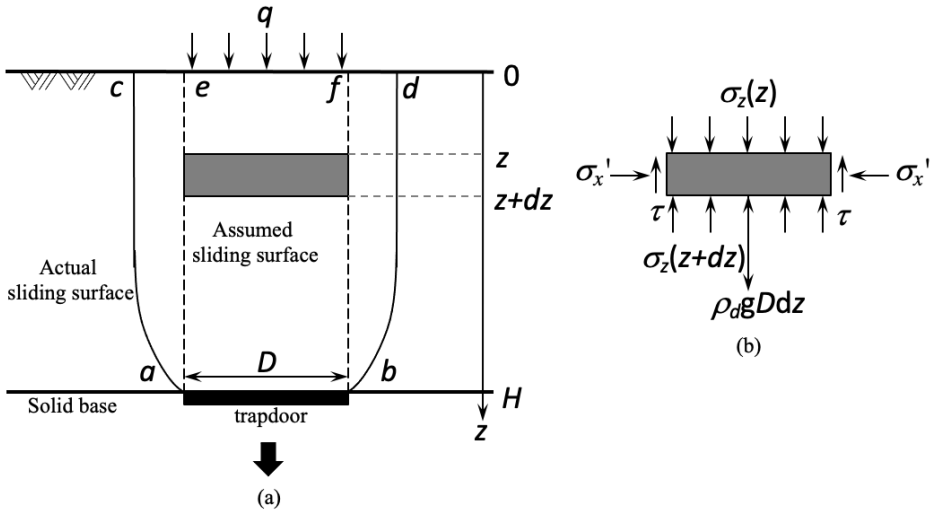

Fig. 2.16 Failure in cohesionless sand preceded by arching, (a) failure surface caused by downward movement of a small section of the base of a layer of sand; (b) a small element of yielding zone between two assumed sliding surfaces, ae and bf (Replotted from Terzaghi, 1943).

Equation (2.1) is available to predict loosening pressure as overburden ratio, *H*/*D* is no larger than 2. When overburden ratio, *H*/*D* is larger than 2, the two sliding surfaces cannot attain to ground surface, hence, the weight of the upper stationary soil zone above the crown of sliding surfaces is assumed to surcharge. However, for this model, the height of the upper soil zone is hardly determined.

Evans (1984) proposed a plasticity theory to evaluate the loosening pressure in granular material. The angle of dilation, ν, no larger than internal friction angle, ϕ, has different value as trapdoor move downwards. According to his assumption, ν is equal to ϕ as minimum loosening pressure is attained and the shape of soil arching is triangular as shown Fig. 2.17 (a), ν is zero as ultimate loosening pressure is attained and the shape of soil arching is rectangular as shown Fig. 2.17 (b). Meanwhile, the shear stress on the boundaries is given as shown in equation (2.2) by considering velocity characteristics (e.g., Jaky, 1948; Evans, 1984).

$$\tau = \sigma_h'\left(\frac{cos\nu\ sin\phi}{1 - sin\nu\ sin\phi}\right) \tag{2.2}$$

where τ is the shear stress; σ_h' is the horizontal effective stress; ν is angle of dilation; ϕ is internal friction angle. For the associated flow rule ($\nu = \phi$), equation (2.2) reduces to the Mohr-Coulomb expression (with cohesion $c' = 0$).

(1) loosening pressure when $\nu = \phi$

As shown in Fig. 2.17 (a), since the vertical components of the shear force N and the normal force T are in opposite direction, and are equal in magnitude, which doesn't contribute to reduce the vertical pressure acting on a trapdoor. Therefore, the load on the trapdoor is only the weight of soil underneath the triangular soil arching.

$$F = \rho_d g D^2/(4tan\phi) \qquad \text{for} \quad H/D \le 1/(2tan\phi) \qquad (2.3\text{ a})$$

$$F = \rho_d g D^2\{1-(H/D)tan\phi\} \qquad \text{for} \quad H/D > 1/(2tan\phi) \qquad (2.3\text{ b})$$

where F is the load acting on a trapdoor; H is overburden height; D is width of trapdoor; ρ_d is dry density.

(2) loosening pressure when $\nu = 0^\circ$

As shown in Fig. 2.17 (b), the model is similar to Terzaghi's model, according to the limit equilibrium theory, the formula for predicting load acting on a trapdoor is written as

$$F = \frac{\rho_d g D^2}{2K_h sin\phi}\left(1 - e^{\frac{-2K_h sin\phi \cdot z}{D}}\right) \qquad \text{for } H/D \le 2 \qquad (2.4\text{ a})$$

$$F = \rho_d g D^2\{\left(1 - e^{\frac{-4K_h sin\phi}{D}}\right)/(2K_h sin\phi) + (H/D-2)e^{\frac{-4K_h sin\phi}{D}} \qquad \text{for } H/D > 2 \qquad (2.4\text{ b})$$

where K_h is 1.2 based on his test results and other researchers, since it affects the prediction of loosening pressure, in his opinion, more research should be required to obtain appropriate value for K_h; z is the distance to ground surface. Soil cohesion is assumed to be zero here.

(3) loosening pressure when $0^\circ < \nu < \phi$

As the normal stress is not known what value should be use at the boundaries, the theoretical solution for predicting loosening pressure is not apparent. However, a conclusion he made is the loosening pressure lie within the limits set by $\nu = 0^\circ$ and $\nu = \phi$.

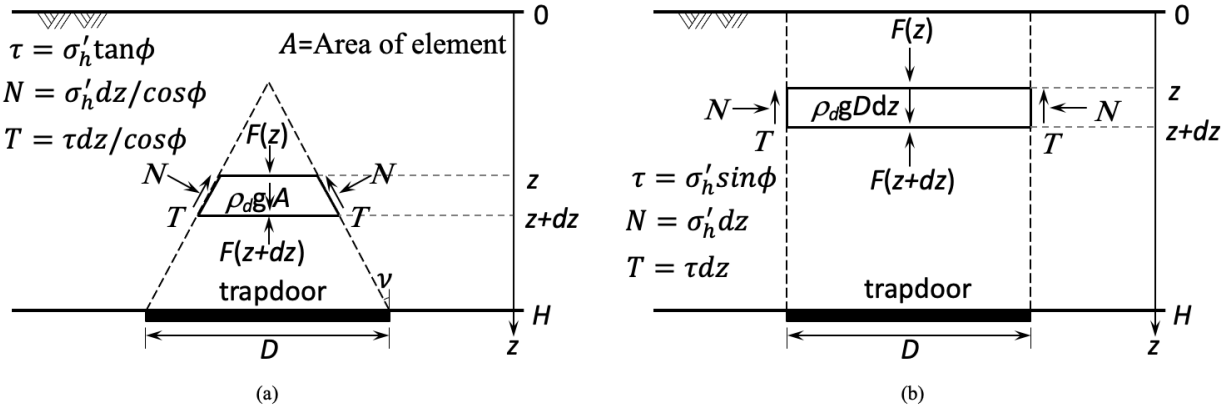

Fig. 2.17 Free body diagrams for active arching in the two-dimensional case, (a) free body diagrams for $\nu = \phi$; (b) free body diagrams for $\nu = 0^\circ$ (Replotted from Evans, 1984).

Consequently, Iglesia (2014) also developed a theory to estimate loosening pressure for the parabolic soil arching and triangular soil arching based on salient aspects of the theories by Engesser (1882) and Evans (1984). In his theory, the angle of the tangent line of the curved soil arching to the horizontal line is defined as θ which is assumed to the complementary of internal friction angle ϕ as shown in Fig. 2.18. This assumption for the curved soil arching by Iglesia is similar to that by Evans (1984). For the load acting on a trapdoor after downwards movement, unlike Evans's assumption, the load defined by Iglesia includes the weight W of soil underneath soil arching and the vertical stress σ_{vr} induced by the intensified lateral stress σ_{hr}.

The weight of soil below soil arching can be calculated by the cross-sectional area of the soil multiplied by the specific weight of the soil. Hence, the weight for the curved soil arching is written as

$$W = \frac{\gamma D^2 tan\theta}{6} = \frac{\rho_d g D^2 \tan(\frac{\pi}{2} - \phi)}{6} = \frac{\rho_d g D^2 \cot\phi}{6} \tag{2.5}$$

For the vertical stress σ_{vr} brought about by the transfer of soil stress to the sides, following Engesser's approach (1882), can be quantified by considering an imaginary structure arch of thickness of dh, and uniformly loaded over its entire span as shown as Fig. 2.19. Therefore, the lateral stress σ_{hr} at the edge of the arch is then the ratio of the lateral thrust reaction dF_h to the lateral area dh (the depth in the normal of soil arch is unity). Herein, the assumption is that the stress state at the edge of arch is the same in the imaginary structure as in the actual case. Meanwhile, the lateral stress σ_{hr} is assumed to be constant, and the stress state of the entire arch attain to the Mohr-Coulomb failure state. The Mohr circle of the stress state at the end of arching can be drawn in Mohr diagram as shown in Fig. 2.20. Hence, the vertical stress σ_{vr} can be written as

$$\sigma_{vr} = K_E \sigma_{hr} \tag{2.6}$$

where

$$K_E = \frac{cos\phi^2}{1 + sin\phi^2} \tag{2.7}$$

Herein, the coefficient of earth pressure K_E is defined as the ratio of the vertical stress to the lateral stress, which is different with Krynine's definition (e.g., Krynine, 1945; Handy, 1985). Moreover, K_E is defined for the incline shear surface, and its value is less than 1 which means the lateral stress σ_{hr} is greater than the vertical stress σ_{vr} at the maximum arching.

For the uniform loading on the imaginary arch structure, it was calculated by Engesser (1882) as

$$q = dh \cdot (\rho_d g - \frac{\sigma_{vr}}{H}) \tag{2.8}$$

As shown in Fig. 19, for the parabolic arch with span D forming an angle θ to horizontal at the end of arch, the lateral thrust reaction dF_h caused by uniform loading q can be written as (e.g., Leontovich, 1959)

$$dF_h = \frac{qD^2}{8f} = \frac{qD}{2tan\theta} = \frac{qD}{2cot\phi} \tag{2.9}$$

Where $f = Dtan\theta/4$, which is the height of the arch. As previous statement, $\sigma_{hr} = dF_h/dh$, combing equations (2.8) and (2.9), the lateral stress σ_{hr} can be obtained as

$$\sigma_{hr} = \frac{D}{2cot\phi}(\rho_d g - \frac{\sigma_{vr}}{H}) \tag{2.10}$$

Substitute equation (2.10) into equation (2.6), the vertical stress σ_{vr} can be written as

$$\sigma_{vr} = \frac{HD\rho_d g K_E}{2Hcot\phi + DK_E} \tag{2.11}$$

Based on the equations (2.5) and (2.11), the loosening pressure σ_z acting on a trapdoor for the curved soil arching can be written as

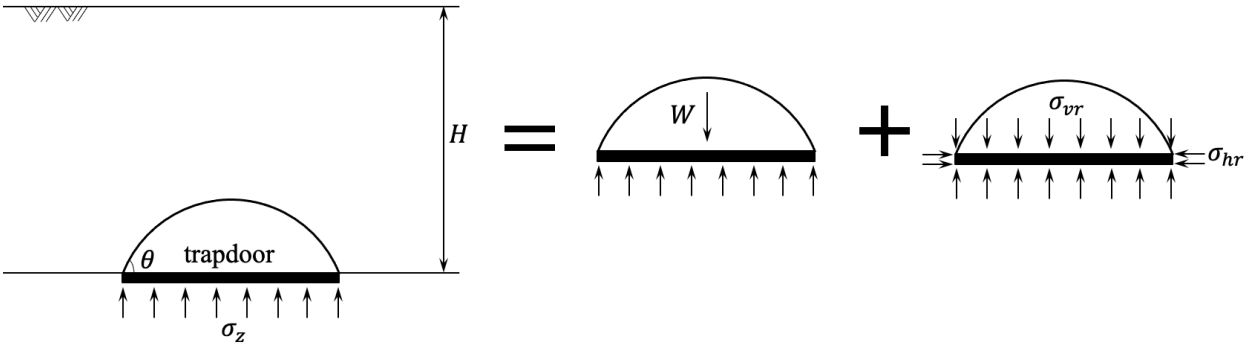

Fig. 2.18 Engesser's approach (replotted from Iglesia et al., 2014).

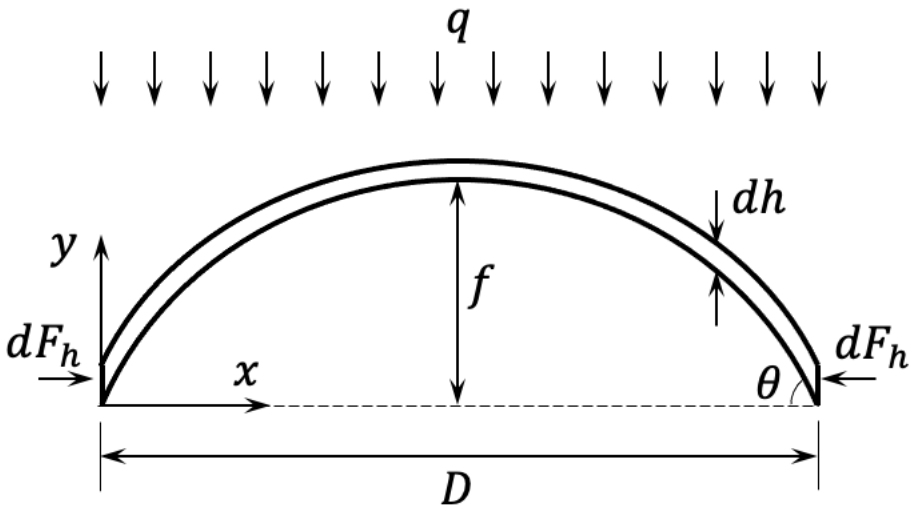

Fig. 2.19 Imaginary structure arch in Engesser's (1882) analysis (replotted from Iglesia et al., 2014).

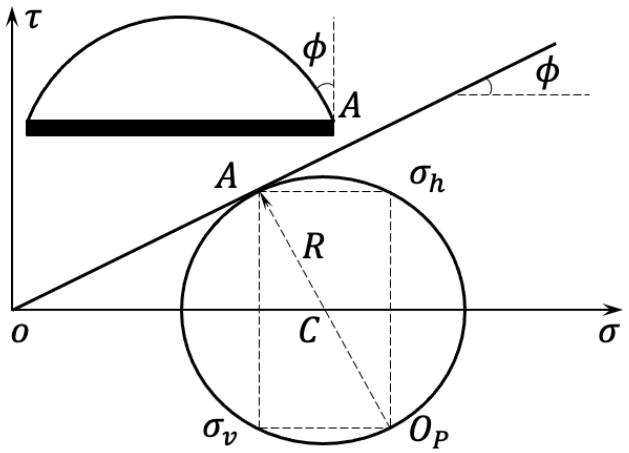

Fig. 2.20 Mohr diagram assuming failure stress at edge of trapdoor (replotted from Iglesia et al., 2014).

$$\sigma_z = \frac{W}{D} + \sigma_{vr} = \rho_d g D\left(\frac{HK_E}{2Hcot\phi + DK_E} + \frac{\cot\phi}{6}\right) \tag{2.12}$$

For the triangular soil arching, the only difference is the calculation of the weight of soil below soil arching W ($\rho_d g D^2 \cot\phi/4$) and the lateral thrust reaction dF_h ($= qDtan\phi/4$). Therefore, a similar expression for predicting the loosening pressure can be written as

$$\sigma_z = \rho_d g D\left(\frac{HK_E}{4Hcot\phi + DK_E} + \frac{\cot\phi}{4}\right) \tag{2.13}$$

According to the comparison of theoretical result calculated by equations (2.12) and (2.13) with the experiment result observed by centrifuge tests, the two equations can nicely capture the experiment results.

Moreover, Kikumoto (2004) proposed a theory to evaluate loosening earth pressure for 3D trapdoor test as shown as Fig. 2.21, which was written as below.

$$\sigma_z = \frac{x(\rho_d g - c/x)}{4K_h tan\phi}\left(1 - e^{\frac{-4K_h tan\phi \cdot z}{x}}\right) \tag{2.14}$$

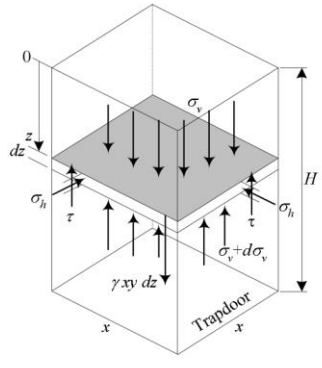

Fig. 4-31 Terzaghiの式[14]の3次元問題への拡張[28]

Fig. 2.21 Diagram for 3D trapdoor (from Kikumoto, 2004).

Currently, the theories proposed by Terzaghi (1943), Evans (1984), Iglesia (2014) and Kikumoto (2004) are the main theoretical solutions for estimation of loosening pressure. Even though, some other researchers also proposed many theories (e.g., Engesser, 1882; Bierbaumer, 1913; Marston and Anderson, 1913; Ladanyi and Hoyaux, 1969; Liang, 2019 2020) to predict loosening pressure, those theories are similar to the three theories, the merely difference is the lateral earth pressure coefficient. However, the loosening pressure estimated by those theories is average pressure acting on a trapdoor, which isn't consistent with the result observed in experiment (e.g., Evans, 1984; Kikumoto, 2004). Tamura (2001) and Kikumoto et al. (2004) proposed a theory to predict the distribution of loosening pressure across a trapdoor and stress redistribution around a trapdoor respectively.

2.3 Behavior of unsaturated soils

In this section, the behavior of unsaturated soils was reviewed, which included soil-water characteristic curve, the principle of effective stress for unsaturated soils and shear strength.

2.3.1 Soil-water characteristic curve

Soil-water characteristic curve (swcc) is the relationship between volumetric water content, gravimetric water content or degree of saturation and soil suction, which plays an important role in application of unsaturated soil mechanics (Fredlund and Rahardjo, 1993). The swcc was firstly plotted by Edgar Buckingham for six soils ranging in texture from sand to clay in 1907 (Leong, 2019). The swcc is also expressed as water retention curve, soil moisture retention curve, soil water release curve, suction-water content relationship and soil moisture characteristic curve in other disciplines, which is usually determined based on test results of water content and suction. swcc in not a unique curve due to hysteresis, which includes the main drying (desorption) swcc curve and the main wetting (adsorption) swcc curve (Fredlund et al., 2011). The main drying swcc curve is frequently measured in laboratory with relative ease (Fredlund and Rahardjo, 1993), which is normally time-consuming and costly. The main wetting swcc curve is generally estimated by the main drying swcc curve and hysteresis as wetting path of experiment is more difficult (e.g., Fredlund et al., 2011). The shape of swcc is also affected by stress history, fabric, confining pressure and density (Fredlund et al., 2002).

Many empirical swcc were proposed to best fit volumetric water content θ_w and suction s data during the past decades (e.g., Gardner, 1958; Brooks and Corey, 1964; McKee and Bumb, 1984 1987; van Genuchten, 1980; Fredlund and Xing, 1994; Pereira and Fredlund, 2000; Fredlund and Phan, 2006), in which θ_s is the saturated volumetric water content and θ_r is the residual volumetric water content. The equations are shown as below.

(1). Gardner (1958)

$$\theta_w = \theta_r + \frac{\theta_s - \theta_r}{1 + (\alpha s)^n} \tag{2.15}$$

where s is soil suction; θ_w is volumetric water content corresponding to any suction; α is a curve fitting parameter related to the air entry value of soil; n is a curve fitting parameter related to the slope at the inflection point on

the swcc.

(2). Brooks and Corey (1964)

$$\theta_w = \theta_r + (\theta_s - \theta_r)(\frac{a}{s})^n \tag{2.16}$$

Equation (2.16) is only valid as s is larger than or equal to α. θ_w is assumed to be equal to θ_r as s is less than α.

(3). McKee and Bumb (1984)

$$\theta_w = \theta_r + (\theta_s - \theta_r)\exp(\frac{a - s}{b}) \tag{2.17}$$

Where a and b are soil parameter.

(4). McKee and Bumb (1984)

$$\theta_w = \theta_r + \frac{\theta_s - \theta_r}{1 + \exp(\frac{s - a}{b})} \tag{2.18}$$

(5). van Genuchten (1980)

$$\theta_w = \theta_r + \frac{\theta_s - \theta_r}{[1 + (\alpha s)^n]^m} \tag{2.19}$$

van Genuchten equation is famous and extensively accepted by many researchers. Equation (2.19) has three fitting parameters of α, n and m. For parameter α, Fredlund and Xing (1994) indicated that $1/\alpha$ is closely related to air entry value, and the air entry value can be used for $1/\alpha$ if m is small. For parameter n and m, van Genuchten indicated that n and m had a fixed relationship of m = 1-2/n based on Burdine theory (Burdine, 1953) or m = 1-1/n based on Mualem theory (Mealem, 1976), so that a closed-form expression for hydraulic conductivity could be obtained.

(6). Fredlund and Xing (1994)

$$\theta_w = \theta_r + \frac{\theta_s - \theta_r}{\{ln[e + (\frac{s}{a})^n]\}^m} \tag{2.20}$$

(7). Pereira and Fredlund (2000)

$$\theta = \theta_u + \frac{\theta_f - \theta_u}{[1 + (\frac{s}{a})^n]^m} \tag{2.21}$$

where α is matirc suction at the inflection point; θ is volumetric water content of a soil under a given net confining stress; θ_f is the final volumetric water content of a soil under a given net confining stress; θ_u is the initial volumetric water content of a soil under a given net confining stress.

(8). Fredlund and Pham (2006)

Fredlund and Pham (2006) intended to propose three linear relationships to express the entire swcc according to the magnitude of suction. The low suction range is from 1 kPa to air entry value s_{AEV}, the intermediate suction range is from s_{AEV} to residual suction s_R, the high suction range is from s_R to 1000000 kPa. The equations for

swcc are written as

$$\theta_w^1 = \theta_u - S_1 \log(s) \qquad 1 \le s < s_{AEV} \qquad (2.22\text{ a})$$

$$\theta_w^2 = \theta_{ae} - S_2 \log(\frac{s}{s_{AEV}}) \qquad s_{AEV} \le s < s_R \qquad (2.22\text{ b})$$

$$\theta_w^3 = -S_3 \log(\frac{s}{10^6}) \qquad s_R \le s < 10^6\ kPa \qquad (2.22\text{ c})$$

where θ_w^i (i = 1, 2, 3) is the volumetric water content of each suction range; S_i (i = 1, 2, 3) is the slope of straight line for each suction range; θ_u is the volumetric water content when suction is 1 kPa; θ_{ae} is the volumetric water content corresponding to air entry value.

Fredlund and Xing (1994) also indicated that the swcc could be predicted by the pore size distribution curve, hence they proposed equation (2.23). And they obtained mathematical equation for swcc by assumed some special pore size function such as a constant pore size function and pore size function varies inversely as r^2. However, it is difficult to obtain the actual pore size function for a soil in reality, which limits the application of this method. Fredlund et al. (2002) indicated that the estimation of swcc by pore size distribution is difficult to predict the swcc of clay, tills and loams.

$$\theta(R) = \int_{R_{min}}^{R} f(r)\, dr \qquad (2.23)$$

where R is the specific pore radius; θ(R) is volumetric water content when all the pores with radius less than or equal to R are filled with water; R_{min} is minimum pore radius in the soil; r is the pore radius; $f(r)$ is the pore size function. When R is equal to maximum pore radius R_{max}, θ(R) equals to volumetric water content θ_s corresponding to saturated case.

Overall, swcc is significantly important to estimate the properties of unsaturated soil such as effective stress and shear strength. In this study, degree of saturation S_r can be obtained by equation (2.19), which is used to evaluate horizontal effective stress at sliding surfaces and wet density for unsaturated zone for trapdoor test. As van Genuchten equation is more prevalent and commonly adopted by other researchers, the parameters of swcc in equation (2.19) are easily found. However, hysteresis is not considered in this study because the groundwater level doesn't change during the trapdoor test.

2.3.2 Effective stress of unsaturated soils

The effective stress concept for saturated soils was proposed by Terzaghi (1936) and is widely accepted and extensively utilized to predict the soil behavior in research and in practice. Two propositions of the effective stress principle for saturated soils are summarized as below (Terzaghi, 1936)

- Compression, distortion and a change of shear resistance of a soil are exclusively caused by changes in effective stress.

- The definition of effective stress of saturated soils based on experiment results is written as

$$\sigma' = \sigma - u_w \tag{2.24}$$

where σ' is effective stress of a soil; σ is total stress of a soil; u_w is the pore water pressure. An assumption made here is that water is incompressible.

As most of soil in nature are in unsaturated state, many researchers have attempted to establish the effective stress principle for unsaturated soil based on extension of effective stress principle of saturated soils. One well known and extensively utilized effective stress principle of unsaturated soils was propose by Bishop in 1959, which is written as

$$\sigma' = \sigma - u_a + \chi(u_a - u_w) \tag{2.25}$$

where u_a is the pore air pressure; u_w is the pore water pressure; χ is the effective stress parameter. Generally, (σ – u_a) and (u_a - u_w) are termed as net stress and soil suction, respectively. χ is an unknown parameter, which is lie in the range from 0 to 1. χ is equal to 1 for saturated soils and χ is equal to 0 for dry soil.

Consequently, Bishop and Donald (1961) carried out triaxial tests on unsaturated silt to verify validity of equation (2.25), in which the cell pressure σ_3, pore water pressure u_w and pore air pressure u_a were varied, however, (σ_3 – u_a) and (u_a - u_w) are held to be constant during shearing. They found that the stress-strain behavior of unsaturated silt was not affected. Hence, they concluded that equation (2.25) was statically correct because the soil behavior was independent with σ_3, u_a and u_w. Meanwhile, effective stress parameter χ is a function of degree of saturation. Bishop and Blight (1963) conducted a series of triaxial tests on four compacted soils to explore the relationship between effective stress parameter χ and degree of saturation S_r as shown in Fig. 2.22. The experiment result in Fig. 2.22 shows a nearly linear relationship between χ and S_r, for simplicity, χ is frequently assumed to be equal to S_r (e.g., Schrefler, 1984; Öberg and Sällfors, 1997; Lu and Likos, 2006; Komolvilas and Kikumoto, 2017). Moreover, Borja (2006) derived this relationship based on the principles of thermodynamics. However, Jennings and Burland (1962) questioned the validity of equation (2.25), Oedometer tests on air-dry silt and silty sand were carried out to investigate soil behavior during socking under constant total stress. They found that the volume of soil decreased during soaking, which was contrary with prediction by equation (2.25). Hence, they pointed out that equation (2.25) was invalid to predict volume change behavior of unsaturated soils. Kohgo et al. (1993) thought suction effects should be considered in two different ways due to the air entry suction value. Firstly, the increase of suction induced the increase in effective stress when suction was less than air entry suction value. Secondly, when suction was larger than air entry suction value, an increase in suction caused an increase not only in yield stress, but also in the stiffness of the soil skeleton against plastic deformation, which was because of the relative sliding between soil particles. Therefore, an empirical effective stress principle for unsaturated soils was proposed as below

$$\sigma' = \sigma - u_{eq} \tag{2.26}$$

where u_{eq} is the equivalent pore pressure.

$$u_{eq} = u_a - s \qquad s \le s_{AEV} \tag{2.27}$$

$$u_{eq} = u_a - \{s_{AEV} + \frac{s_C - s_{AEV}}{s - s_{AEV} + a_e}(s - s_{AEV})\} \qquad s > s_{AEV} \tag{2.28}$$

where s is soil suction ($s = u_a - u_w$), s_c is a critical suction; s_{AEV} is the air entry suction value; a_e is a material parameter. As suction is less than air entry suction value, equation (2.27) reduces to equation (2.24) (Terzaghi, 1936).

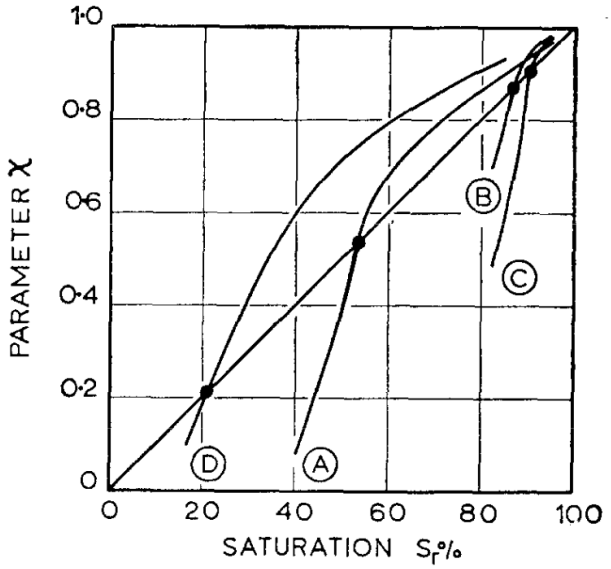

Fig. 2.22 Summary of measured effective stress parameter versus degree of saturation for compacted soils: (A) Talybont clay; (B) Selset clay; (C) Mangla shale; (D) Vaich moraine (from Bishop and Blight, 1963).

Khalili et al. (2004) thought equation (2.25) was validity to predict shear strength and volume change of unsaturated soils by using a modified χ. χ has a unique relationship with the ratio of suction to air entry value (Khalili and Khabbaz, 1998), which is written as

$$\begin{aligned} \chi &= 1 && s \le s_{AEV} \\ \chi &= (\frac{s}{s_{AEV}})^{-0.55} && s > s_{AEV} \end{aligned} \tag{2.29}$$

Meanwhile, they carried out compression tests with Kaolin clay and Glenmore Park silt in a modified oedometer and obtained the curve of suction versus axial strain, which was successfully predicted by equation (2.25) combined with equation (2.29).

Since Bishop's effective stress for unsaturated soils is commonly accepted by many researchers, equation (2.25) is adopted to predict effective stress in this study because volume change is not considered. Meanwhile, χ is

assumed to be equal to S_r for simplicity.

2.3.3 Shear stress of unsaturated soils

After effective stress of saturated soils was proposed by Terzaghi (1936), he deduced shear stress of saturated soils by combining Mohr-Coulomb failure criterion (Terzaghi, 1943), which is written as

$$\tau = c' + (\sigma - u_w)tan\phi \tag{2.30}$$

where τ is shear stress; c' is effective cohesion; σ is total normal stress on the failure plane; u_w is pore water pressure; ϕ is internal friction angle. The shear stress proposed by Terzaghi (1943) is a classic theory which is commonly accepted and utilized in geotechnical engineering. Equation (2.30) is revealed that shear stress τ has a linear relationship with effective normal stress (σ- u_w). Therefore, many researchers attempted to extend theory of shear stress of saturated soils to generate a modified theory to predict shear stress of unsaturated soils (e.g., Bishop and Blight, 1963; Lamborn, 1986, Khalili and Khabbaz, 1998), which is termed as effective stress state variable method. Another way to estimate the unsaturated shear strength is independent stress state variable method (e.g., Fredlund et al., 1978; Tekinsoy et al., 2004; Lee et al., 2005).

Unlike the saturated soils, the unsaturated soils are generally termed as three-phase system, in which it has solid phase, air phase and water phase (Fredlund and Rahardjo, 1993). After effective stress of unsaturated soils proposed by Bishop (1959), many researchers recognized that suction ($u_a - u_w$) has significant influence on the behavior of unsaturated soils except net stress ($\sigma - u_a$) (e.g., Gan et al., 1988; Khalili et al., 2004; Tekinsoy et al., 2004; Kim and Borden, 2011). The two independent stress state variables of net stress ($\sigma - u_a$) and suction ($u_a - u_w$) to describe the mechanical behavior of unsaturated soils because only one stress variable is affected as pore water pressure varies, and pore air pressure is usually assumed to be zero relative to atmosphere in practice application (e.g., Fredlund et al., 1978; Pufahl et al., 1983). Therefore, shear stress of unsaturated soils is dominated by net stress ($\sigma - u_a$) and suction ($u_a - u_w$), based on that, many prediction equations and empirical equations have been proposed.

Bishop and Blight (1963) proposed a modified shear stress of unsaturated soils by combining Bishop's effective stress of unsaturated soils (Bishop, 1959) and the classic Mohr-Coulomb failure criterion. The modified shear stress of unsaturated soils is written as

$$\tau = c' + [(\sigma - u_a) + \chi(u_a - u_w)]tan\phi \tag{2.31}$$

where τ is shear stress; c' is soil cohesion; σ is the total normal stress applied on the failure plane; u_a is the pore air pressure; u_w is the pore water pressure; ϕ is the internal friction angle; χ is the effective stress parameter and depends mainly on degree of saturation S_r. As χ equals to one, equation (2.31) reduces to equation (2.30) of saturated case. Triaxial shear test on unsaturated Mangla shale was also carried out and the curve of shear stress versus effective stress was shown in Fig. 2.23. It is revealed that this shear stress of unsaturated soils is an extension of shear stress of saturated soils. Oberg and Sallfors (1997) pointed out that equation (2.31) with

assumption of $\chi = S_r$ can give reasonable accuracy prediction only for non-clayey materials and the condition of S_r higher than around 50 %.

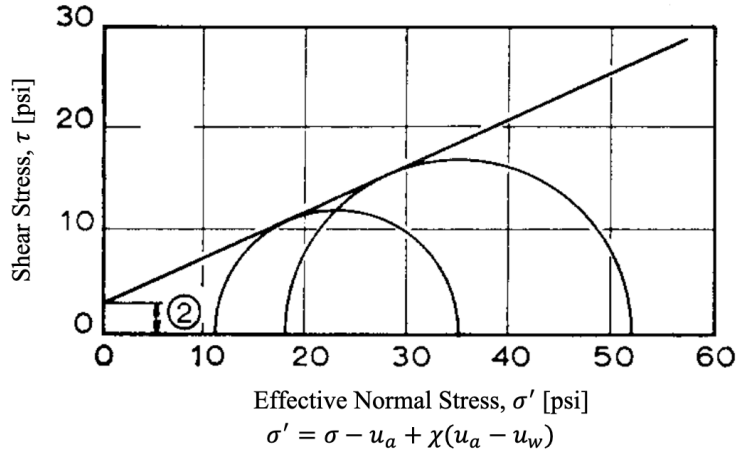

Fig. 2.23 Shear stress versus effective normal stress (from Bishop and Blight, 1963).

Similarly, Lamborn (1986) predicted shear stress of unsaturated soils with equation (2.31) in which χ was equal to volumetric water content θ. Khalili and Khabbaz (1998) indicated that equation (2.31) with a modified χ evaluated by equation (2.29) could predict shear stress of unsaturated soils, and a series of triaxial shearing test were carried out to validate the prediction result and a good agreement was observed (e.g., Khalili and Khabbaz, 1998; Khalili et al., 2004).

Fredlund et al. (1978) indicated that the failure envelope for shear stress of unsaturated soils should be plotted on three-dimension diagram because the shear stress of unsaturated soils is frequently described with two independent stress state variables of $(\sigma - u_a)$ and $(u_a - u_w)$, which is totally unlike that of saturated soils. The equation for prediction of shear stress of unsaturated soils is written as

$$\tau = c' + (\sigma - u_a)tan\phi + (u_a - u_w)tan\phi^b \tag{2.32}$$

where ϕ^b is the angle indicating the rate of increase in shear stress relative to a change in suction $(u_a - u_w)$. c' and ϕ could be evaluated by direct shear tests on the specimens of saturated soil (e.g., Gan et al., 1988; Khalili et al., 2004; Schnellmann, 2015). According to the direct shear tests on unsaturated glacial till with constant net stress of 72.6 kPa, it was revealed that the curve of ϕ^b versus $(u_a - u_w)$ exhibited a significantly nonlinearity (Gan et al., 1988), which is shown in Fig. 2.24. From Fig. 2.24, we can see that ϕ^b is equal to or close to ϕ when $(u_a - u_w)$ is less than air entry value, then ϕ^bdecreases rapidly as $(u_a - u_w)$ gradually increases. Finally, ϕ^b attains a fairly constant value when $(u_a - u_w)$ becomes higher (Gan et al., 1988). However, Schnellmann (2015) indicated that ϕ^b decreased to zero when $(u_a - u_w)$ reached the suction value corresponding to the residual water content on swcc, under which suction has no contribution to shear stress (Schnellmann, 2015). The failure envelope of shear stress of unsaturated soils proposed by Schnellmann is shown in Fig. 2.25.

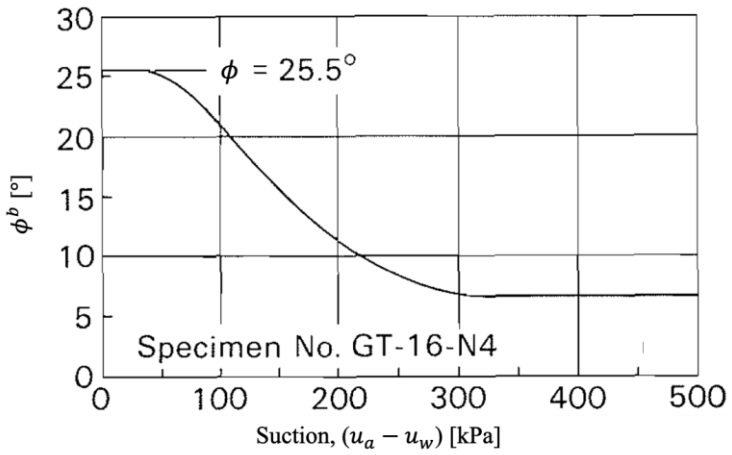

Fig. 2.24 ϕ^b versus $(u_a - u_w)$ from direct shear test on unsaturated glacial till specimen (from Gan et al., 1988).

Equation (2.32) could be rewritten as

$$\tau = c' + [(\sigma - u_a) + \beta(u_a - u_w)]tan\phi \tag{2.33}$$

where $\beta = tan\phi^b / tan\phi$. In this case, equation (2.33) reduces to equation (2.31), in which χ equals to β.

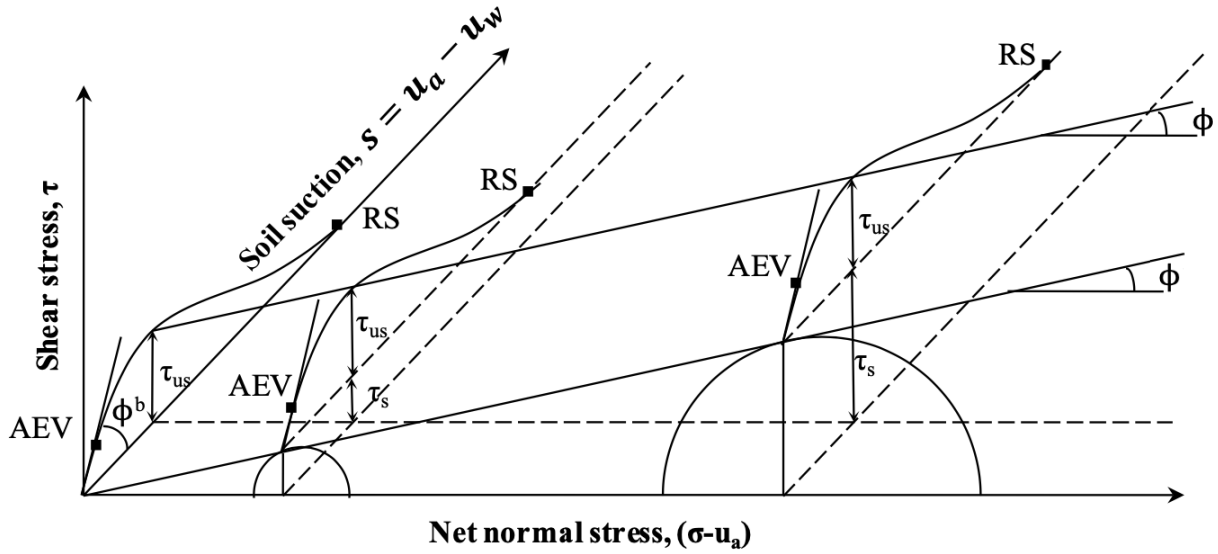

Fig. 2.25 Extend Mohr-Coulomb failure surface for the Schnellmann's model behaviour of the shear strength with respect to soil suction for coarse-grained soils (from Schnellmann, 2015).

Fredlund et al. (1995) deduced an analytical equation to predict shear stress of unsaturated soils in which a soil parameter κ depended on soil type, which is written as

$$\tau = c' + (\sigma - u_a)tan\phi + (u_a - u_w)(\frac{\theta_w - \theta_r}{\theta_s - \theta_r})^{\kappa} tan\phi \tag{2.34}$$

where κ is a soil parameter dependent upon the soil type; θ_w is volumetric water content corresponding to any suction; θ_s is the saturated volumetric water content; θ_r is the residual volumetric water content. Equation (2.34) could satisfactorily predict shear stress of sandy soils when κ is equal to one, and κ gradually increases as soil plasticity increases.

Vanapalli and Fredlund (2000) proposed a model to mathematically evaluate κ with plasticity index of the soils, which is written as

$$\kappa = -0.0080(I_p)^2 + 0.0801I_p + 1 \tag{2.35}$$

where I_p is plasticity index.

Furthermore, Garven and Vanapalli (2006) proposed a new model to evaluate κ for different compacted soils such as clay, silt and tills, which is written as

$$\kappa = -0.0016(I_p)^2 + 0.0975I_p + 1 \tag{2.36}$$

Bao et al. (1998) proposed a modified model based on equation (2.34), in which a change of air entry value was linear in the change of residual soil suction on a semi-logarithmic plot. The modified model is expressed as

$$\tau = c' + (\sigma - u_a)tan\phi + (u_a - u_w)[\frac{\log(s_R) - \log(s)}{\log(s_R) - \log(s_{AEV})}]tan\phi \tag{2.37}$$

where s_R is the residual soil suction.

Rassam and Cock (2002) proposed a prediction function to evaluate shear stress for unsaturated soils, which is written as

$$\tau = c' + (\sigma - u_a)tan\phi + stan\phi - \varphi(s - s_{AEV})^{\beta} \tag{2.38}$$

where φ and β are fitting parameters, the estimation of which are shown as below

$$\varphi = \frac{s_R tan\phi - \tau_{Sr}}{(s_R - s_{AEV})^{\beta}} \tag{2.39}$$

$$\beta = \frac{tan\phi(s_R - s_{AEV})}{s_R tan\phi - \tau_{Sr}} \tag{2.40}$$

where τ_{Sr} is the contribution of matric suction to the shear strength at the residual suction, which should be determined experimentally.

However, the prediction function is only applicable for sand, silt and their mixture because the residual suction can be experimentally estimated by modified direct shear or triaxial apparatus.

Aubeny and Lytton (2003) extended the prediction equation proposed by Lamborn (1986) for shear stress of unsaturated soils, which is written as

$$\tau = c' + (\sigma - u_a)tan\phi + f_1\theta_w(u_a - u_w)tan\phi \tag{2.41}$$

where f_1 is a function related to volumetric water content, the determination of f_1 is shown as below.

$$f_1 = \frac{1}{\theta_w} \qquad S_r = 100\ \%$$

$$f_1 = 1 + (\frac{S_r - 85}{15})(\frac{1}{\theta_w} - 1) \qquad 85\ \% \leq S_r \leq 100\ \%$$

$$f_1 = 1 \qquad S_r < 85\ \%$$

Tekinsoy et al. (2004) proposed an empirical logarithmic function with best fitting to experiment data to predict the shear stress of unsaturated soils, which is written as

$$\tau = c' + (\sigma - u_a)tan\phi + (s_{AEV} + P_{at})\ln(\frac{s + P_{at}}{P_{at}})tan\phi \tag{2.42}$$

where P_{at} is atmospheric pressure; s ($s = u_a - u_w$) is soil suction. Tekinsoy indicated that equation (2.42) has a good agreement with the experiment data of fine-grained soils.

As the swcc and shear stress of unsaturated soils are significantly affected by net confining stress shown in experiment results, Lee et al. (2005) proposed a modified prediction equation of unsaturated shear stress based on the model proposed by Fredlund et al. (1995), in which the influence of net confining stress on suction was taken into considered, hence, a linear term about net confining stress was incorporated in the proposed model. The proposed model (Lee et al., 2005) is written as

$$\begin{aligned} &\tau = c' + (\sigma - u_a)tan\phi + stan\phi && s < s_{AEV} \\ &\tau = c' + [(\sigma - u_a) + s_{AEV}]tan\phi + (s - s_{AEV})\left(\frac{\theta_w - \theta_r}{\theta_s - \theta_r}\right)^{\kappa}[1 + \lambda(\sigma - u_a)]tan\phi && s \geq s_{AEV} \end{aligned} \tag{2.43}$$

where λ is the fitting parameter; κ is a soil parameter dependent upon the soil type, which could be obtained through regression analysis using strength test results at zero net confining stress. Lee et al. (2005) concluded that the proposed model could effectively predict shear stress of weathered granite under various conditions without performing additional unsaturated triaxial tests.

According to the indication that shear stress of unsaturated soils involve two independent stress state variables of net stress ($\sigma - u_a$) and suction ($u_a - u_w$) (e.g., Fredlund et al., 1978), Guan et al. (2010) proposed a prediction equation for shear stress of unsaturated soils by considering hysteresis, which is written as

$$\begin{aligned} &\tau = c' + (\sigma - u_a)tan\phi + stan\phi && s < s_{AEV} \\ &\tau = c' + [(\sigma - u_a) + s_{AEV}]tan\phi + (s - s_{AEV})b(\frac{\theta_w - \theta_r}{\theta_s - \theta_r})^{\kappa}tan\phi && s \geq s_{AEV} \end{aligned} \tag{2.44}$$

$$\kappa = [\log(s) - \log(s_{AEV})]^{y}$$

where y and b are constant controlling parameters.

For the drying path that the soil specimen loses water, y and b in equation (2.44) are given as below

$$y = y_d = 0.502\ln(I_p + 2.7) - 0.387$$
$$b = b_d = -0.245\{\ln[n_d(I_p + 2.7)]\}^2 + 2.114\{\ln[n_d(I_p + 4.4)]\} - 3.522 \quad (2.45)$$

where I_p is plasticity index; n_d is soil parameter n of the main drying SWCC curve proposed by Fredlund and Xing (1994).

For the wetting path that the soil specimen soaks water, y and b in equation (2.44) are given as below

$$y = y_w = 3.55y_d - 3.00$$
$$b = b_w = 0.542b_d\frac{n_d}{n_w} + 0.389 \quad (2.46)$$

where n_w is soil parameter n of the main wetting SWCC curve proposed by Fredlund and Xing (1994).

The prediction equation of shear stress of unsaturated soils (Guan et al., 2010) can exhibit two boundaries of shear stress in the space of net normal stress, suction and shear stress, for an unsaturated soil specimen with any degree of saturation S_r, the surface of shear stress in the space should not beyond the boundaries evaluated by equation (2.44).

2.4 Summary

Many studies already have been conducted to explore the mechanism of shallow tunnel excavation in fully-dried ground through trapdoor test. The distribution of earth pressure across a trapdoor and stress redistribution around the trapdoor, failure mechanism and surface settlement profile were investigated by 2D or 3D trapdoor test in model ground or sand ground under. Furthermore, some researchers proposed new theoretical approaches to estimate average loosening earth pressure for 2D and 3D trapdoor test. Other researchers developed new theories based on Terzaghi's theory to evaluate loosening earth pressure by modifying lateral earth pressure coefficient. Most of trapdoor test were carried out in ground with fully-dried state so as the Terzaghi's theory or other theoretical solution could be applied to predict loosening earth pressure and compare theoretical result with that obtained from experiment. However, the ground in reality is usually in unsaturated state, the studies on shallow tunnel excavation in unsaturated ground are hardly to be found. Although numerical solution is a good way to explore complex research circumstance, an appropriate soil model of unsaturated soils is needed and many parameters of unsaturated soils should be determined, so there is no numerical research on trapdoor test in unsaturated ground.

Therefore, the mechanism of shallow tunnel excavation in unsaturated ground was explored in this study, for which behavior of unsaturated soils was reviewed. Soil water characteristic curve predicted by van Genuchten (1980), Bishop's effective stress for unsaturated soils (1959) and shear stress of unsaturated soils evaluated by Bishop and Blight (1963) were adopted to evaluate loosening earth pressure in this study.

Overall, the novelties of the thesis were summarized as following.

- For shallow tunnel excavation in unsaturated ground, series of trapdoor test in unsaturated ground were carried out to explore soil mechanics, failure mechanism and surface settlement. And effect of the depth of groundwater level on loosening earth pressure was also investigated.
- A rational model was proposed to evaluate loosening earth pressure on the crown of a tunnel in unsaturated ground. Effect of depth of groundwater level and soil types on loosening earth pressure, and scale effect in saturated and unsaturated ground were investigated. Furthermore, the consistency of experimental loosening earth pressure and that predicted by the proposed theory was also investigated.
- Theories was proposed to predict distribution of loosening earth pressure and stress redistribution based on the proposed theory.
- The changing in loosening earth pressure due to the raise of groundwater level was investigated to explore tunnel stability.

CHAPTER 3 TRAPDOOR TEST IN SATURATED AND UNSATURATED GROUND

Trapdoor test developed by Terzaghi (1936) is a useful tool to investigate tunnel excavation. Many studies for trapdoor test in fully-dried ground (e.g., Evans, 1984; Tanaka and Sakai, 1987; Sadrekarimi and Abbasnejad, 2010) or model ground with aluminum bar (e.g., Park and Adachi, 2002; Kikumoto, 2014; Bhandari and Han, 2018) had been carried out to explore soil mechanics, failure mechanism and surface settlement. However, the studies on trapdoor test in saturated and unsaturated ground (e.g., Song at al., 2018) are hardly to be found. In this chapter, trapdoor test in saturated and unsaturated ground was carried out to investigate the distribution of earth pressure, evolution of shear bands and surface settlement profile. Furthermore, the effect of depth of groundwater level on total and effective loosening pressures were also investigated.

3.1 Apparatus, test patterns and test process

To carry out trapdoor test in saturated and unsaturated ground, a new apparatus should be appropriately designed and constructed, because water inflow or outflow from the ground and changing in width of trapdoor should be considered. According to the objectives of trapdoor test in saturated and unsaturated ground, test patterns and test process should be carefully designed.

3.1.1 Apparatus

The new apparatus for trapdoor test in saturated and unsaturated ground was shown in Fig. 3.1, the size of soil chamber is 80.5 cm × 30.5 cm × 60.0 cm, so the bottom area A of soil chamber was 2455.3 cm^2. To generate unsaturated ground, water was slowly drained out from saturated ground to lower the groundwater level. Hence, a perforated acrylic plate with strainer was to separate water tank and soil chamber as shown as Fig. 3.1 (a), so water not only could be flowed in soil chamber through the bottom of soil chamber, but also could be flowed in through the perforated acrylic plate, however, sand could not pass through the strainer into the two water tanks. At the bottom of soil chamber, there were five independent metal boxes (a, b, c, d, e), which could be controlled to be fixed or moved by the clamps. Therefore, the width of trapdoor could be adjusted. As trapdoor test was carried out in saturated and unsaturated ground, so each metal box was covered with a membrane to prevent water flowing into it to protect load cells inside it, as shown as in Fig. 3.1 (c).

To measure surface settlement of trapdoor test, the device shown in Fig. 3.1 (a) was put on a pair of independent beams above the apparatus, so the surface settlement measurement would not affect earth pressure given by load cells. The device included a fixed laser displacement scanner X and a moveable laser displacement scanner Y scanning the ground surface to obtain surface settlement profile (Kikumoto, 2004; Adachi et al., 2003). To investigate the evolution of shear bands during trapdoor test by PIV, a camera was fixed in front of the acrylic wall to take a series of photographs based on the displacement of trapdoor, as shown as in Fig. 3.1 (b).

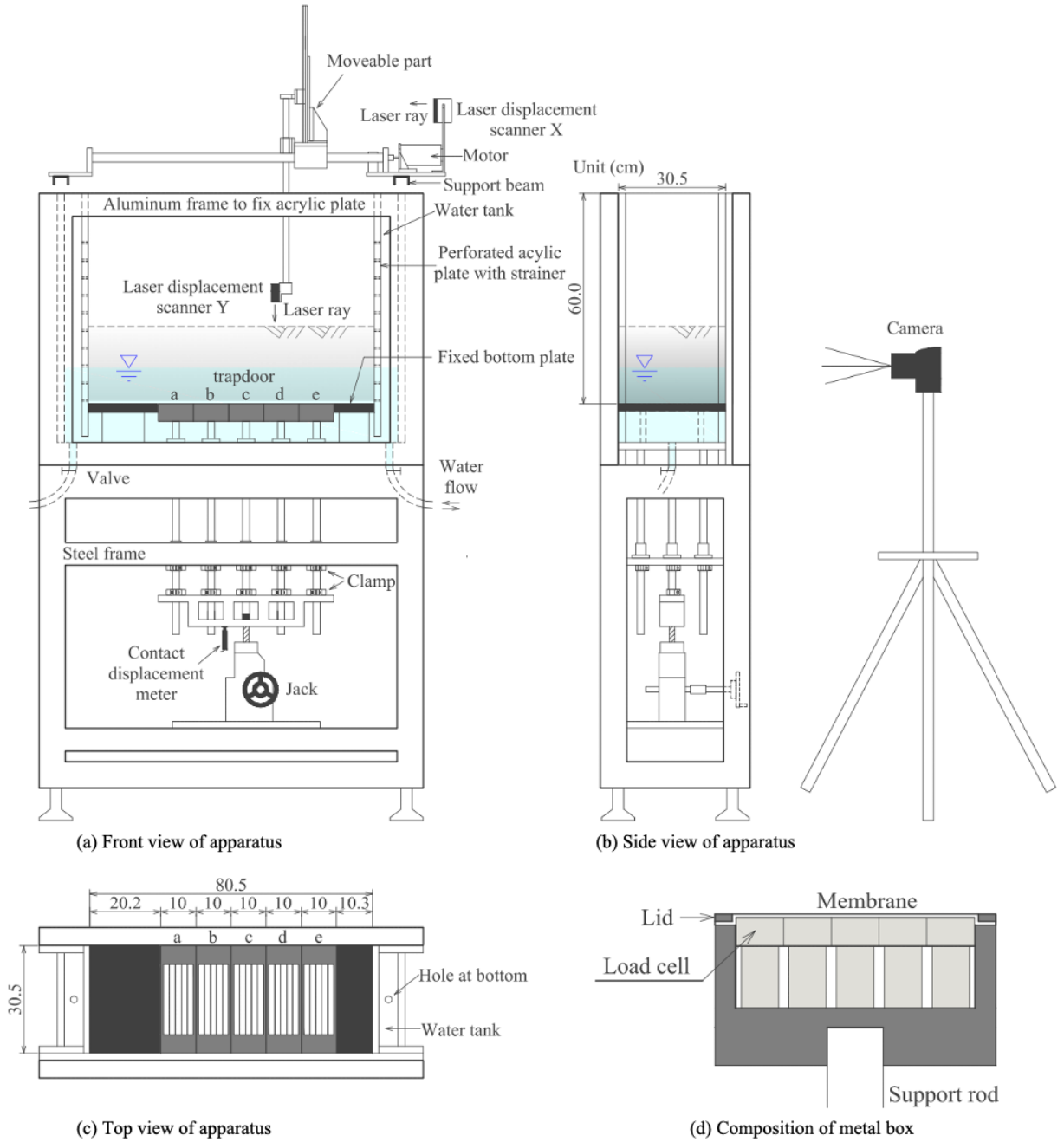

Fig. 3.1 Schematic diagram of (a) front view of apparatus; (b) side view of soil chamber; (c) top view of apparatus; (d) the composition of single metal box .

3.1.2 Test patterns

As shallow tunnel excavation was considered in this study, overburden ratio was no larger than 2 (e.g., McNulty, 1965; Evans, 1984; Koutsabeloulis and Griffiths, 1989; Sloan, 1990; Kikumoto and Kishida, 2003; Dewoolkar et. al., 2007). The height of soil chamber was 60 cm, so the width of trapdoor could be 10 cm and 20 cm. As we known, there was no scale effect for trapdoor test in dry ground (e.g., Evans, 1984, Tanaka and Sakai, 1993),

therefore, to investigate scale effect in saturated ground, trapdoor test under the same overburden ratio H/D with different width of trapdoor D were carried out to check the normalized loosening earth pressure by initial pressure. For the scale effect in unsaturated ground, trapdoor test under the same overburden ratio H/D and ratio of depth of groundwater level to overburden height of H_w/H with different width of trapdoor D was carried out to check the normalized loosening earth pressure by initial pressure of saturated ground.

Furthermore, the effect of the depth of groundwater level on total and effective loosening earth pressure were also investigated, so trapdoor test under the same overburden ratio H/D and width of trapdoor D but different depth of groundwater level H_w was also carried out to explore the changing in loosening earth pressure. Moreover, as the repeatability of experiment was extremely important, most circumstances of trapdoor test were conducted for three times. Based on the above discussion, test patterns were summarized as shown in Table 3-1.

Table 3-1 Test patterns for trapdoor test in saturated and unsaturated ground.

Schematic diagram	State of ground	D (cm)	H/D	H_w/H
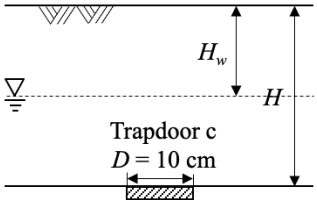	Saturated	10	1.0, 1.5, 2.0	0.00
	Unsaturated		1.0	0.50, 1.00
			1.5	0.50, 1.00
			2.0	0.25, 0.50, 1.00
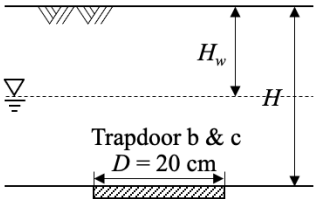	Saturated	20	0.5, 1.0, 2.0	0.00
	Unsaturated		0.5	1.00
			1.0	0.50, 1.00
			2.0	0.25, 0.50, 0.75, 1.00

3.1.3 Test process

In this study, the experiment material for trapdoor test was Toyoura sand (soil particle density $\rho_s = 2.65\ g/cm^3$). The process of trapdoor test in saturated and unsaturated ground:

- Teflon was sprayed on the front and back acrylic wall of soil chamber to reduce the friction between ground and wall. Then load cells were calibrated with water to get the coefficients of load cells, the calibration process and the coefficient of one load cell was shown in Fig. 3.2,
- Water was poured into soil chamber until the height of water head from the bottom of soil chamber being 15 cm. A suction sensor was placed at the bottom of soil chamber. Toyoura sand was deposited in soil chamber through a sieve until overburden height being H, during which the distance of water head to ground surface should be around 15 cm, so that the dry density of ground would be uniformity, especially for large

overburden height (e.g., H = 40 cm), meanwhile, a suction sensor was placement on ground surface as overburden height increased every 10 cm,

- Water head was slowly decreased to the position close to ground surface, and then ground surface was made flat. After that, to complete the generation of saturated ground, water head should be continued to decrease to the position of one more centimeter lower than ground surface, so water would not affect the measurement of the laser displacement scanner. To make unsaturated ground, water head was continued to be decrease to the corresponding depth of groundwater level H_w of unsaturated test case. Then the two valves were closed. Initial pressure was recorded,
- The device for surface settlement measurement was put on a pair of independent beams above apparatus. The laser displacement scanner Y shown in Fig. 3.1 (d) was moved from right to left to scan ground surface. A camera was fixed in front of apparatus, as shown in Fig. 3.1 (e). And a photograph was taken with the remote of camera,
- Trapdoor was lowered, earth pressure for each displacement of trapdoor δ was recorded, the setting displacement of trapdoor was shown in Table 3-2. At the same time, the data of surface settlement was recorded, a series of photographs were obtained,
- The two valves were opened, the water drained out from ground was gathered and weighted. And the wet sand was also taken out and weighted.

Herein, the dry density of saturated and unsaturated should be determined. Based on the total mass of water and wet sand M for saturated ground, total initial pressure σ_{z0} ($\sigma_{z0} = Mg/A$) could be calculated, so that the saturated density ρ_{sat} ($\rho_{sat} = M/AH$) could be obtained. Then dry density ρ_d ($\rho_d = \rho_s(\rho_{sat} - \rho_w)/(\rho_s - \rho_w)$) of saturated ground could be obtained, the dry density of unsaturated ground should be equal to that of saturated ground because the ground of saturated and unsaturated was made by the same way. In this study, the dry density of saturated and unsaturated ground was 1.57 g/cm^3.

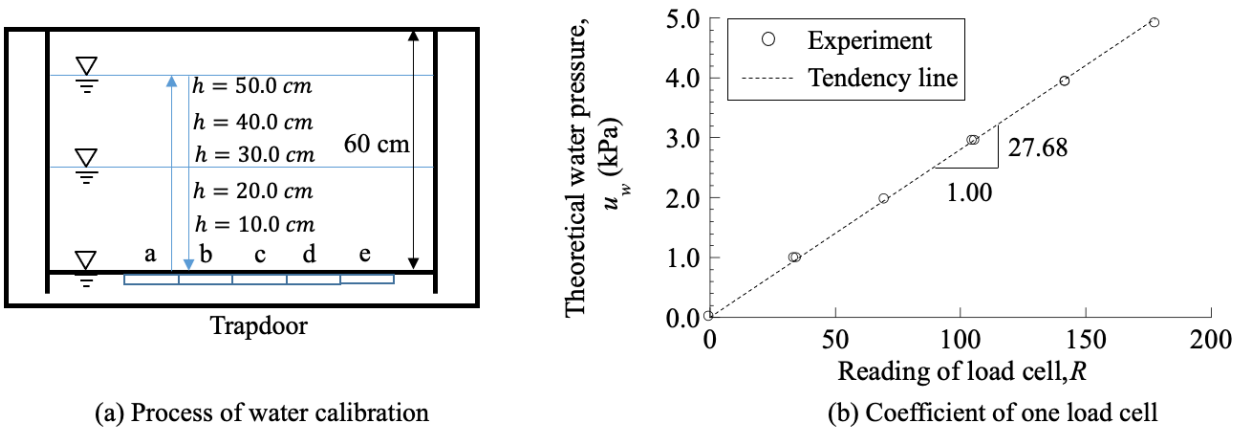

(a) Process of water calibration (b) Coefficient of one load cell

Fig. 3.2 Water calibration for the load cells (a) the calibration process; (b) coefficient of one load cell.

Table 3-2 The setting displacement of trapdoor.

Step No.	1	2	3	4	5	6	7	8	9
Displacement, δ (mm)	0.00	0.05	0.10	0.20	0.30	0.40	0.50	0.75	1.00

Step No.	10	11	12	13	14	15	16	17
Displacement, δ (mm)	1.25	1.50	1.75	2.00	2.50	3.00	4.00	5.00

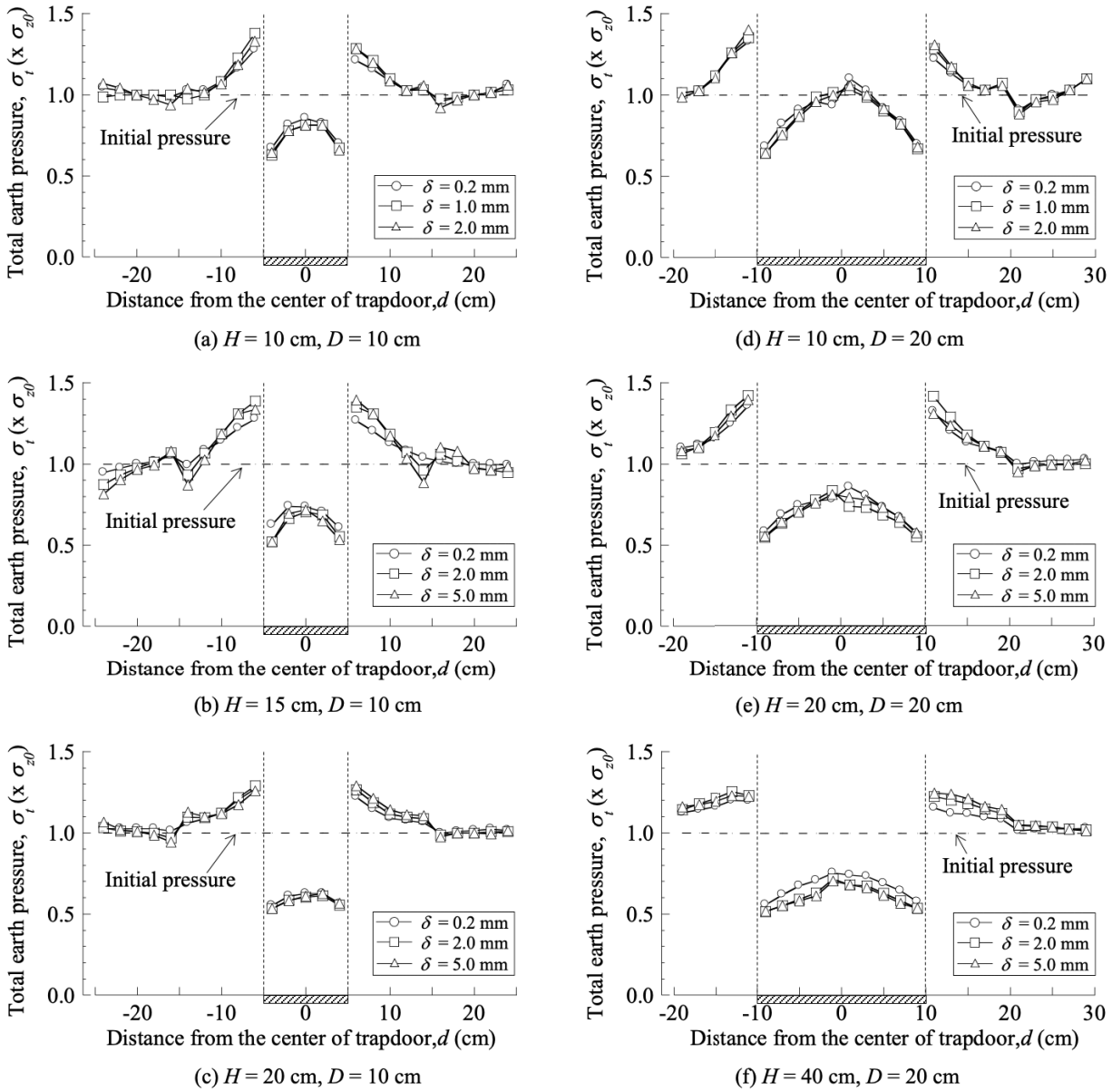

Fig. 3.3 Distribution of earth pressure for trapdoor test in saturated ground (a) H/D = 1.0, D = 10 cm, H_w = 0 cm; (b) H/D = 1.5, D = 10 cm, H_w = 0 cm; (c) H/D = 2.0, D = 20 cm, H_w = 0 cm; (d) H/D = 0.5, D = 20 cm, H_w = 0 cm; (e) H/D = 1.0, D = 20 cm, H_w = 0 cm; (f) H/D = 2.0, D = 20 cm, H_w = 0 cm.

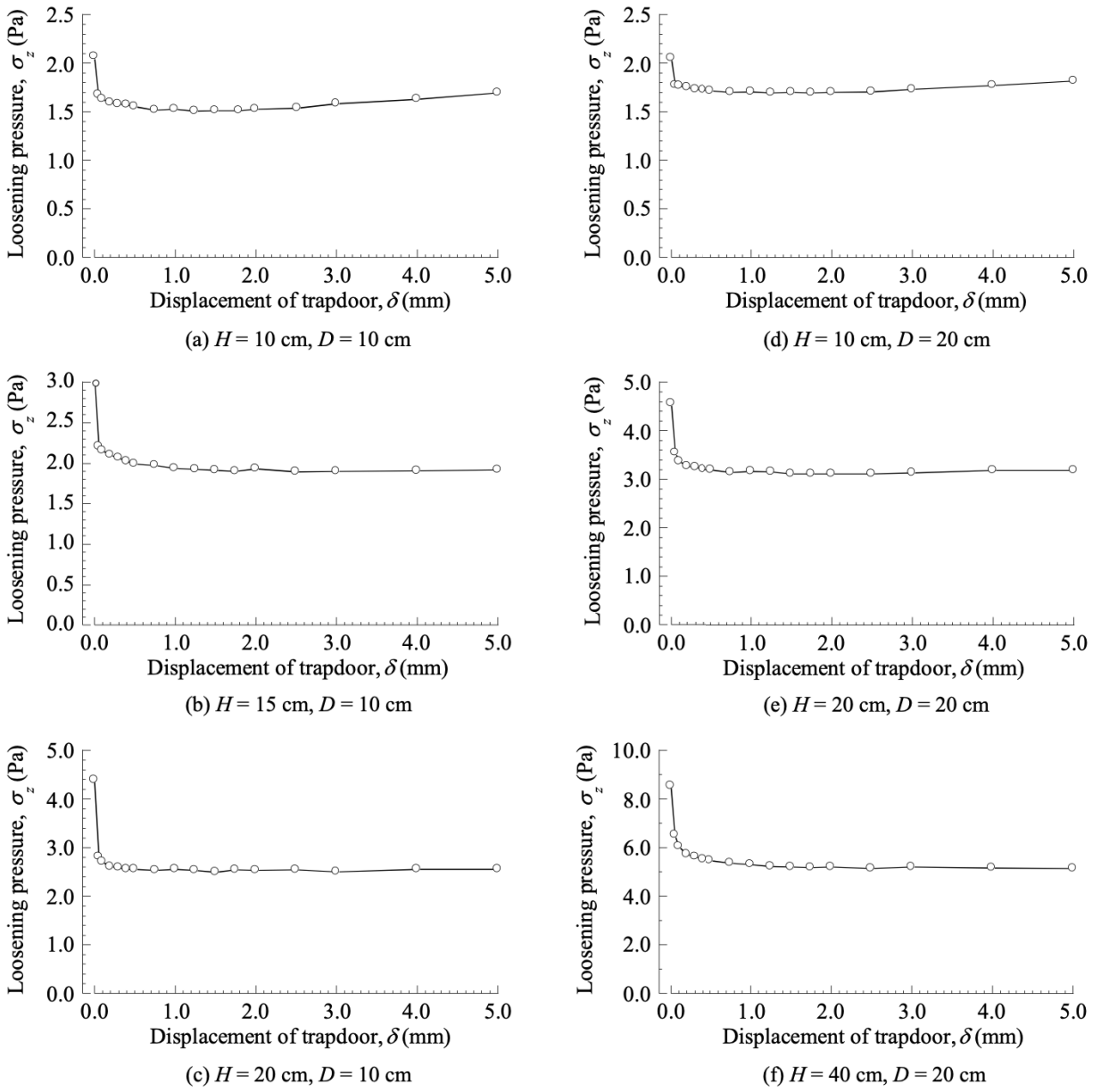

Fig. 3.4 The variation of loosening pressure with the displacement of trapdoor in saturated ground (a) H/D = 1.0, D = 10 cm, H_w = 0 cm; (b) H/D = 1.5, D = 10 cm, H_w = 0 cm; (c) H/D = 2.0, D = 20 cm, H_w = 0 cm; (d) H/D = 0.5, D = 20 cm, H_w = 0 cm; (e) H/D = 1.0, D = 20 cm, H_w = 0 cm; (f) H/D = 2.0, D = 20 cm, H_w = 0 cm.

3.2 Distribution of earth pressure in saturated and unsaturated ground

Herein, the distribution of loosening earth pressure acting on a trapdoor and stress redistribution around the trapdoor would be explored for trapdoor test in saturated and unsaturated ground. Then the evolution of loosening earth pressure acting on a trapdoor with the displacement of trapdoor and the profile of pore water pressure were also investigated.

3.2.1 Distribution of earth pressure in saturated ground

A series of trapdoor tests in saturated ground were conducted with overburden ratio *H*/*D* of 0.5, 1.0, 1.5, 2.0 as shown in Table 3-1. The distribution of loosening earth pressure acting on trapdoor and stress redistribution around the trapdoor was shown in Fig. 3.3. We could see that the shape of loosening earth pressure in saturated ground was symmetric, and its magnitude was less than initial pressure σ_{z0} observed by load cells. However, loosening earth pressure at the center of trapdoor was larger than initial pressure as overburden ratio was 0.5 and width of trapdoor was 20 cm, the reason was that the trapdoor b and trapdoor c had slight relative displacement. At stationary zone, the earth pressure was larger than initial pressure, and gradually decreased to initial pressure. Meanwhile, the average total loosening earth pressure with the displacement of trapdoor was shown in Fig. 3.4. It was shown that total loosening earth pressure rapidly decreased to a minimum value and kept constant as overburden height was larger than 10 cm. Therefore, as the displacement of trapdoor was 0.2, 2.0, 5.0 mm respectively, the earth pressure observed by load cells was chosen to explore the distribution of earth pressure. As overburden height was no larger than 10 cm, total loosening pressure rapidly decreased to a minimum value, then it gradually increased. In this case, as the displacement of trapdoor was 0.2, 1.0, 2.0 mm respectively, the corresponding earth pressure observed by the load cells was chosen to explore the distribution of earth pressure.

3.2.2 Distribution of earth pressure in unsaturated ground

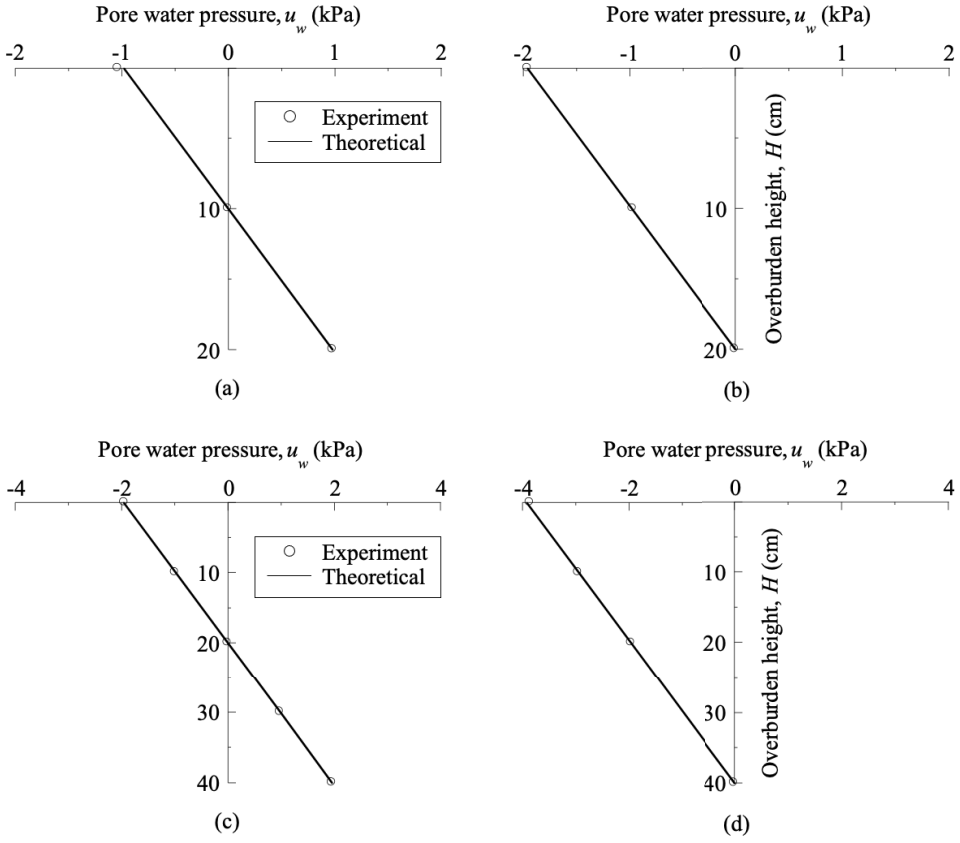

Fig. 3.5 Suction profiles in unsaturated ground (a) *H*/*D* = 2.0, *D* = 10 cm, H_w = 10 cm; (b) *H*/*D* = 2.0, *D* = 10 cm, H_w = 20 cm; (c) *H*/*D* = 2.0, *D* = 20 cm, H_w = 20 cm; (d) *H*/*D* = 2.0, *D* = 20 cm, H_w = 40 cm.

Trapdoor tests in unsaturated ground were conducted under the same overburden ratio H/D (H/D = 1.0, 2.0) and width of trapdoor D (D = 10, 20 cm) with different depth of groundwater level H_w. Since ground was in unsaturated state, the crucial point was suction profile. Therefore, pore water pressure was measured by transducer in trapdoor test, then suction could be estimated by its definition ($s = u_a - u_w$), in which pore air pressure was assumed to be zero because the density of air was negligible (Pufahl et al., 1983, Vahedifard et al., 2016, Sahoo et al., 2018). The pore water pressure profiles were shown in Fig. 3.5, it was shown that pore water pressure profile was linear, and it could be also evaluated theoretically ($u_w = \rho_w g(z - H_w)$).

The distribution of earth pressure was shown in Fig. 3.6 ~ 3.9. We can see that loosening earth pressure in unsaturated ground was also symmetric, and it was significant less than initial pressure observed by load cells. At stationary zone, when overburden height was no larger than 10 cm, the earth pressure was larger than initial pressure, and it gradually decreased to initial pressure. As overburden height was larger than 10 cm, the earth pressure was no less than initial pressure, and it increased firstly, then it started to decrease. The probable reason was that the friction between ground and wall was too large compared with that in saturated ground, and the larger confining pressure due to larger suction may cause the larger friction. The average total loosening pressure with the displacement of trapdoor was shown in Fig. 3.10. Similarly, loosening earth pressure rapidly decreased to a minimum value, and it kept constant as overburden height was larger than 10 cm, otherwise, it had the tendency of increasement.

Similarly, as overburden height was no larger than 10 cm, the corresponding earth pressure of displacement of trapdoor of 0.2, 1.0, 2.0 mm were chosen to explore the distribution of earth pressure. As overburden height was larger than 10 cm, the corresponding earth pressure of displacement of trapdoor of 0.2, 2.0, 5.0 mm were chosen to explore the distribution of earth pressure.

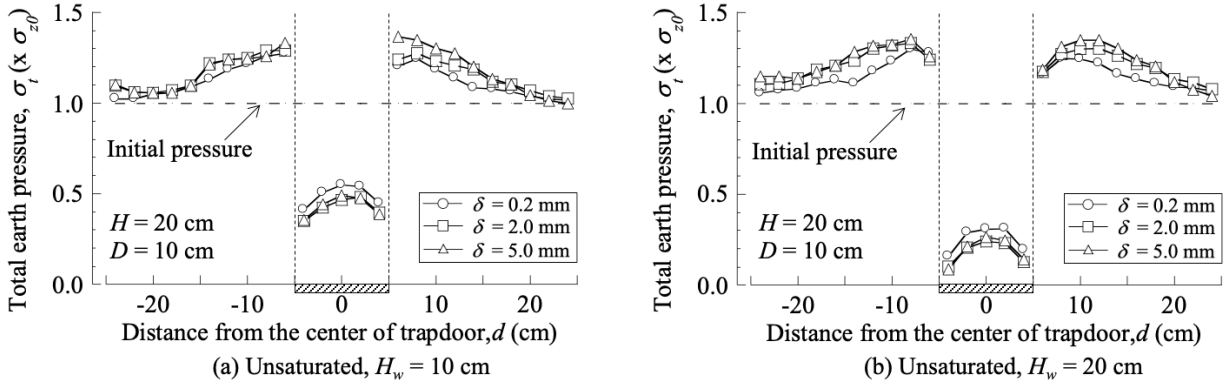

Fig. 3.6 Distribution of earth pressure for trapdoor test in unsaturated ground (a) H/D = 2.0, D = 10 cm, H_w = 10 cm; (b) H/D = 2.0, D = 10 cm, H_w = 20 cm.

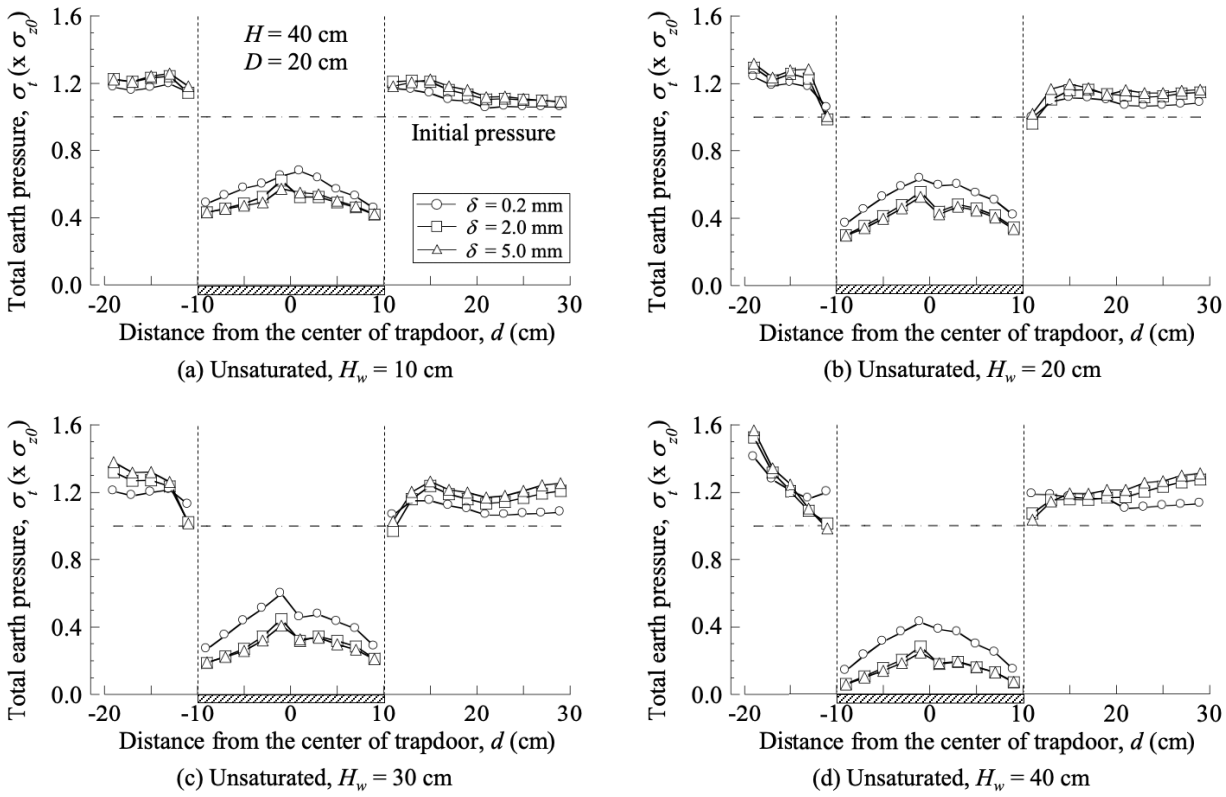

Fig. 3.7 Distribution of earth pressure for trapdoor test in unsaturated ground (a) H/D = 2.0, D = 20 cm, H_w = 10 cm; (b) H/D = 2.0, D = 20 cm, H_w = 20 cm; (c) H/D = 2.0, D = 20 cm, H_w = 30 cm; (d) H/D = 2.0, D = 20 cm, H_w = 40 cm.

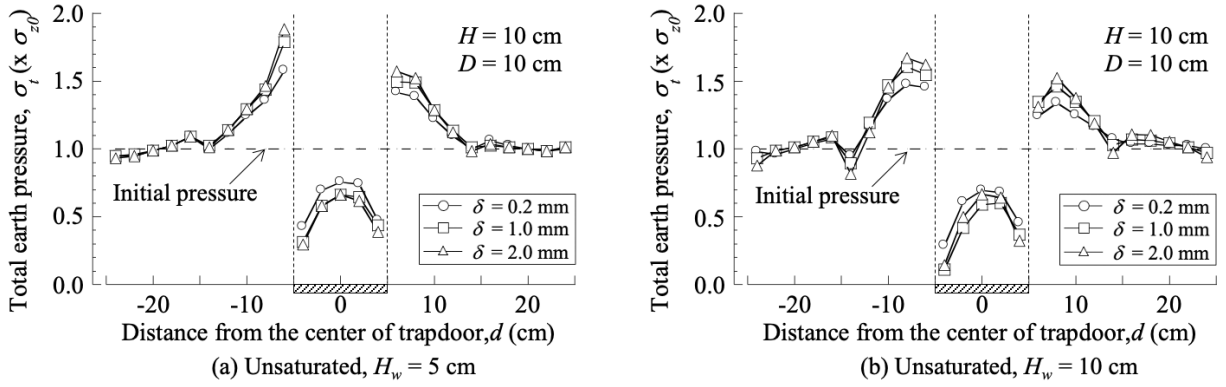

Fig. 3.8 Distribution of earth pressure for trapdoor test in unsaturated ground (a) H/D = 1.0, D = 10 cm, H_w = 5 cm; (b) H/D = 1.0, D = 10 cm, H_w = 10 cm.

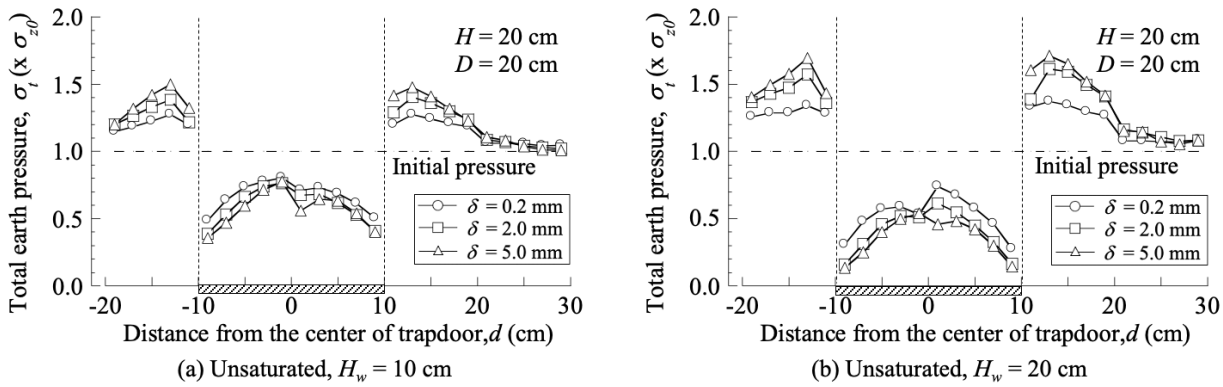

Fig. 3.9 Distribution of earth pressure for trapdoor test in unsaturated ground (a) H/D = 1.0, D = 20 cm, H_w = 10 cm; (b) H/D = 1.0, D = 20 cm, H_w = 20 cm.

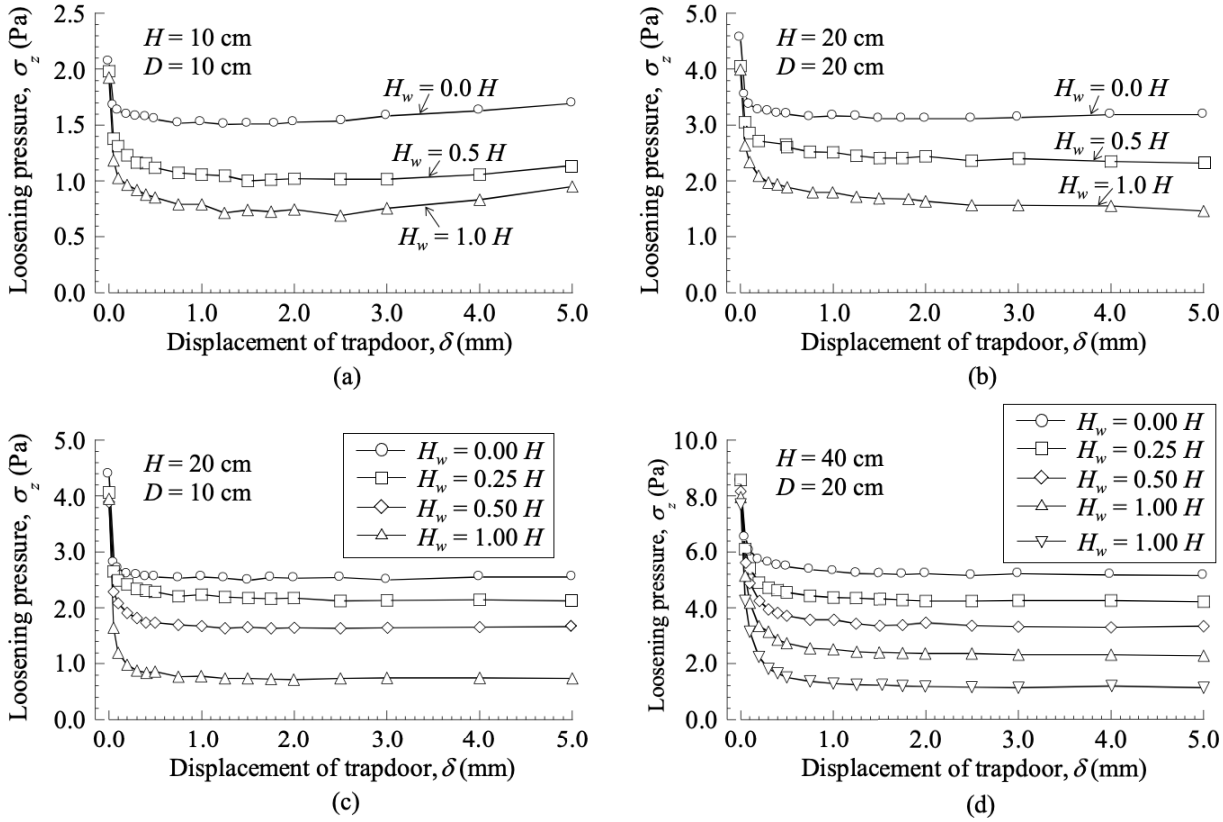

Fig. 3.10 The variation of loosening pressure with the displacement of trapdoor in unsaturated ground (a) H/D = 1.0, D = 10 cm, H_w = 0.0, 0.5, 1.0 H; (b) H/D = 1.0, D = 20 cm, H_w = 0.0, 0.5, 1.0 H; (c) H/D = 2.0, D = 10 cm, H_w = 0.00, 0.25, 0.50, 1.00 H; (d) H/D = 2.0, D = 20 cm, H_w = 0.00, 0.25, 0.50, 0.75, 1.00 H.

3.2.3 Summary

In this section, the linear profiles of pore water pressure in unsaturated ground were measured and observed, according to the definition of suction, the linear suction profiles could be evaluated. Furthermore, the distribution of loosening earth pressure acting on a trapdoor and stress redistribution around the trapdoor in saturated and unsaturated ground were explored, And the changing in loosening earth pressure with displacement of trapdoor was investigated.

Loosening earth pressure after trapdoor being lowered was significant less than initial pressure due to soil arching effect, and it gradually decreased from the center to the end of trapdoor. At stationary zone, earth pressure at the end of trapdoor was larger than initial pressure, and then gradually decreased to initial pressure as the position was far from the end of trapdoor. Total loosening pressure rapidly decreased as the displacement of trapdoor was less than 1.0 mm, then it was almost constant as overburden height was larger than 10 cm. contrarily, total loosening earth pressure started to increase as the displacement of trapdoor was larger than 2.0 mm.

3.3 Shear bands

Previous studies for shear bands were revealed that overburden ratio, stress level, soil particle size, dilatancy behavior and so on affected shear bands formation in dry ground (e.g., Stone and Wood, 1992; Dewoolkar et al., 2007). However, the failure mechanism of trapdoor test in saturated and unsaturated ground was still unknown. Hence, the shear bands and its evolution with displacement of trapdoor δ in saturated and unsaturated ground were discussed in this section.

3.3.1 Shear bands in saturated ground

For shear bands in saturated ground, the effect of overburden ratio H/D on it was investigated. Hence, shear bands under different overburden ratio of 1.0, 1.5, 2.0 with the same width of trapdoor D of 10 cm were shown in Fig. 3.11. And shear bands under different overburden ratio of 0.5, 1.0, 2.0 with the same width of trapdoor of 20 cm were shown in Fig. 3.12. It was revealed that shear bands were affected by overburden ratio. Shear bands were more oblique as overburden ratio was larger, and multiple shear bands were observed as overburden ratio was larger than 1.0. As overburden ratio was no larger than 1.0, only one shear bands were observed, and it was not vertical.

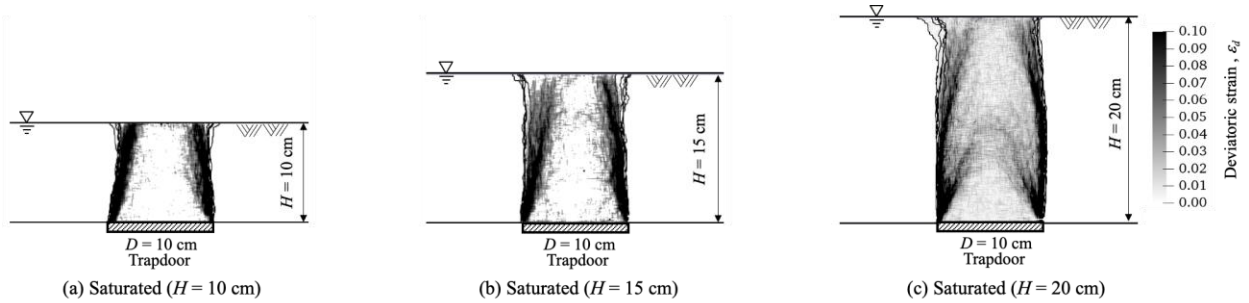

(a) Saturated (H = 10 cm) (b) Saturated (H = 15 cm) (c) Saturated (H = 20 cm)

Fig. 3.11 Shear bands with different overburden ratio for trapdoor test in saturated ground (a) H/D = 1.0, D = 10 cm, H_w = 0 cm; (b) H/D = 1.5, D = 10 cm, H_w = 0 cm; (c) H/D = 2.0, D = 10 cm, H_w = 0 cm.

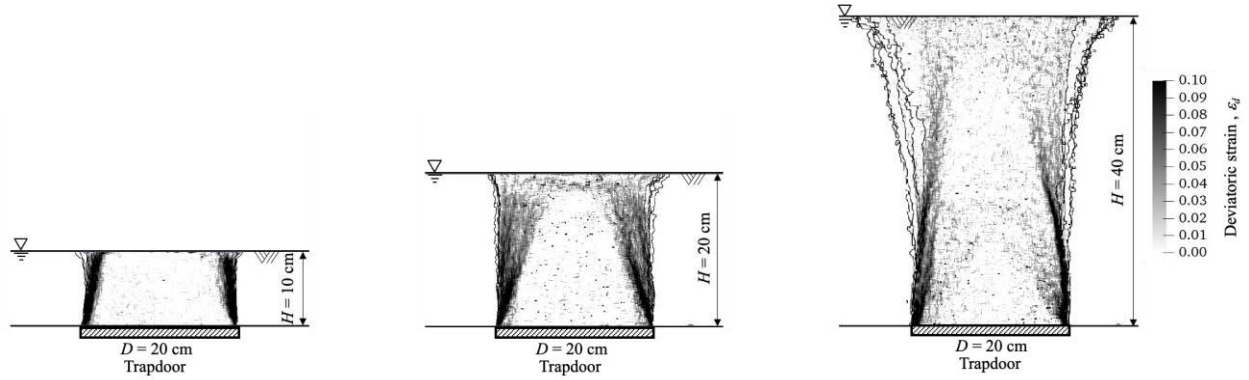

(a) Saturated (H = 10 cm) (b) Saturated (H = 20 cm) (c) Saturated (H = 40 cm)

Fig. 3.12 Shear bands with different overburden ratio for trapdoor test in saturated ground (a) H/D = 0.5, D = 20 cm, H_w = 0 cm; (b) H/D = 1.0, D = 20 cm, H_w = 0 cm; (c) H/D = 2.0, D = 20 cm, H_w = 0 cm.

3.3.2 Shear bands in unsaturated ground

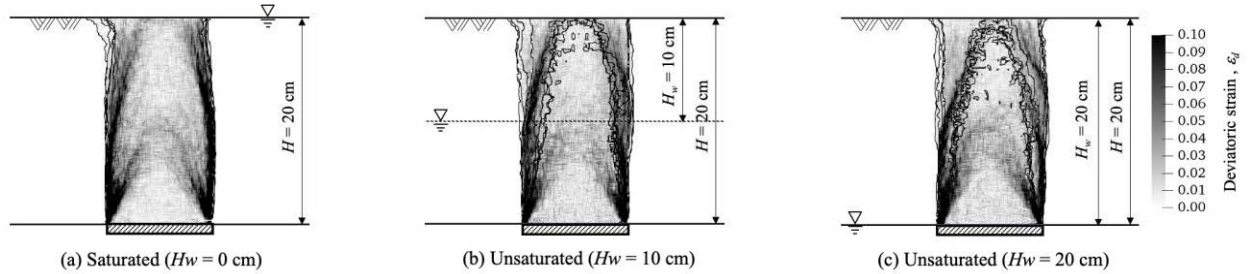

(a) Saturated (Hw = 0 cm) (b) Unsaturated (Hw = 10 cm) (c) Unsaturated (Hw = 20 cm)

Fig. 3.13 Shear bands with different depth of groundwater level for trapdoor test in unsaturated ground (a) H/D = 2.0, D = 10 cm, H_w = 0 cm; (b) H/D = 2.0, D = 10 cm, H_w = 10 cm; (c) H/D = 2.0, D = 10 cm, H_w = 20 cm.

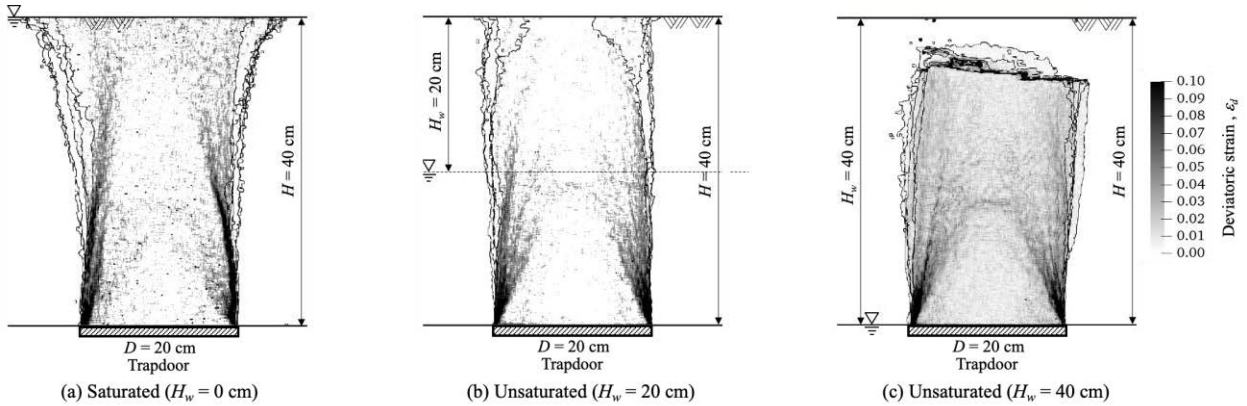

Fig. 3.14 Shear bands with different depth of groundwater level for trapdoor test in unsaturated ground (a) H/D = 2.0, D = 20 cm, H_w = 0 cm; (b) H/D = 2.0, D = 20 cm, H_w = 20 cm; (c) H/D = 2.0, D = 20 cm, H_w = 40 cm.

For shear bands in unsaturated ground, we intended to investigate the effect of the depth of groundwater level H_w on it as overburden ratio H/D and width of trapdoor D were identical, which was shown in Fig. 3.13 and 3.14. It was shown that multiple shear bands were observed. As shown in Fig. 3.13, it was revealed that the open of intermediate shear bands was smaller when the depth of groundwater level was deeper. However, a crack was observed as overburden height was 40 cm and the depth of groundwater level was 40 cm, as shown in Fig. 3.14. This was because confining pressure and shear stress were larger due to larger suction as the depth of groundwater level was deeper, hence, the shear strength near ground surface was significant close to the weight of soil, the soil above the crack was hardly to move downwards compared with soil below the crack. Therefore, shear bands in unsaturated ground could be significantly affected by suction, the open of shear bands became smaller as suction was larger due to the depth of groundwater level. And the crack near ground surface would be emerged as suction was larger enough so that shear strength was close to the weight of soil.

3.3.3 Evolution of shear band with displacement of trapdoor

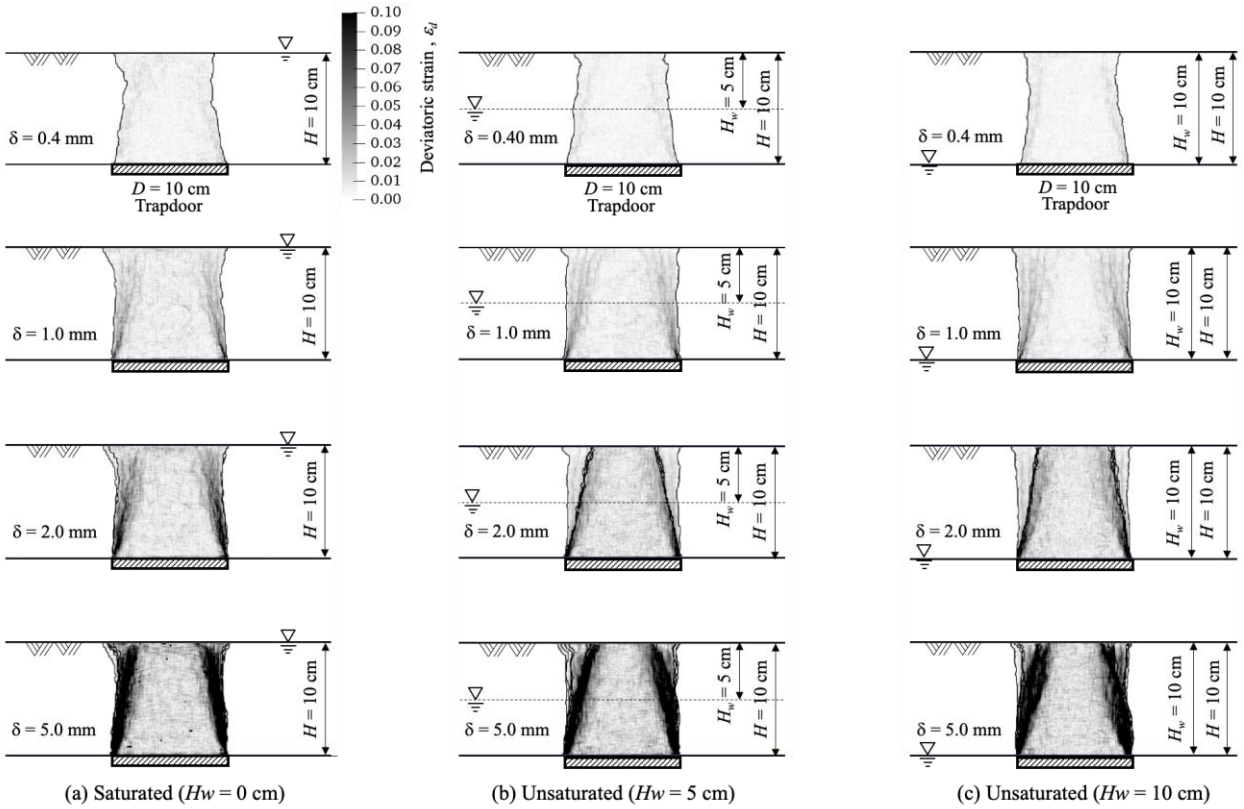

Fig. 3.15 Evolution of shear bands with displacement of trapdoor in (a) saturated ground (D = 10 cm, H/D = 1.0, H_w = 0 cm); (a) saturated ground (D = 10 cm, H/D = 1.0, H_w = 5 cm); (a) saturated ground (D = 10 cm, H/D = 1.0, H_w = 10 cm).

Previous discussion was shown multiple shear bands were emerged for trapdoor test in saturated and unsaturated ground. Herein, the evolution of shear bands with displacement of trapdoor δ would be investigated. For the evolution of shear bands shown in Fig. 3.15, overburden ratio H/D was 1.0 and width of trapdoor D was 10 cm, the depth of groundwater level Hw was 0, 5, 10 cm respectively. It was shown that the formation of the first shear bands was ceased as the displacement of trapdoor was 1.0 mm, and the shape of shear bands was similar as the displacement of trapdoor was less than 1.0 mm even if the depth of groundwater level was different. The second shear bands were observed as the displacement of trapdoor was larger than 1.0 mm. And the open of the second shear bands with the same displacement of trapdoor (δ = 2.0, 5.0 mm) was smaller as the depth of groundwater level was deeper.

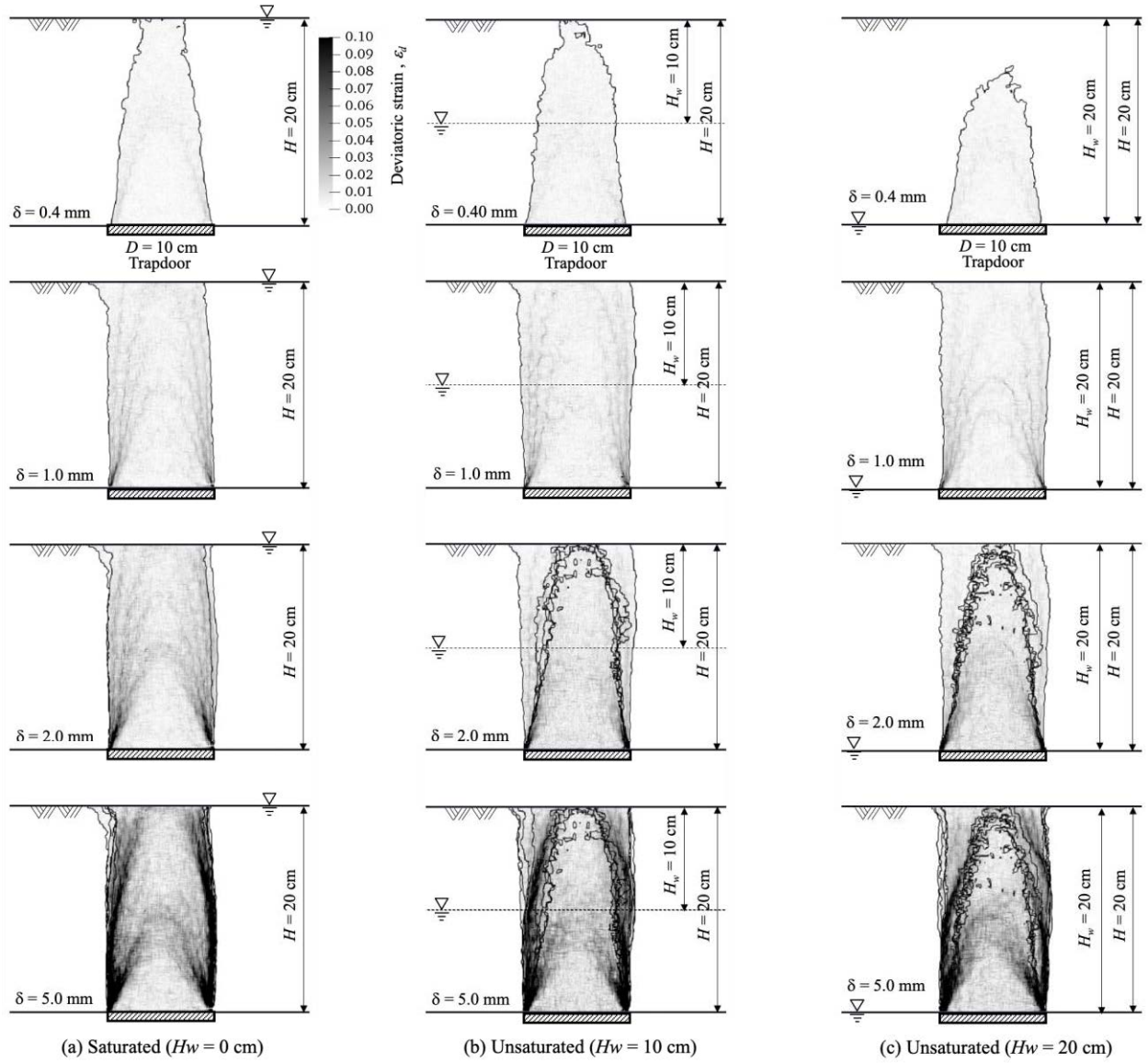

Fig. 3.16 Evolution of shear bands with displacement of trapdoor in (a) saturated ground (D = 10 cm, H/D = 2.0, H_w = 0 cm); (b) unsaturated ground (D = 10 cm, H/D = 2.0, H_w = 10 cm); (c) unsaturated ground (D = 10 cm, H/D = 2.0, H_w = 20 cm).

When overburden ratio was 2.0 and width of trapdoor was 10 cm, the depth of groundwater level was 0, 10, 20 cm respectively, the evolution of shear bands was shown in Fig. 3.16. It was revealed that the open of the first shear bands was smaller due to the deeper depth of groundwater level as the displacement of trapdoor was 0.4 mm, the whole soil arching was observed as the depth of groundwater level was 20 cm. And the formation of the first shear bands was ceased as the displacement of trapdoor was 1.0 mm. After that, the second shear bands inside the first shear bands started to develop, and it became steady as the displacement of trapdoor was 2.0 mm. It was also revealed that the open of the second shear bands was smaller as the depth of groundwater level was deeper. When the displacement of trapdoor was 5.0 mm, the third shear bands was observed, which was similar in the ground with different depth of groundwater level.

3.3.4 Summary

(1) Shear bands in saturated ground was affected by overburden ratio *H*/*D*, it was more oblique as overburden ratio was larger. And multiple shear bands were observed as overburden ratio was larger than 1.0. When overburden ratio was no larger than 1.0, only one shear bands was emerged, and it was not vertical. This was because confining pressure and shear strength were larger as overburden ratio was larger, which made the shear bands more curvature until the whole soil arching being emerged.
(2) Sher bands in unsaturated ground was significantly affected by the depth of groundwater level *Hw*, the open of shear bands was smaller as the depth of groundwater level was deeper, because larger suction due to the deeper depth of groundwater level caused larger confining pressure and shear stress, so the soil arching effect was more obvious. And crack could be observed as suction was large enough. Meanwhile, multiple shear bands were observed in unsaturated ground, the numbers of shear bands were affected by overburden height.
(3) for the evolution of shear bands with displacement of trapdoor, it was revealed the first shear bands was gradually expanded until the displacement of trapdoor δ of 1.0 mm, then the first shear bands formation was ceased. After that, a new shear bands would be generated inside the previous shear bands sequentially.

3.4 Surface settlement

Herein, we intended to discuss the effect of overburden ratio *H*/*D* on surface settlement of trapdoor test in saturated ground, and the effect of the depth of groundwater level on surface settlement of trapdoor test in unsaturated ground.

3.4.1 Surface settlement of trapdoor test in saturated ground

As shown in Fig. 3.4, the loosening earth pressure for all overburden height (H = 10, 15, 20, 40 cm) was already a minimum value as displacement of trapdoor was 2.0 mm. Therefore, herein the corresponding surface settlement was shown when the displacement of trapdoor was 2.0 mm. The surface settlement profiles of trapdoor tests in saturated ground under different overburden ratio *H*/*D* with the same width of trapdoor *D* were shown in Fig. 3.17 (a-10) and (a-20). We could see that the soil above the trapdoor significantly moved downwards, and the surface settlement profiles was different as overburden ratio was different.
To explore the effect of overburden ratio on surface settlement, the maximum surface settlement S_{max} was defined as shown in Fig. 3.17 (a-10), which was the distance from the current ground surface to its original position. Firstly, the relationship of maximum surface settlement and displacement of trapdoor δ were explored as shown as Fig. 3.17 (b-10) and (b-20). It was revealed that maximum surface settlement was larger as displacement of trapdoor was larger. Meanwhile, the corresponding maximum surface settlement was equal to displacement of trapdoor (d = 1.0, 2.0, 3.0, 4.0, 5.0 mm) as overburden ratio was no larger than 1.0, because shear bands were almost vertical as shown as Fig. 3.11 and 3.12, soil arching effect was weak, the soil above the trapdoor shifted with the displacement of trapdoor. However, the corresponding maximum surface settlement was less than

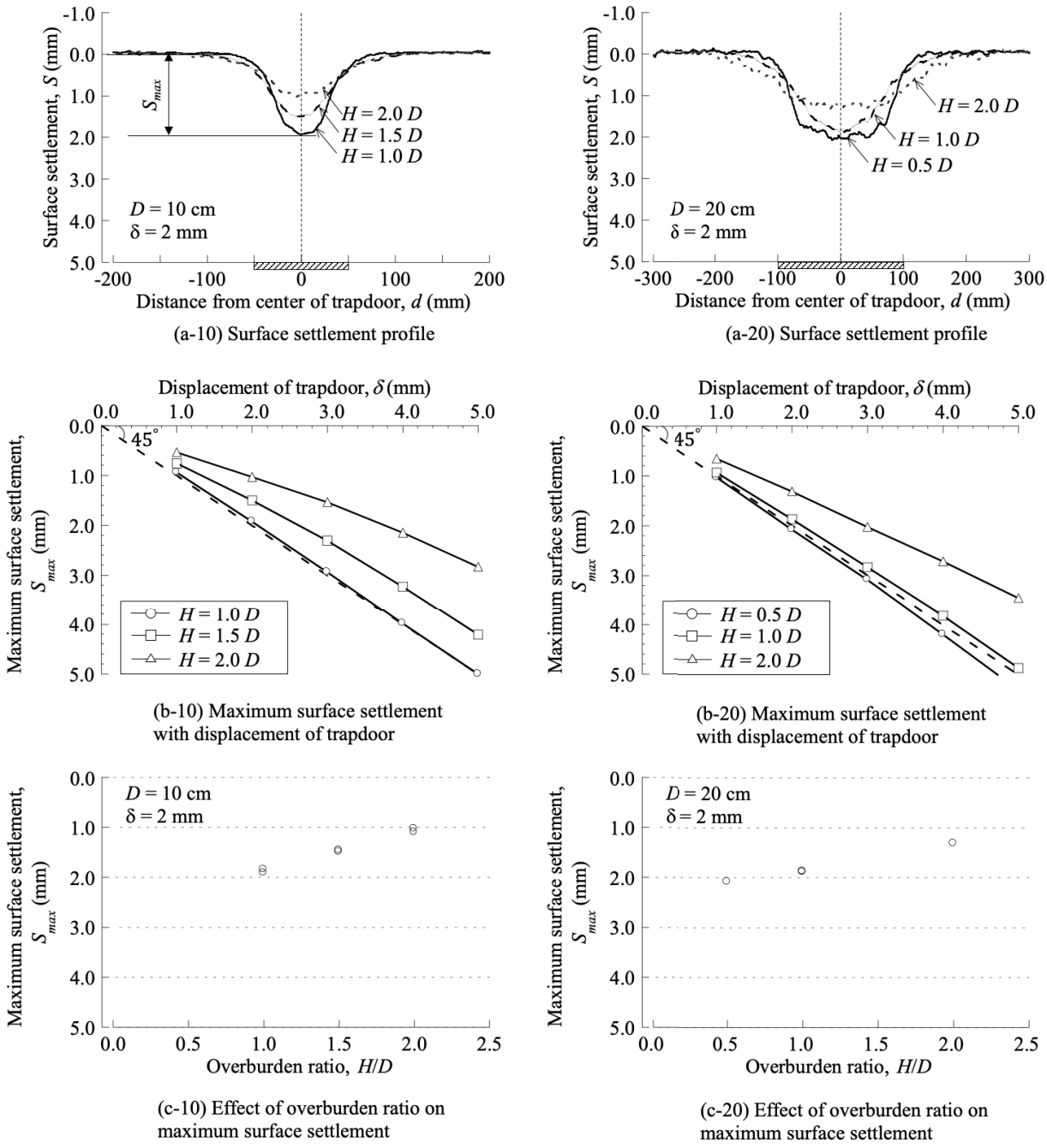

Fig. 3.17 Surface settlement for trapdoor test in saturated ground (a-10) surface settlement profile, D = 10 cm; (b-10) maximum surface settlement with displacement of trapdoor, D = 10 cm; (c-10) effect of depth of groundwater level on the maximum surface settlement, D = 10 cm; (a-20) surface settlement profile, D = 20 cm; (b-20) maximum surface settlement with displacement of trapdoor, D = 20 cm; (c-20) effect of depth of groundwater level on the maximum surface settlement, D = 20 cm.

displacement of trapdoor as overburden ratio was larger than 1.0 because shear bands became more oblique, soil arching effect was strong, so the soil above the trapdoor was prevented to be move downwards. Meanwhile, the corresponding maximum surface settlement for each displacement of trapdoor was smaller as overburden ratio

was larger. Therefore, when displacement of trapdoor was 2.0 mm, the effect of overburden ratio on maximum surface settlement, and the repeatability was shown in Fig. 3.17 (c-10) and (c-20). It was revealed that maximum surface settlement was smaller as overburden ratio was larger.

3.4.2 Surface settlement of trapdoor test in unsaturated ground

The effect of the depth of groundwater level H_w on surface settlement was discussed herein. As overburden ratio H/D and width of trapdoor D were identical, the surface settlement profiles with different depth of groundwater level were shown in Figs. 3.18 (a-10, a-20) and 3.19 (a-10, a-20). It was shown that the surface settlement profiles were almost overlapped as overburden height H was no larger than 20 cm, however, they had significant difference as overburden height was 40 cm.

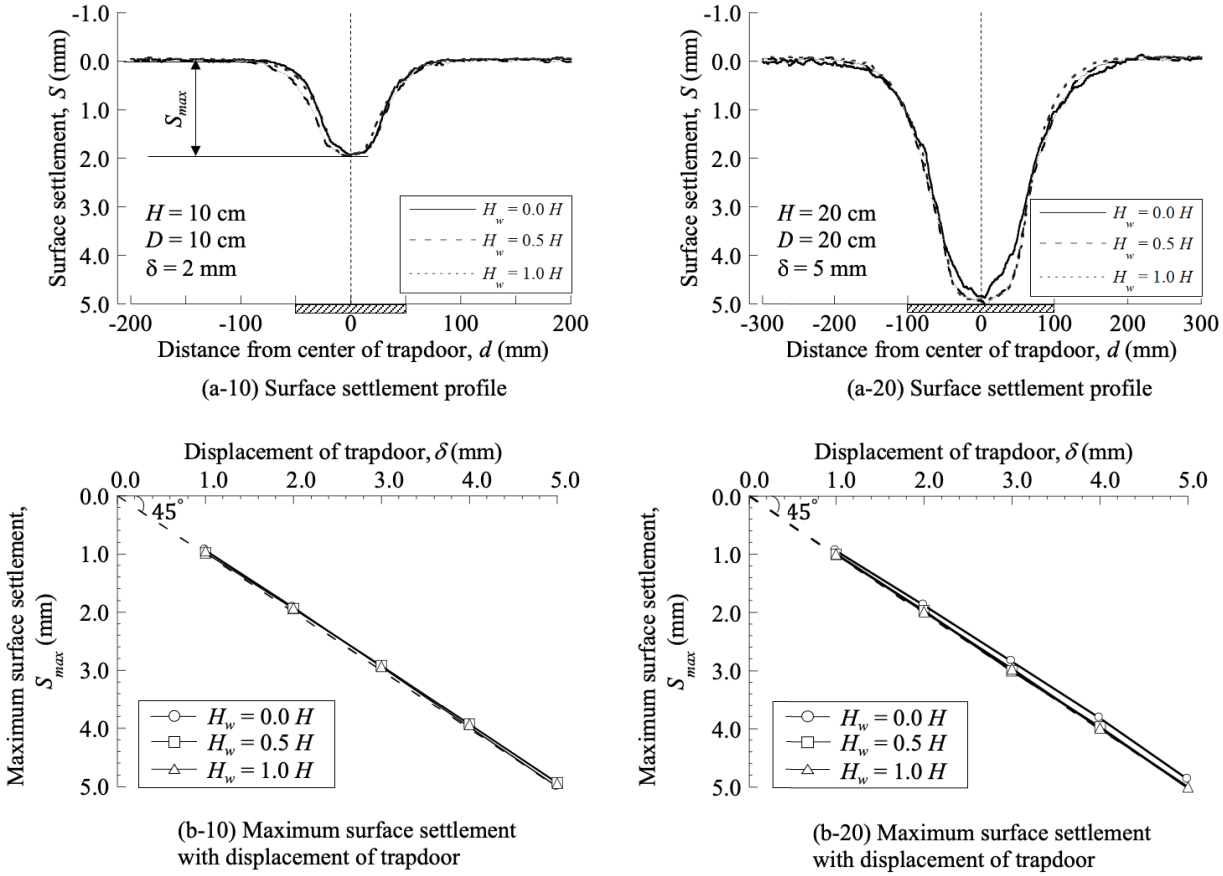

Fig. 3.18 Surface settlement for trapdoor test in unsaturated ground (a) D = 10 cm, H = 1.0 D, H_w = 0.0, 0.5, 1.0 H; (b) D = 20 cm, H = 1.0 D, H_w = 0.0, 0.5, 1.0 H.

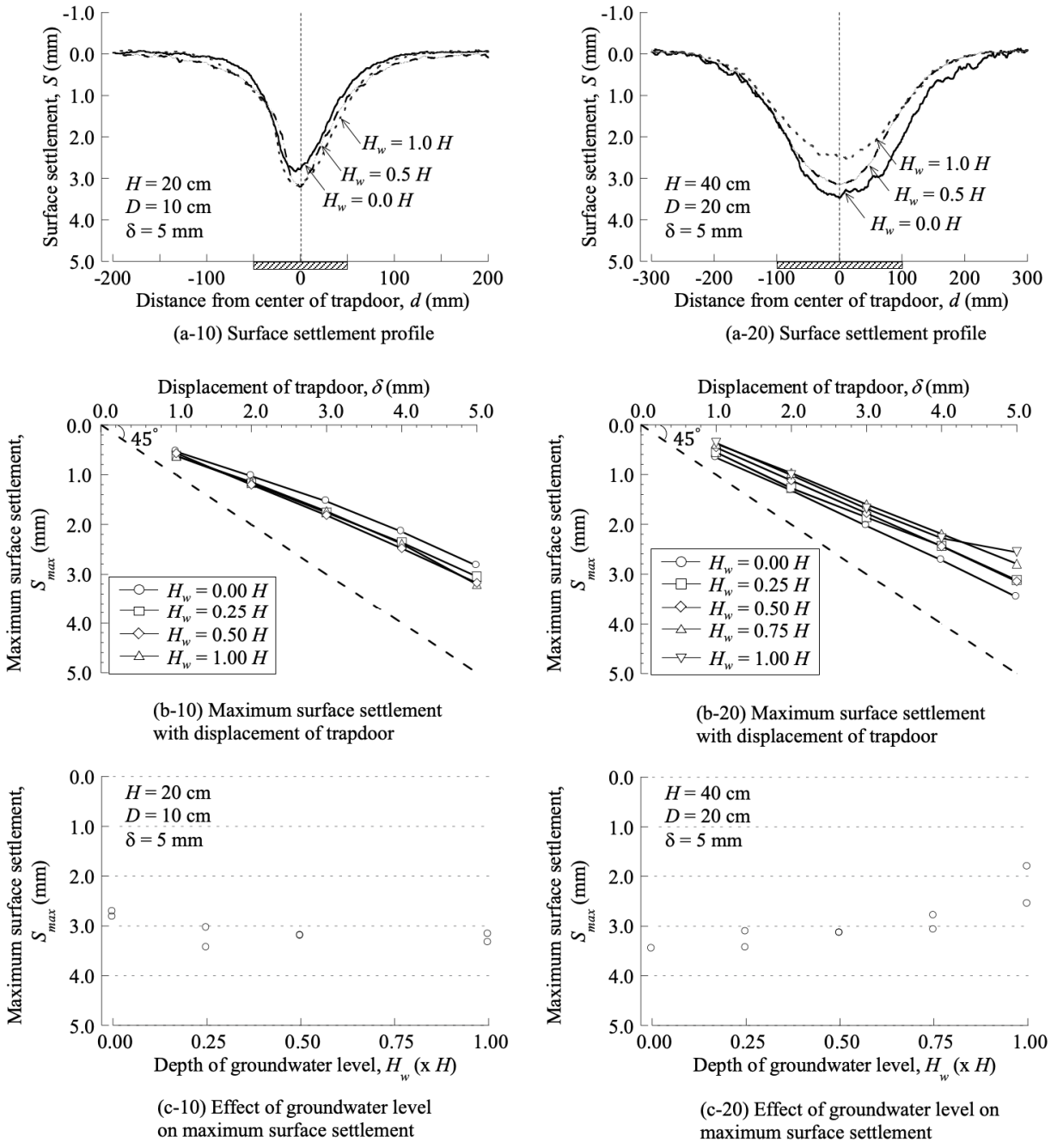

Fig. 3.19 Surface settlement for trapdoor test in unsaturated ground (a-10) surface settlement profile, D = 10 cm, H/D = 2.0, H_w = 0.00, 0.25, 0.50, 1.00 H; (b-10) maximum surface settlement with displacement of trapdoor, D = 10 cm, H/D = 2.0, H_w = 0.00, 0.25, 0.50, 1.00 H; (c-10) effect of depth of groundwater level on the maximum surface settlement, D = 10 cm, H/D = 2.0, H_w = 0.00, 0.25, 0.50, 1.00 H; (a-20) surface settlement profile, D = 20 cm, H/D = 2.0, H_w = 0.00, 0.25, 0.50, 0.75, 1.00 H; (b-20) maximum surface settlement with displacement of trapdoor, D = 20 cm, H/D = 2.0, H_w = 0.00, 0.25, 0.50, 0.75, 1.00 H; (c-20) effect of depth of groundwater level on the maximum surface settlement, D = 20 cm, H/D = 2.0, H_w = 0.00, 0.25, 0.50, 0.75, 1.00 H.

The changing in maximum surface settlement S_{max} with displacement of trapdoor δ was shown in Figs. 3.18 (b-10, b-20) and 3.19 (b-10, b-20). It was shown that the corresponding maximum surface settlement was equal to displacement of trapdoor as shown as in Fig. 3.18 (b-10, b-20) as overburden ratio was no larger than 1.0, which meant the influence of suction on maximum surface settlement could be ignored. The corresponding maximum surface settlement was less than displacement of trapdoor in Figs. 3.19 (b-10, b-20) as overburden ratio was larger than 1.0. However, the influence of suction on maximum surface settlement was not observed for each displacement of trapdoor as overburden ratio was 2.0 and width of trapdoor was 10 cm, the reason was that suction was too small to significantly affect shear bands as shown as Fig. 3.13. When overburden ratio was 2.0 and width of trapdoor was 20 cm, maximum surface settlement was smaller as depth of groundwater level was larger for each displacement of trapdoor, especially the displacement of trapdoor was 5.0 mm. Because suction was large enough to affect shear bands, as shown as Fig. 3.14, shear bands didn't attain to ground surface as depth of groundwater level was 40 cm, a crack was observed.

Moreover, when displacement of trapdoor was 5.0 mm, the effect of overburden ratio on maximum surface settlement, and the repeatability was shown in Fig. 3.19 (c-10) and (c-20). It was revealed that the effect of depth of groundwater level on maximum surface settlement could be ignored as overburden ratio was 2.0 and width of trapdoor was 10 cm. When overburden ratio was 2.0 and width of trapdoor was 20 cm, maximum surface settlement was smaller as depth of groundwater level was deeper.

3.4.3 Summary

(1) For trapdoor test in saturated ground, as overburden ratio H/D was no larger than 1.0, the corresponding maximum surface settlement S_{mlax} was equal to the displacement of trapdoor, the effect of overburden ratio on the maximum surface settlement could be ignored. Contrarily, the corresponding maximum surface settlement was smaller as overburden ratio ($H/D > 1.0$) was larger.

(2) For maximum surface settlement of trapdoor test in unsaturated ground, when overburden ratio was 2.0 and width of trapdoor overburden ratio was 20 cm, it was smaller as the depth of groundwater level H_w was deeper, this was because the larger suction caused larger confining pressure and shear stress. As overburden height H was less than 40 cm, suction was too small to affect the maximum surface settlement.

3.5 Effect of depth of groundwater level on loosening earth pressure

For trapdoor test in unsaturated ground, overburden ratio H/D and width of trapdoor D were identical, total loosening pressure σ_z was smaller as the depth of groundwater level H_w was deeper as shown as Fig. 3.10. In this section, the effect of the depth of groundwater level on loosening earth pressure was investigated in more details. In the total or effective loosening earth pressure versus depth of groundwater level plane, overburden ratio H/D and width of trapdoor D were identical, total or effective initial pressure and total or effective loosening earth pressure for different depth of groundwater level were shown in Figs. 3.20 ~3.23. It was revealed that total loosening earth pressure gradually became smaller as the depth of groundwater level was deeper. This reduction

was not due to the decreasing of the mass of water of different thickness of unsaturated zone, because total initial pressure with different depth of groundwater level were almost identical. The reason for the reduction of total loosening earth pressure was soil arching effect, the larger confining pressure and shear stress caused by the larger suction transferred more weight of soil above the trapdoor to the stationary zone. Contrarily, effective loosening earth pressure slightly increased, however, effective initial pressure was also larger as depth of groundwater level was deeper.

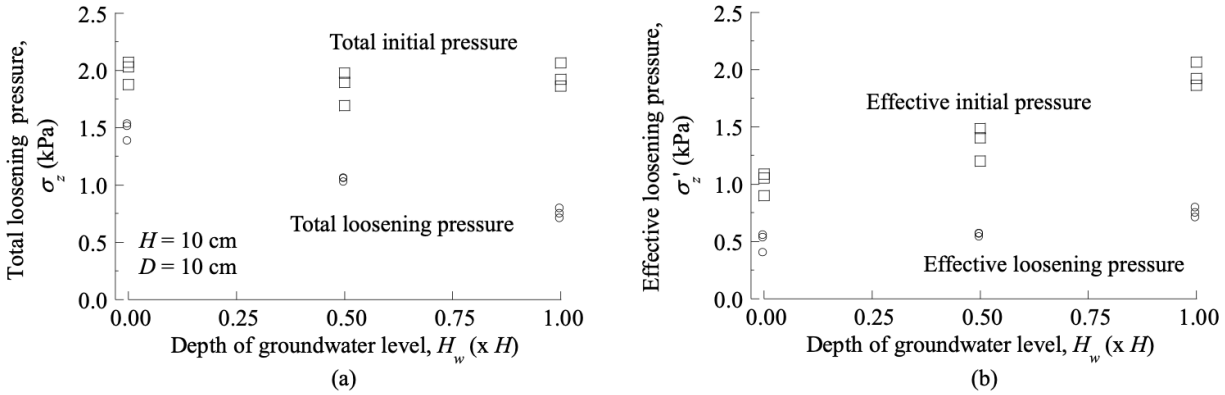

Fig. 3.20 The effect of depth of groundwater level on (a) total loosening earth pressure (H = 10 cm, D = 10 cm); (b) effective loosening earth pressure (H = 10 cm, D = 10 cm).

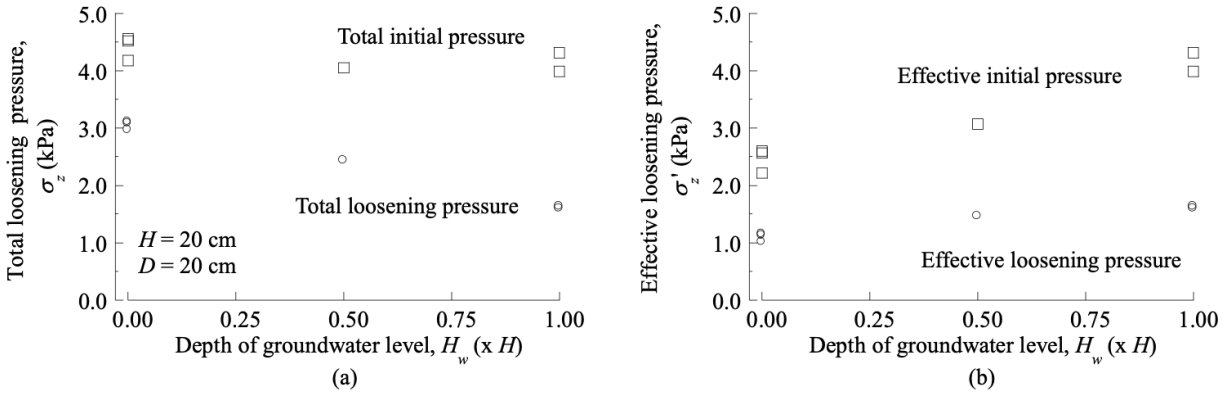

Fig. 3.21 The effect of depth of groundwater level on (a) total loosening earth pressure (H = 20 cm, D = 20 cm); (b) effective loosening earth pressure (H = 20 cm, D = 20 cm).

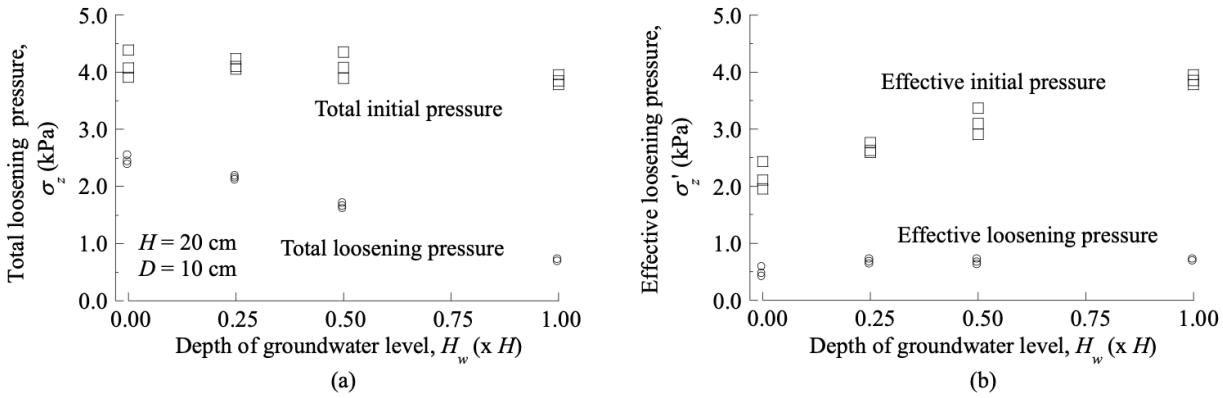

Fig. 3.22 The effect of depth of groundwater level on (a) total loosening earth pressure (H = 20 cm, D = 10 cm); (b) effective loosening earth pressure (H = 20 cm, D = 10 cm).

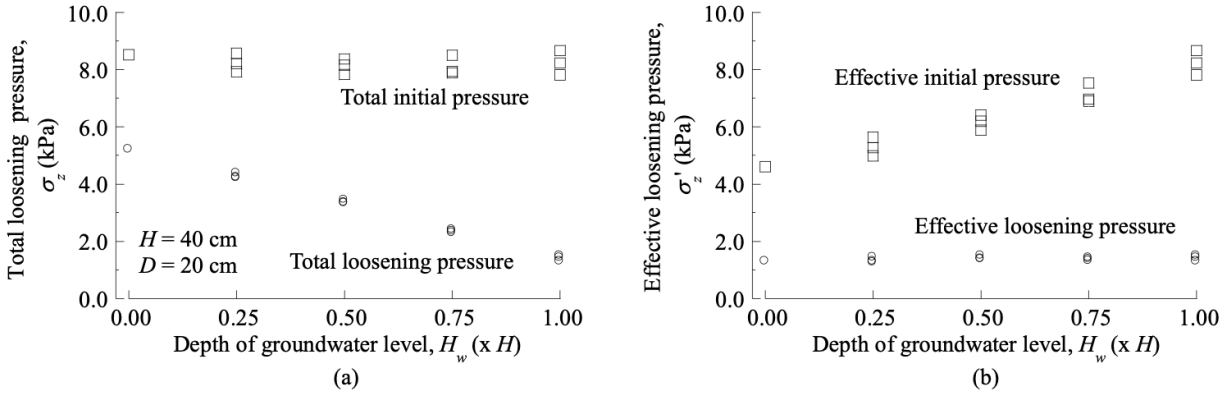

Fig. 3.23 The effect of depth of groundwater level on (a) total loosening earth pressure (H = 40 cm, D = 20 cm); (b) effective loosening earth pressure (H = 40 cm, D = 20 cm).

3.6 Summary

In this chapter, trapdoor tests in saturated and unsaturated ground were carried out to explore the distribution of earth pressure, shear bands and surface settlement. Based on the experimental result, the effect of the depth of groundwater level on loosening earth pressure and scale effect in saturated and unsaturated ground were also discussed. Conclusions were written as following:

(1) Loosening earth pressure was significant smaller compared with initial pressure, and it gradually decreased from the center of trapdoor to the end of trapdoor. The shape of loosening earth pressure was symmetric. Meanwhile, the average loosening earth pressure acting on trapdoor rapidly decreased as displacement of trapdoor was no larger than 1.0 mm, and it was already a minimum value as displacement of trapdoor was 2.0 mm. At stationary zone, when the distance to the end of trapdoor was larger, earth pressure was larger than initial pressure and gradually decreased to initial pressure.

(2) Shear bands in saturated ground was more oblique as overburden ratio was larger. For shear bands in

unsaturated ground, as the depth of groundwater level was deeper, the open of it was smaller. Meanwhile, multiple shear bands were observed in saturated and unsaturated ground, the first shear bands was gradually expanded until it became steady as displacement of trapdoor was no larger than 1.0. As displacement of trapdoor continued to be larger, a new shear bands were emerged inside the previous shear bands sequentially.

(3) In saturated ground, the maximum surface settlement was smaller as overburden ratio was larger. In unsaturated ground, the maximum surface settlement was smaller as the depth of groundwater level was deeper. However, as overburden ratio is no larger than 1.0, the effect of overburden ratio on the maximum surface settlement in saturated ground and the effect of the depth of groundwater level on maximum surface settlement in unsaturated ground could be ignored, the corresponding maximum surface settlement was always equal to displacement of trapdoor.

(4) The depth of groundwater level significantly affected total and effective loosening earth pressure. The experiment result was shown that total loosening earth pressure was smaller as the depth of groundwater level was deeper, contrarily, effective loosening earth pressure was slightly larger, the reason was that the larger confining pressure and shear stress caused by the larger suction transferred more weight of soil above a trapdoor to stationary zone.

CHAPTER 4 A THEORY TO EVALUATE LOOSENING EARTH PRESSURE IN UNSATURATED GROUND

Trapdoor test in saturated and unsaturated ground was carried out to explore the distribution of earth pressure and loosening earth pressure with displacement of trapdoor. Then we intended to propose a simple theory to evaluate loosening earth pressure acting on a trapdoor in unsaturated ground. The proposed theory was deduced based on the limit equilibrium theory, combining soil-water characteristic curves, Mohr-Coulomb failure criteria and effective stress for unsaturated soils. The proposed theory was validated by comparing loosening earth pressure in fully-dried and fully-saturated ground with that evaluated by Terzaghi's theory (1943). Furthermore, the proposed theory was applied to evaluate the vertical distribution of loosening earth pressure in unsaturated ground, which shown the totally difference comparing with that in saturated ground. Then the effect of movement of groundwater level and soil type on loosening earth pressure were also explored. And the scale effect in saturated and unsaturated ground was discussed. Finally, the loosening earth pressure observed by trapdoor test in chapter 3 was compared with that predicted by the proposed theory.

4.1 The proposed theory for loosening earth pressure in unsaturated ground

This section uses a trapdoor problem in unsaturated ground as shown in Fig. 4.1. The z coordinate is taken vertically downward with the ground surface as the origin and groundwater level is set as H_w. A trapdoor of width D, located near the ground surface at a depth H, simulates stress release during tunnel excavation by its downward movement. The ground is assumed to be uniform, having a solid density of ρ_s and dry density of ρ_d (void ratio, $e = \frac{\rho_s}{\rho_d} - 1$).

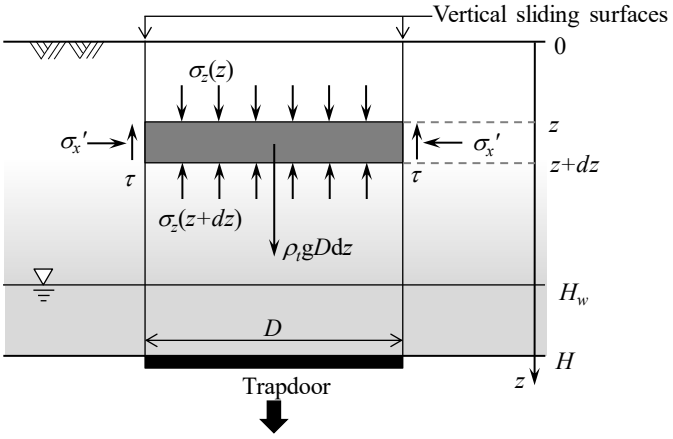

Fig. 4.1 Trapdoor problem in unsaturated soil.

4.1.1 Failure mode, equilibrium and boundary conditions

Several studies have indicated that shear bands tend to develop vertically upward from both ends of a trapdoor and reach the ground surface when the overburden height, H, is no more than 2–3 times larger than the trapdoor width, D (e.g., McNulty, 1965; Evans, 1984; Koutsabeloulis and Griffiths, 1989; Sloan, 1990; Kikumoto and Kishida, 2003; Dewoolkar et. al., 2007). As the study uses a shallow trapdoor problem, vertical failure surfaces are assumed as shown in Fig. 4.1. For this failure mode, an equation of equilibrium of vertical force acting on a small soil element above the trapdoor is given as

$$-\sigma_z(z+dz)D - 2\tau dz + \sigma_z(z)D + \rho_t g D dz = 0 \tag{4.1}$$

where $\sigma_z(z)$ is the vertical earth pressure in the ground above the trapdoor at a depth of z; τ is shear stress on the side boundary of the soil element; ρ_t is the wet density of soil; g is gravity. Applying Taylor's expansion, the equilibrium equation (4.1) reduces to equation (4.2)

$$\frac{d\sigma_z}{dz} = \rho_t g - \frac{2}{D}\tau \tag{4.2}$$

As we consider a traction-free condition at the ground surface, the boundary condition is given as $\sigma_z(0) = 0$ kPa.

4.1.2 Pore pressure and soil suction

Pore air pressure ($u_a(z)$) and pore water pressure ($u_w(z)$) are assumed to be under static pressure conditions. The value of u_a is usually assumed to be zero (atmospheric pressure) at any depth as the density of air is negligible (Pufahl et al., 1983; Vahedifard et al., 2016; Sahoo et al., 2018) and u_w is assumed to have a linear distribution in the vertical direction with a slope of $\rho_w g$ (ρ_w is the density of water) (Pufahl et al., 1983; Ng and Menzies, 2007; Vahedifard et al., 2016). The value of u_w becomes zero at the groundwater surface, is negative above the groundwater level, and can be written as

$$u_w = \rho_w g(z - H_w) \tag{4.3}$$

Soil suction, s, is given as the difference between pore air pressure, u_a, and pore water pressure, u_w .

$$s = (u_a - u_w) = \rho_w g(H_w - z) \tag{4.4}$$

A simple, linear suction profile is assumed herein. However, the proposed method can incorporate the effects of infiltration and evaporation further by introducing a nonlinear suction profile (e.g., Vo and Russell, 2006).

4.1.3 Degree of saturation and wet density

The degree of saturation, S_r, is usually given as a function of suction. Although any soil-water characteristic curve can be applied to the proposed theory, the classical equation proposed by van Genuchten (1980) is employed herein.

$$S_r = (S_{max} - S_{min})\{1 + \langle \alpha s \rangle^n\}^{-m} + S_{min} \tag{4.5}$$

where $\langle\ \rangle$ denotes Macaulay brackets; S_{max} and S_{min} are the maximum and minimum degrees of saturation, respectively; and α, m, and n are material parameters. From equations (4.4) and (4.5), S_r is given as a function of depth, $S_r(z)$. Note that the proposed method can incorporate several factors affecting the soil-water characteristic curve such as the air-entry suction (Fredlund and Xing, 1994), hydraulic hysteresis (Hains, 1930), or the effect of density (Tarantino and Tombolato, 2005) by replacing equation (4.5) with an advanced soil-water characteristic curve model (e.g., Fredlund and Xing, 1994; Kikumoto et al., 2010; Komolvilas and Kikumoto, 2017).

Wet density, ρ_t, is given as a function of the degree of saturation, $S_r(z)$, by its definition, which is written as

$$\rho_t = \frac{\rho_s + eS_r(z)\rho_w}{1 + e} \tag{4.6}$$

From equations (4.4) to (4.6), S_r and ρ_t are uniquely given by depth z, respectively. ρ_t equals saturation density (ρ_{sat}) at the saturated state ($S_r = 1$) and equals dry density (ρ_d) at the dry state ($S_r = 0$).

4.1.4 Effective stress and shear resistance

The effective stress proposed by Bishop (1959) is usually used for unsaturated soils, as it can uniquely arrange the critical state stress ratio of unsaturated soils regardless of suction, *s*, as shown in Fig. 4.2. By using this, the vertical effective stress corresponding to σ_z in equation (4.2) is given as

$$\sigma_z' = \sigma_z - \{\chi u_w + (1 - \chi)u_a\} \tag{4.7}$$

where χ is the effective stress parameter, for which S_r is usually applied (e.g., Schrefler, 1984; Öberg and Sällfors, 1997; Lu and Likos, 2006; Komolvilas and Kikumoto, 2017). Borja (2006) derived this relationship based on the principles of thermodynamics. Therefore, in the proposed theory, equation (4.7) can be written as

$$\sigma_z' = \sigma_z - u_a + S_r s \tag{4.8}$$

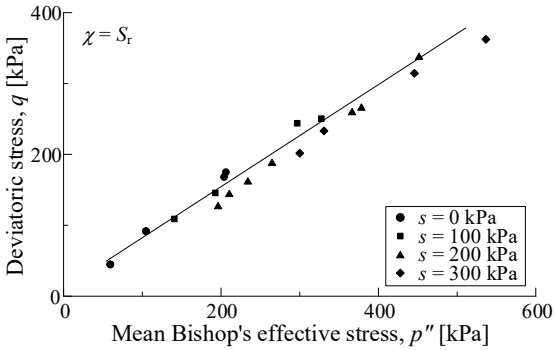

Fig. 4.2 Relation between mean stress, p'', and deviator stress, q, of Bishop's effective stress (replotted from Sivakumar, 1993).

The Mohr-Coulomb failure criterion is assumed to be satisfied by Bishop's effective stress along vertical failure surfaces (Fig. 4.1), hence, the shear stress is written as

$$\tau = \sigma_x' \tan\phi \tag{4.9}$$

Where σ_x' is Bishop's horizontal effective stress; and ϕ is the internal friction angle of soil. Herein, the internal friction angle is almost constant regardless of the degree of saturation (e.g., Gan et al., 1988; Khalili et al., 2004; Schnellmann, 2015), which can be determined by direct shear test or triaxial shear test on the specimens of saturated soil. Cohesion is not considered herein.

4.1.5 Earth pressure coefficient

A coefficient of earth pressure, K_h, is considered for Bishop's effective stress in the ground above the trapdoor similarly as the saturated ground (Terzaghi, 1943)

$$K_h = \frac{\sigma_x'}{\sigma_z'} \tag{4.10}$$

Terzaghi (1943) empirically recommended K_h to be at unity. According to experiment result and numerical simulation of the trapdoor problem in fully–dried ground, K_h tends to be larger than the earth pressure coefficient at rest and is around unity (e.g., Evans, 1984; Kikumoto et al., 2003; Kikumoto, 2004).

4.1.6 Loosening earth pressure

Substituting equations (4.4) to (4.10) into equation (4.2), we can write the ordinary differential equation as

$$\frac{d\sigma_z}{dz} = \frac{\rho_s + eS_r(z)\rho_w}{1+e} g - \frac{2}{D} K[\sigma_z - u_a + S_r(z)\rho_w g(H_w - z)]\tan\phi \tag{4.11}$$

Then the loosening earth pressure, $\sigma_z(z)$, is derived by solving differential equation (4.11) under the boundary condition that $\sigma_z(0) = 0$ kPa. For this, a simple and explicit numerical scheme with incremental depth Δz is applied shown as below.

$$\sigma_z(z + \Delta z) - \sigma_z(z) = \frac{d\sigma_z}{dz}\Delta z \tag{4.12}$$

4.2 Evaluation of Loosening Earth Pressure

The proposed theory was first applied to evaluate loosening earth pressure (vertical earth pressure after lowering the trapdoor) in loamy ground under fully-dried and fully-saturated conditions to check the validity of the theory against the classical Terzaghi's theory. The loosening earth pressure in an unsaturated, loamy ground was then evaluated using the proposed theory. Afterward, the loosening earth pressures in three types of unsaturated ground (sandy, loamy and silty clay soils) were investigated. The simulations in this section were performed under an overburden height, H, of 10.0 m and trapdoor width, D, of 10.0 m. Thus, the overburden ratio (H/D) was 1.0, for which a shallow failure mechanism with vertical failure surfaces was expected. For simulation of

unsaturated ground, the groundwater level was set to 5.0 m and the vertical distributions of suction in the different ground types were the same, as shown in Fig. 4.3 (b). The principal difference between the different soils is their water holding capacity. In general, water holding capacity is controlled primarily by the particle size distribution of the soil. Smaller particles such as clay and silt tend to have richer capillaries than the larger sand particles as they tend to have smaller pore sizes and stronger capillary action. The richer capillaries allows the finer soils to retain a higher degree of saturation. Parameters for the soil-water characteristic curves of the ground types were referred to the following Hodnett and Tomasella (2002; Table 4-2). An assumption herein is that the physical properties (such as density and friction angle) were the same for the different soils (Table 4-1). The soil-water characteristic curves are compared in Fig. 4.4, and the vertical distributions of the degree of saturation, S_r, for sand, loam, and silty clay are shown in Fig. 4.3 (c).

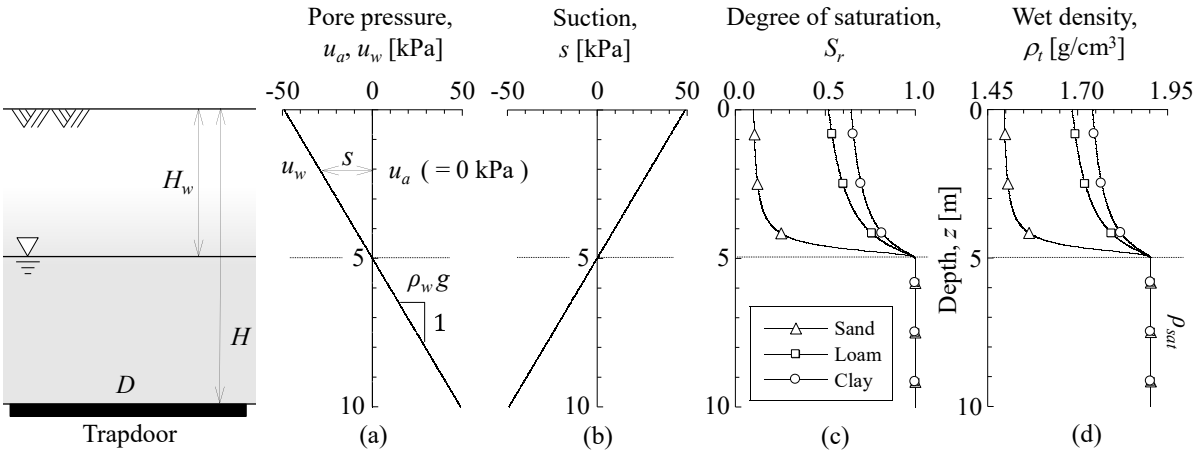

Fig. 4.3 Vertical distribution of (a) pore pressure, u_a, u_w; (b) suction, s; (c) degree of saturation, S_r; (d) wet density, ρ_t (overburden height, H = 10 m, width of trapdoor, D = 10 m, and groundwater level, H_w = 5.0 m).

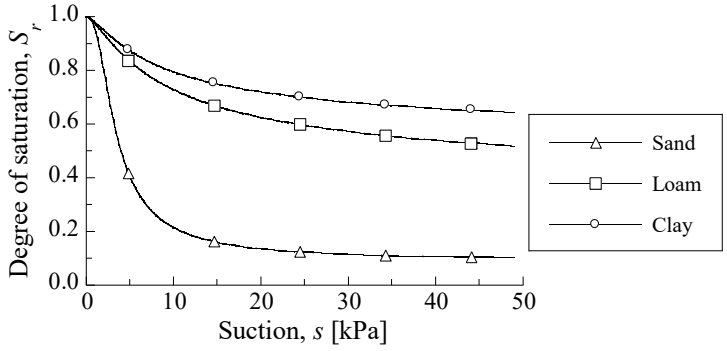

Fig. 4.4 Soil water characteristic curves for sand, loam, and silty clay.

Table 4-1 Soil physical and mechanical properties (the same values were used for the sand, silt, and clay soil types).

ρ_s (g/cm^3)	2.65	Soil particle density
ρ_d (g/cm^3)	1.45	Dry density
ϕ (degree)	30.0	Internal friction angle

Table 4-2 Parameters of the soil–water characteristic curves for sand, loam, and silty clay soil types.

	Sand	Loam	Silt clay
S_{max}	1.000	1.000	1.000
S_{min}	0.090	0.298	0.488
α (kPa^{-1})	0.380	0.246	0.258
m	0.596	0.316	0.318
n	2.474	1.461	1.466

4.2.1 Validation of the proposed theory

Loosening earth pressures in loamy ground under fully-dried and fully-saturated conditions were evaluated by the proposed theory and Terzaghi's theory. To model the fully-dried condition using the proposed theory for unsaturated soils, the groundwater level, H_w, was set to be very deep (10^6 m) so that soil suction, *s,* was remarkably large and the degree of saturation, S_r, was almost zero. For saturated ground, H_w was set to 0.0 m. Comparison of the loosening earth pressure evaluated by the proposed theory and Terzaghi's theory in the fully-dried and fully-saturated conditions are shown in Figs 4.5 and 4.6. The initial earth pressure distribution is calculated as the overburden pressure, which represents the earth pressure at rest before lowering of the trapdoor. The saturation density, $\rho_{sat}\left(=\rho_d-\frac{\rho_s-\rho_d}{\rho_s}\rho_w\right)$, is 1.90 g/cm^3. Figures 4.5 and 4.6, show that both the total and effective loosening earth pressures are lower than the corresponding initial values. This suggests that the earth pressure becomes reduced by vertical-upward shear stress along failure surfaces acting on the ground above the trapdoor. Both the total and effective loosening earth pressures calculated by the proposed theory were identical with those calculated by Terzaghi's theory, which validates the consistency of the proposed theory.

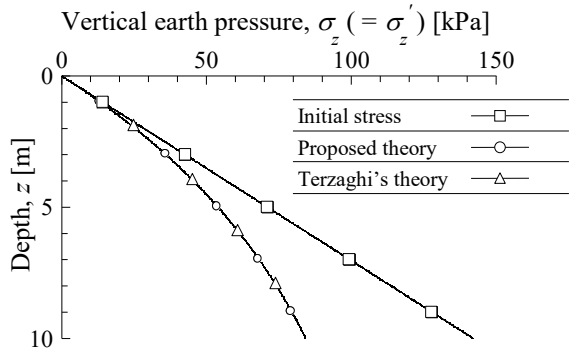

Fig. 4.5 Depth vs. loosening earth pressure in fully-dried ground.

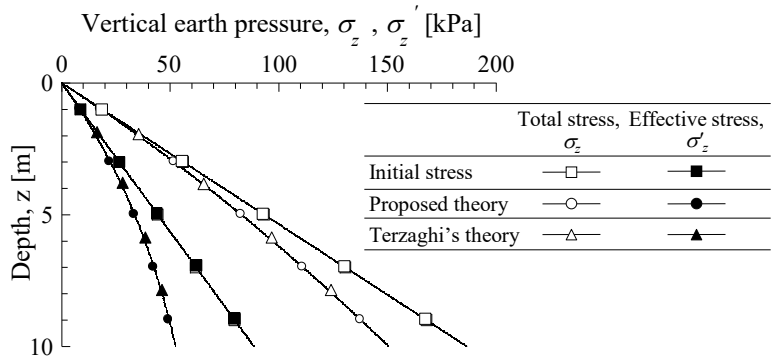

Fig. 4.6 Depth vs. total and effective loosening earth pressures in fully-saturated ground. (Groundwater level, H_w = 0.0 m).

4.2.2 Loosening earth pressure in the unsaturated ground

The proposed theory was applied further to investigate loosening earth pressure in unsaturated loamy ground. Total and effective loosening earth pressures were lower than the corresponding initial earth pressures at all depths (Figure 4.7). In the unsaturated zone above the groundwater level (z < 5 m), the effective loosening earth pressure was larger than the total loosening earth pressure. This indicates that the proposed theory can consider the contribution of matric suction to the increase in effective confining pressure and increase in frictional resistance (τ) in the unsaturated zone. Therefore, the more significant arching effect in unsaturated ground, which is known to occur, can be appropriately evaluated. On the other hand, the correlation between total and effective loosening earth pressure magnitudes is reversed in the saturated zone below the groundwater level.

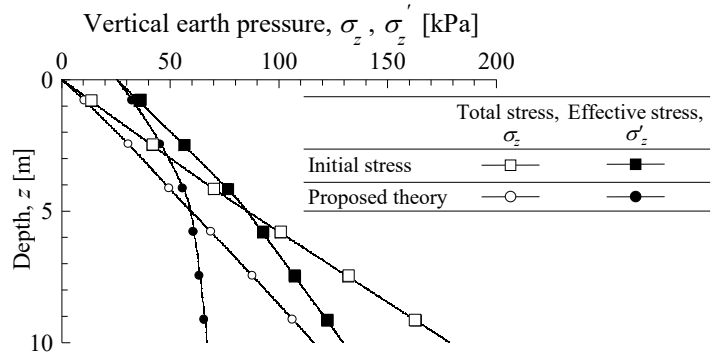

Fig. 4.7 Depth vs. total and effective loosening earth pressures in unsaturated ground (Groundwater level, H_w = 5.0 m).

4.2.3 Loosening earth pressure in different types of unsaturated ground (sand, loam and silty clay soils)

The loosening earth pressure in three types of unsaturated ground (sandy, loamy, and silty clay soils) were investigated. The same physical properties were assumed for the different ground types as shown in Table 4-1. The distributions of soil suction in the different ground types were identical as shown in Fig. 4.3 (b). This is because the groundwater levels were identical (H_w= 5.0 m). However, vertical distribution of the degree of saturation were different (Fig. 4.3 (c)) as different sets of parameters (Table 4-2; Hodnett and Tomasella, 2002)

were applied for the soil-water characteristic curves. Differences in the distributions of degree of saturation resulted in differences in the distribution of wet density as shown in Fig. 4.3 (d).

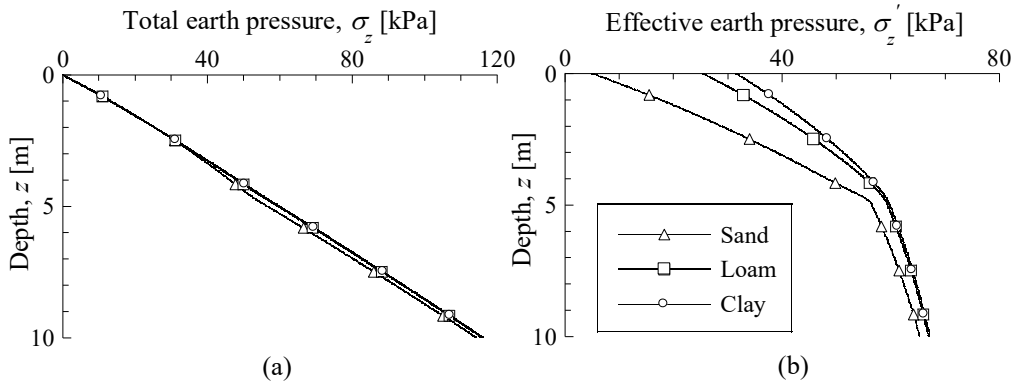

Fig. 4.8 Vertical distribution of (a) total loosening earth pressure; (b) effective loosening earth pressure in sand, loam and silty clay (overburden height, H = 10 m, and groundwater level, H_w = 5.0 m).

Figure 4.8 shows the distributions of the loosening earth pressure for the three ground types. The effective earth pressure in clay and loam ground is much higher than that in the sandy ground. This suggests that shear resistance of the soil along the sliding surfaces, which is usually referred to as "arching effect", becomes more substantial in the clayey and loamy ground compared with the sandy ground. This can explain why the excavation of a tunnel in the sandy ground is relatively more challenging than that in the clayey and loamy ground. However, the differences between the total loosening earth pressures of the ground types is small, although the total loosening earth pressure in the sandy ground is slightly higher than that in the other types of soils.

4.3 Effect of the depth of groundwater level on loosening earth pressure

A series of simulations was carried out using the proposed theory using different groundwater levels to explore its effect on loosening earth pressure. The trapdoor width, D, was fixed to 10.0 m throughout this section.
The overburden height, H, was set to $1.0D$ and the groundwater level, H_w was set to different depths (0.0 m, 2.5 m, 5.0 m, 7.5 m and 10.0 m) for each simulation. Figure 4.9 shows the vertical distributions of the degree of saturation, S_r, the product of suction and degree of saturation, sS_r, and total and effective loosening earth pressures. As the effective stress, σ_z', in equation (4.8) can be decomposed into net stress, $\sigma_z^{net}(=\sigma_z - u_a)$, sS_r represents the contribution of suction on the increase in effective confining pressure. In the case of a deeper H_w, the degree of saturation was smaller at any depth in the unsaturated zone (Fig. 4.9 (a)) and the wet density was also lower. This made overburden pressure lower in the deeper H_w case. Meanwhile, sS_r is larger (Fig. 4.9 (b)) in the deeper H_w case, which made effective loosening earth pressure become higher (Fig. 4.9 (d)). According to equation (4.9), the shear resistance along the vertical slip surfaces, which works to reduce the vertical earth pressure on the trapdoor, also becomes more substantial in the case of a deeper H_w. Owing to the effects of a

lower overburden pressure and higher shear resistance, the total loosening pressure becomes significantly smaller in the deeper H_w case.

The effect of the groundwater level on the loosening earth pressure acting on the trapdoor was further investigated under different overburden height, $H(\leq 30.0\ \text{m})$, and the depth of groundwater level, $H_w(= 0.0, 5.0, 10.0, 15.0, 20.0\ \text{m})$. Figure 4.10 (a) and 4.10 (b) show the total and effective loosening pressures normalized by total and effective overburden pressure at the depth, H, of $1.0D$, respectively (where ρ_{sat} and ρ_{sub} are the saturation and submerged densities, respectively).

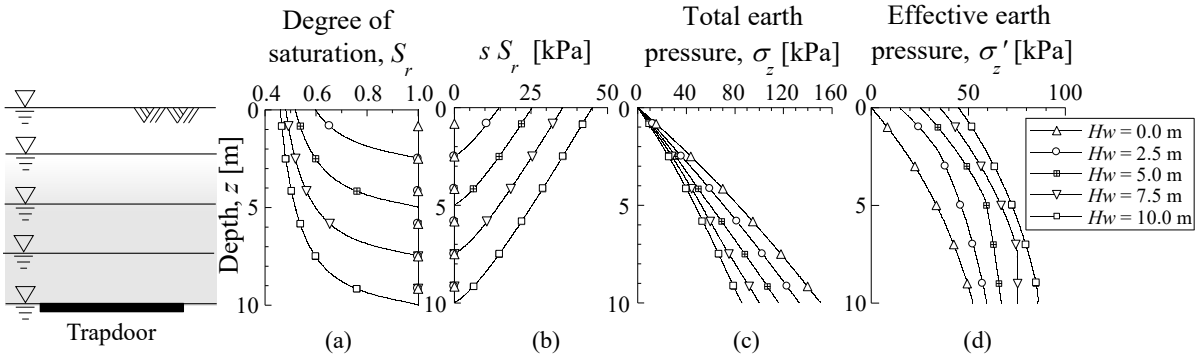

Fig. 4.9 Vertical distribution of (a) degree of saturation; (b) product of degree of saturation and suction; (c) total loosening earth pressure; (d) effective loosening earth pressure in loamy ground (overburden height, H = 10 m, and groundwater level, H_w = 0.0, 2.5, 5.0, 7.5, 10.0 m).

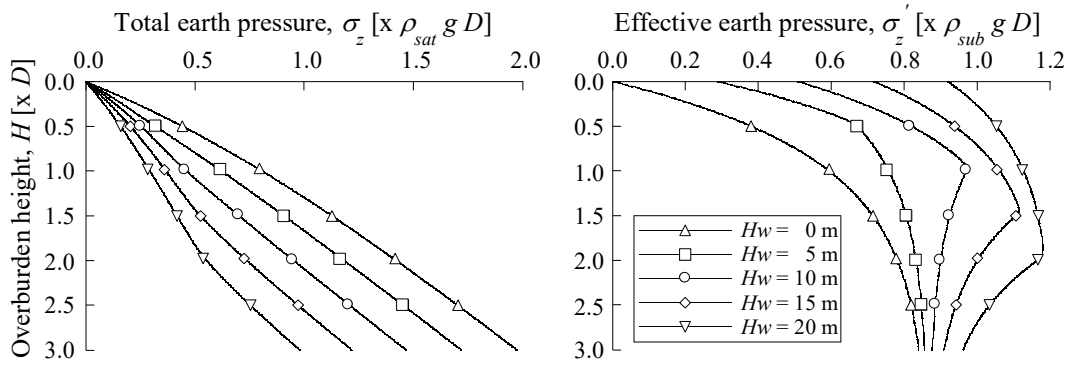

Fig. 4.10 Overburden height vs. (a) normalized total loosening earth pressure; (b) normalized effective loosening earth pressure in unsaturated ground at different groundwater levels (overburden height, H = 0.0-3.0D, width of trapdoor, D = 10 m, and groundwater level, H_w = 0, 5, 10, 15, 20 m).

The total loosening earth pressure became higher both with the increase in overburden height, H, and decrease in the groundwater level, H_w. Therefore, groundwater level and overburden height, had a significant effect on the total loosening pressure. On the other hand, the mean effective stress varied depending on whether the groundwater level is shallower or deeper than the overburden height. The effective earth pressure increased monotonically with the overburden height in the unsaturated zone where the overburden height, H, was less than

the groundwater level H_w. In the case where the trapdoor is located below the groundwater level ($H > H_w$), the effective loosening earth pressure would still increase with the increase in the overburden height when H_w = 5.0 m, but it would decrease with the overburden height when H_w is 10.0 m or larger.

4.4 Scale effect on loosening earth pressure

The characteristics of the loosening earth pressures in unsaturated ground were further investigated in terms of the scale effect. In this section, a series of simulations were carried out by varying the width of the trapdoor, D (i.e. 5.0 m, 10.0 m, and 20.0 m). For each trapdoor width, the overburden height, H, was varied from 0.0 to $3.0D$ with keeping the ratio of the groundwater level, H_w, to the trapdoor width constant.

4.4.1 Scale effect in saturated ground (H_w/D = 0)

The scale effect on the total and effective loosening earth pressures in the fully-saturated ground ($H_w = 0.0$ m) was investigated herein. Figure 3.11 shows the total and effective loosening earth pressures normalized by the corresponding overburden pressures for the overburden height of $1.0D$. The normalized total and effective loosening earth pressures were identical, regardless of the width of the trapdoor, D. Therefore, trapdoor scale can be ignored in fully-saturated ground, which has been demonstrated by previous studies (e.g., Evans, 1984).

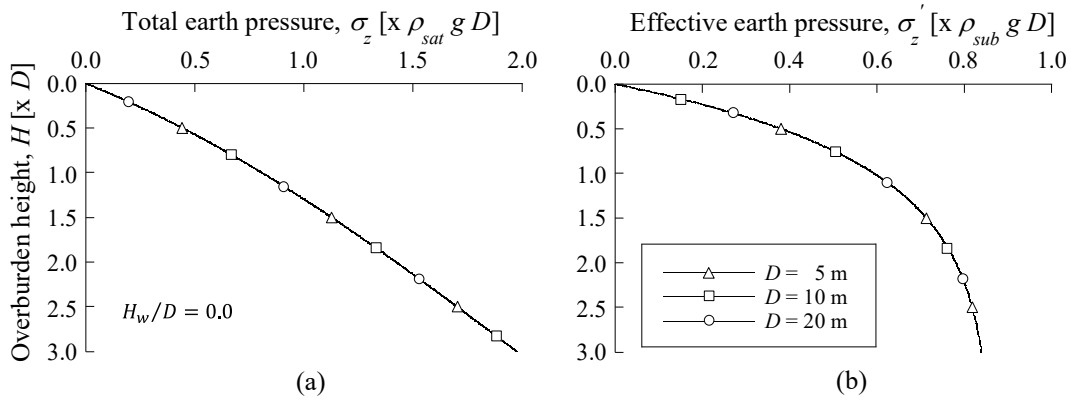

Fig. 4.11 Vertical distribution of (a) total loosening earth pressure; (b) effective loosening earth pressure in saturated, loamy ground (overburden ratio, H = 0.0–3.0D, and groundwater level, H_w = 0.0D).

4.4.2 Scale effect in unsaturated ground ($H_w/D > 0$)

The scale effect on the total and effective loosening earth pressures in the partially-saturated ground for three kinds of groundwater level ratio, H_w/D, were investigated. The total and effective loosening earth pressures were normalized by their initial values of saturated ground for the overburden depth of $1.0D$.

Figure 4.12 shows the vertical distribution of the normalized total and effective loosening earth pressures, degree of saturation, and wet density for the case where the groundwater level, H_w, was $1.5D$. The normalized total and effective pressures in the unsaturated zone for the different trapdoor widths were different, which implies trapdoor scale affects the normalized loosening earth pressure in the unsaturated ground. For the case of the

larger trapdoor width, the normalized effective loosening earth pressure in the unsaturated zone tended to be lower and the normalized total loosening earth pressure tended to be higher. These differences in the distributions of the normalized loosening pressures are related to the differences in the distributions of saturation degree and wet density.

Figures 4.13 and 4.14 show the distributions of the normalized loosening pressures, degree of saturation, and wet density for the cases where the groundwater level, H_w, was $0.5D$ and $2.0D$, respectively. The scale effect was more significant in the higher H_w case. This is because, in the higher H_w case, the unsaturated zone was thicker, suction tended to be stronger, and the shear resistance along the slip surfaces was larger.

These results suggest that the scale effect on the normalized total and effective loosening earth pressure exists in unsaturated grounds, especially with the deeper groundwater levels. This should be considered in the excavation shallow tunnels in unsaturated ground.

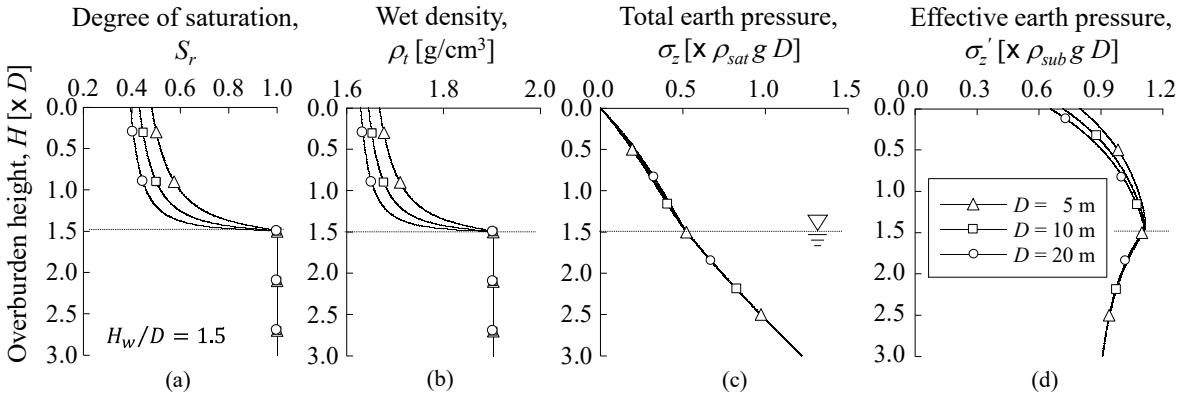

Fig. 4.12 Vertical distribution of (a) degree of saturation; (b) wet density; (c) normalized total loosening earth pressure; (d) normalized effective loosening earth pressure in loamy ground (overburden, H = 0.0–3.0D, and the groundwater level ratio, H_w = 1.5D).

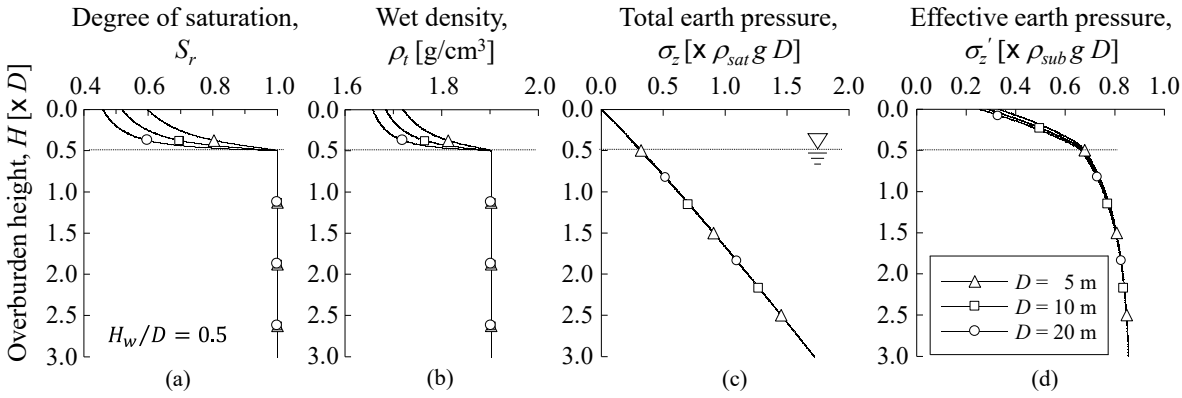

Fig. 4.13 Vertical distribution of (a) degree of saturation; (b) wet density; (c) normalized total loosening earth pressure; (d) normalized effective loosening earth pressure in loamy ground (overburden ratio, H = 0.0–3.0D, and the groundwater level ratio, H_w = 0.5D).

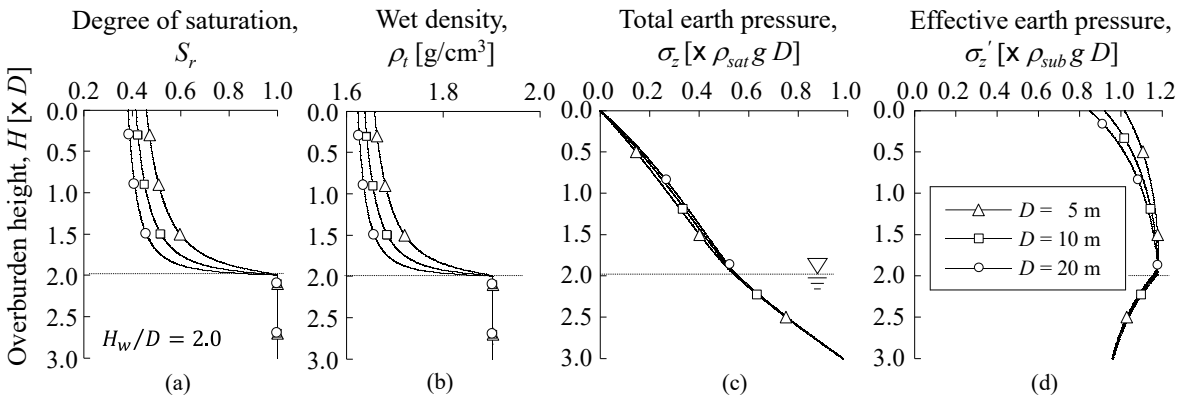

Fig. 4.14 Vertical distribution of (a) degree of saturation; (b) wet density; (c) normalized total loosening earth pressure; (d) normalized effective loosening earth pressure in loamy ground (overburden ratio, H = 0.0–3.0D, and groundwater level ratio, H_w = 2.0D).

4.4.3 The uniqueness of loosening pressures in unsaturated ground

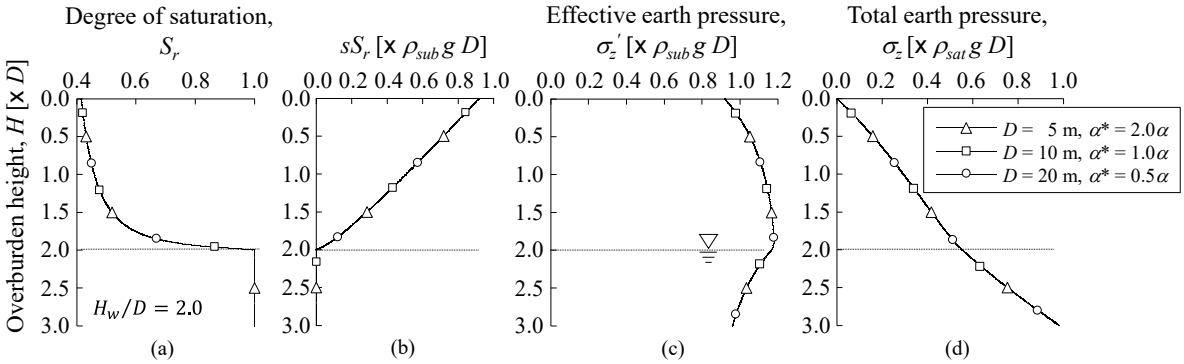

Fig. 4.15 Vertical distribution of (a) normalized degree of saturation; (b) normalized sS_r; (c) normalized effective loosening earth pressure; (d) normalized total loosening earth pressure in loamy ground (overburden ratio, H = 0.0–3.0D, and groundwater level ratio, H_w = 2.0D).

Table 4-3 Scaled parameters of the soil–water characteristic curves for different overburden heights.

	D = 5 m	D = 10 m	D = 20 m
S_{max}		1.000	
S_{min}		0.298	
α (kPa^{-1})	0.492	0.246	0.123
m		0.316	
n		1.461	

In this section, we investigated the uniqueness of total and effective loosening earth pressures in partially-saturated ground by varying width of trapdoor (e.g., 5 m, 10 m, 20 m) and keeping the identical overburden ratio, H/D of 3 and groundwater ratio, H_w/D of 2. Herein, the swcc model is normalized by varying the parameter of

swcc model, α^*. α^* is assumed to be equal to 2.0α, 1.0α, 0.5α (α is given in Table 4-1) as shown in Table 4-3 when the width of Trapdoor, D is 5 m, 10 m, 20 m. Then the normalized degree of saturation, the normalized product of suction and normalized degree of saturation, normalized total and effective loosening pressures are shown in Figure 4.15.

As show in Figure 4.15, we can see that the distribution of the normalized degree of saturation and the sS_r normalized by initial effective overburden pressure at the depth, H, of $1.0D$ are identical as overburden height increases. And it is revealed that the uniqueness of the normalized total and effective loosening earth pressures are observed after scaling the initial effective overburden pressure and the SWCC. The normalized total loosening earth pressure increases as overburden height increases. However, as the overburden height increases, the change of the normalized effective loosening earth pressure depends on the groundwater level, it increases above the groundwater level and decreases below the groundwater level.

4.5 Scale effect in unsaturated ground predicted by the proposed theory

In section 3.6, the scale effect in unsaturated ground was not observed, the probable reason was that the limitation of the scale size of apparatus. Therefore, we intended to apply the proposed theory to predict the scale effect. For the application of the proposed theory, the parameters for the soil-water characteristic curve of Toyoura sand, the internal friction angle of Toyoura sand, and lateral earth pressure coefficient should be determined firstly.

4.5.1 Parameters determination for the proposed theory

Soil-water characteristic curve

As discussion in 4.1.1, van Genuchten equation (1980) was utilized in the proposed theory, in which there were four parameters of S_{min}, α, m, n. Unno at al. (2008) carried out a test to obtain the relationship of suction and degree of saturation following a drying path of Toyoura sand. Hence, experiment data (Unno at al., 2008) was adopted to determine the parameters in van Genuchten equation (1980), which was listed in Table 4-4. Then the observed swcc of Toyoura sand and that predicted by van Genuchten equation (1980) was shown in Fig. 4.16.

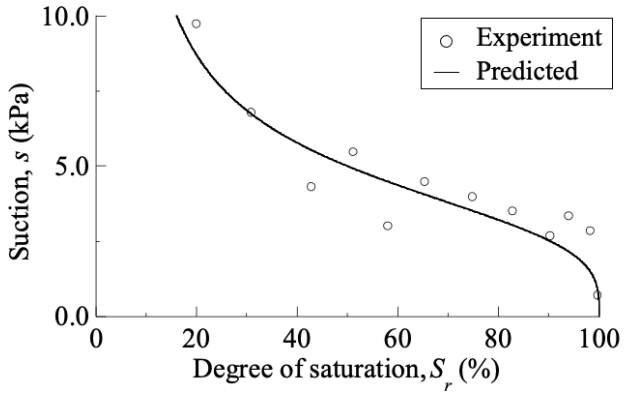

Fig. 4.16 Soil water characteristic curves for Toyoura sand.

Table 4-4 Parameters of the soil–water characteristic curves for Toyoura sand.

S_{max}	1.00	Maximum degree of saturation
S_{min}	0.06	Minimum degree of saturation
α (kPa^{-1})	0.24	Fitting parameter
m	0.71	Fitting parameter
n	3.54	Fitting parameter

Internal friction angle

The internal friction angle of Toyoura sand was determined by direct shear test, herein, the relationship of normal stress and residual shear stress was shown in Fig. 4.17. Hence, internal friction angle of Toyoura sand could be determined as 33.7 degree.

Even though the previous studies indicated that internal friction angle was sensitive to normal stress level (e.g., Palmeira and Gomes, 1996; Zarnani et al., 2011) and inherent anisotropic (e.g., Potts et al., 1987), the internal friction angle corresponding to residual shear stress was adopted here, so the effect of inherent anisotropic could be ignored somewhat. For the effect of normal stress level, internal friction angle was underestimated because normal stress in direct shear test was larger than that in trapdoor test. In this case, the magic parameter, lateral earth pressure coefficient, would be larger, so that the theoretical result could still capture the experimental result.

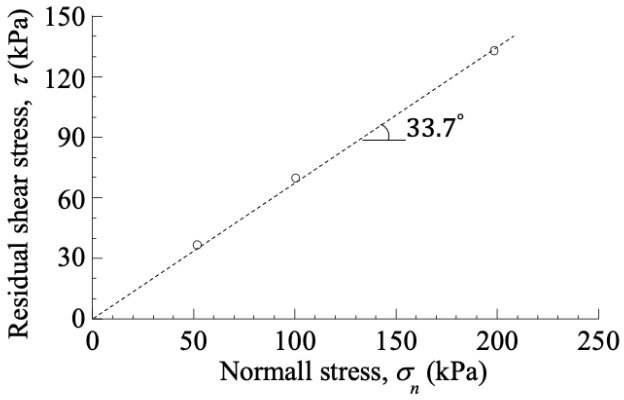

Fig. 4.17 Internal friction angle was determined by direct shear test.

Lateral earth pressure coefficient

Since the dry density (refer to 3.1.3, ρ_d = 1.57 g/cm^3) parameters of swcc and internal friction angle was determined, the lateral earth pressure coefficient K_h for the sand ground above a trapdoor could be determined by comparing the observed loosening earth pressure with that predicted by the proposed theory with different of K_h (= 0.8, 1.0, 1.2, 2.0), which was shown in Fig. 4.18. It was shown that the lateral earth pressure coefficient K_h was better to be 1.2.

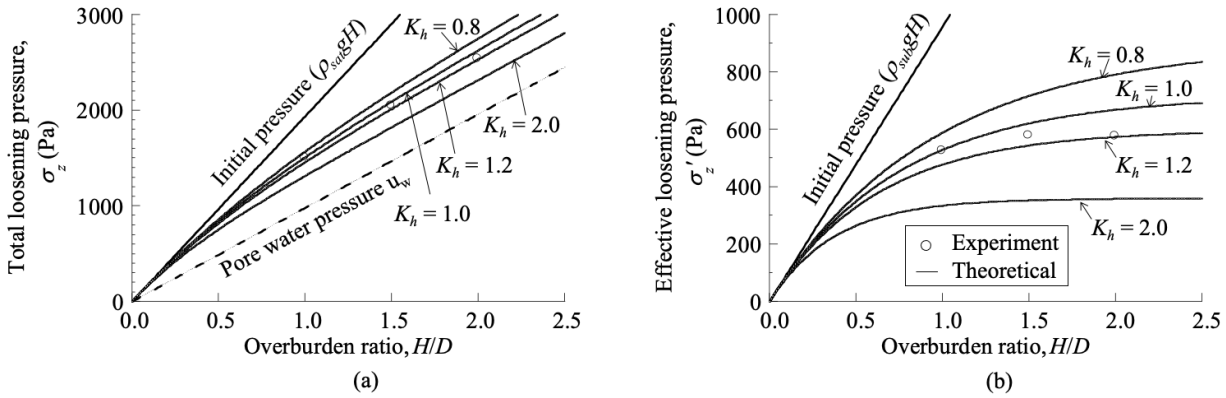

Fig. 4.18 Lateral earth pressure coefficient was determined by comparison of (a) total loosening earth pressure and theoretical prediction with different under of K_h; (b) effective loosening earth pressure and theoretical prediction under different value of K_h.

4.5.2 Scale effect in saturated and unsaturated ground

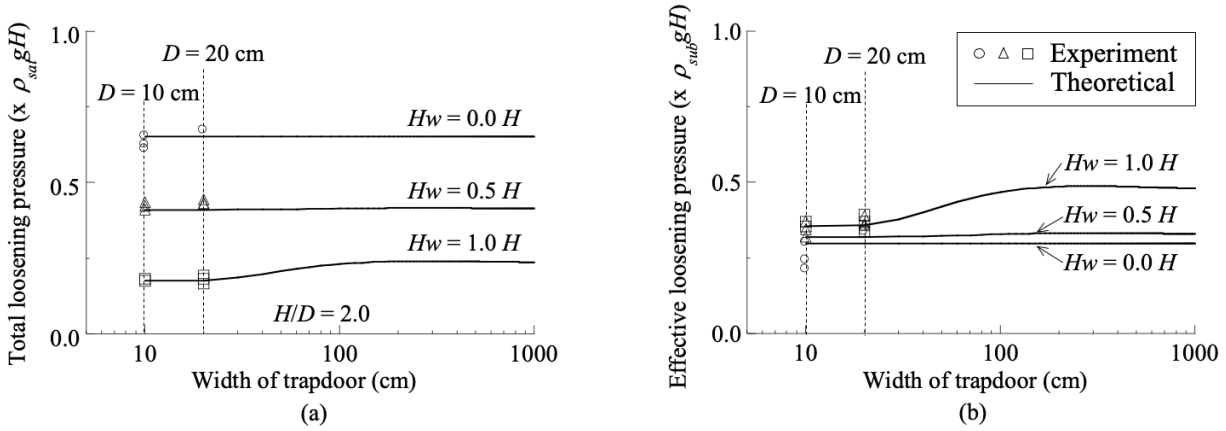

Fig. 4.19 Scale effect was investigated by (a) total loosening pressure (x $\rho_{sat}gH$); (b) effective loosening pressure (x $\rho_{sub}gH$).

Based on the parameters determined in above paragraph, the proposed theory could be applied to predict the scale effect in saturated and unsaturated ground. Overburden ratio was identical (H/D = 2.0), the depth of groundwater level was 0.0, 0.5, 1.0 H respectively. The total and effective loosening earth pressures were normalized by total initial pressure ($\rho_{sat}\ gH$) of saturated ground and effective initial pressure ($\rho_{sub}\ gH$) of saturated ground respectively. The normalized loosening earth pressure under different width of trapdoor for saturated ground (H_w = 0.0 H) and unsaturated ground (H_w = 0.5, 1.0 H) were shown in Fig. 4.19. For the trapdoor test in saturated ground, both the observed normalized total and effective loosening earth pressure and that predicted by the proposed theory were identical even if width of trapdoor was different, which meant there was no scale effect in saturated ground.

For trapdoor test in unsaturated ground, the observed normalized total and effective loosening earth pressure with different width of trapdoor (D = 10, 20 cm) were the same, however, the predicted normalized total and effective loosening pressure with different width of trapdoor were not a straight line, especially the ground was

totally unsaturated (H_w = 1.0 H), which meant scale effect in unsaturated ground existed. The scale effect for trapdoor test in unsaturated ground could not be observed, because the limitation of scale size of width of trapdoor.

4.6 The observed loosening earth pressure compared with that predicted by the proposed theory

Based on the experiment result in chapter 3 and the proposed theory, the comparison of observed and predicted total and effective loosening earth pressures were explored, which was shown in Figs. 4.20 and 4.21. For most of trapdoor tests in saturated and unsaturated ground, it was carried out for three times to validate the repeatability of experiment result. We could see that the observed total and effective loosening earth pressure was consistent with that predicted by the proposed theory. It was revealed that the proposed theory could precisely evaluate the loosening earth pressure acting on a trapdoor, and it could be adopted in practice project in future.

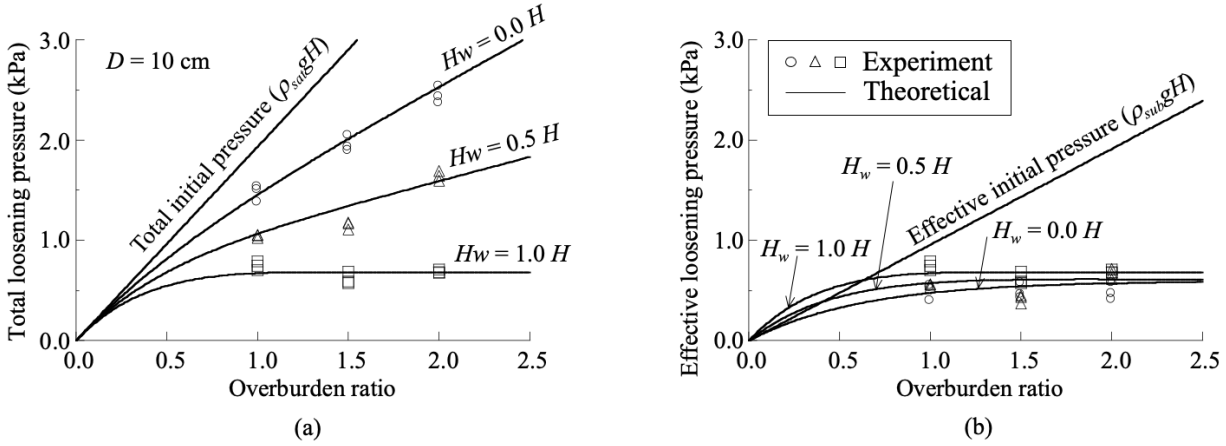

Fig. 4.20 The comparison of experimental and predicted (a) total loosening pressure (D = 10 cm); (b) effective loosening pressure (D = 10 cm).

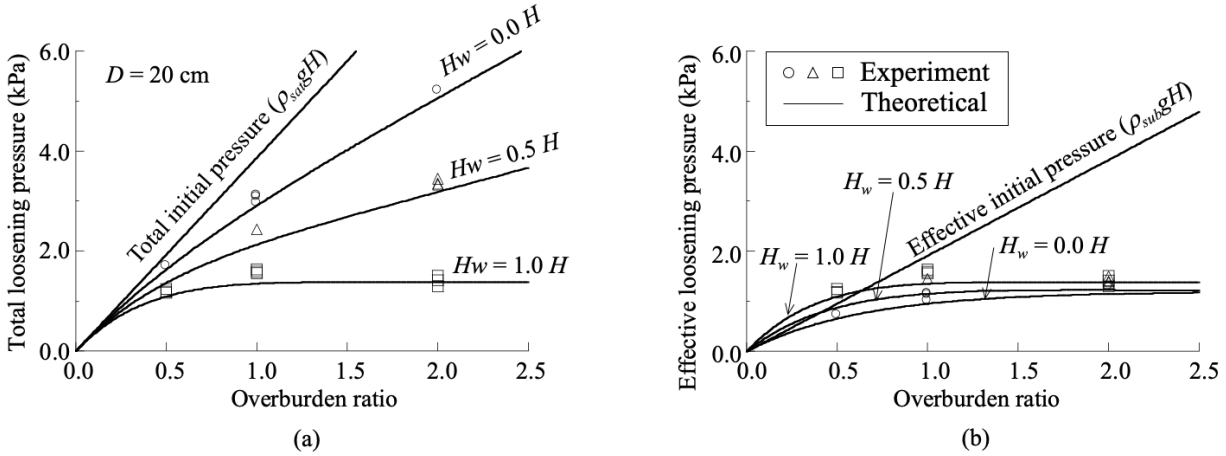

Fig. 4.21 The comparison of experimental and predicted (a) total loosening pressure (D = 20 cm); (b) effective loosening pressure (D = 20 cm).

4.7 Summary

A simple theory for evaluating loosening earth pressure acting on a shallow trapdoor in unsaturated ground was proposed in this paper. The proposed theory was developed based on the limit equilibrium method by combining Bishop's effective stress for unsaturated soils, a classic soil-water characteristic curve, and Mohr-Coulomb failure criteria. The proposed theory predicted valid loosening earth pressures in both fully-saturated and fully-dried grounds compared to pressures calculated by Terzaghi's theory.

Differences in effective loosening earth pressure were demonstrated for different types of unsaturated ground (sandy, loamy and silty clay grounds). In unsaturated ground with high water retention (such as clay soils), higher effective confining pressure and higher shear resistance along the slip surfaces can be expected.

Depth of the groundwater level was shown to have a significant effect on total and effective loosening earth pressures. In unsaturated ground, the total loosening earth pressure was lower than in the saturated ground, but the effective loosening earth pressure tended to be higher. Therefore, the mechanical stability of a shallow tunnel in unsaturated ground will vary with groundwater level fluctuations.

The normalized loosening pressure was identical irrespective of scale in fully-saturated ground, confirming that the scale effect is not significant in fully-saturated ground. In unsaturated ground however, the scale effect on the normalized loosening earth pressure was significant, especially in the case of deeper groundwater level. With a wider trapdoor, the normalized effective loosening earth pressure in the unsaturated zone tended to be smaller, but the normalized total loosening earth pressure tended to be larger.

However, we can also see that the uniqueness of loosening earth pressures is emerged as the loosening pressures and swcc model are normalized by initial pressures and modified swcc parameter α. So by scaling overburden height, loosening pressures and swcc, the scale effect on loosening pressures can be ceased.

Furthermore, the scale effect in unsaturated ground was predicted by the proposed theory, which successfully verified that scale effect in unsaturated ground was existed, it could not be observed in trapdoor test because the limitation of scale size of width of trapdoor. The comparison result of the observed loosening earth pressure with that predicted by the proposed theory was also shown the proposed theory was simple and rational to evaluate loosening earth pressure in unsaturated ground.

CHAPTER 5 THEORIES TO PREDICT THE DISTRIBUTION OF EARTH PRESSURE

In chapter 4, the predicted loosening earth pressure acting on a trapdoor was explored, which was an average pressure. However, experimental result (e.g., Evans, 1984; Kikumoto, 2004) have shown that the distribution of loosening earth pressure on a trapdoor is a symmetric parabola. There are few studies to theoretically evaluate the distribution of loosening earth pressure acting on trapdoor and stress redistribution around the trapdoor. Tamura (2001) proposed a theory to predict the distribution of the passive earth pressure acting on a trapdoor by extending Terzaghi's theory (1943), in which the ground was assumed to be dry state. Kikumoto et al. (2004) also proposed a theory to predict the stress redistribution at stationary zone. However, there is no study on the evaluation of the distribution of loosening earth pressure and stress redistribution in unsaturated ground. Therefore, in this chapter, theories for predicting the distribution of loosening earth pressure across a trapdoor and stress redistribution around the trapdoor respectively were deduced based on the proposed theory and previous theories for trapdoor test in dry ground (Tamura, 2001; Kikumoto et al., 2004). Furthermore, the theories were applied to capture the distribution of earth pressure for trapdoor test in saturated and unsaturated obtained in chapter 3.

5.1 Theories for the distribution of earth pressure

5.1.1 A theory I for the distribution of loosening earth pressure

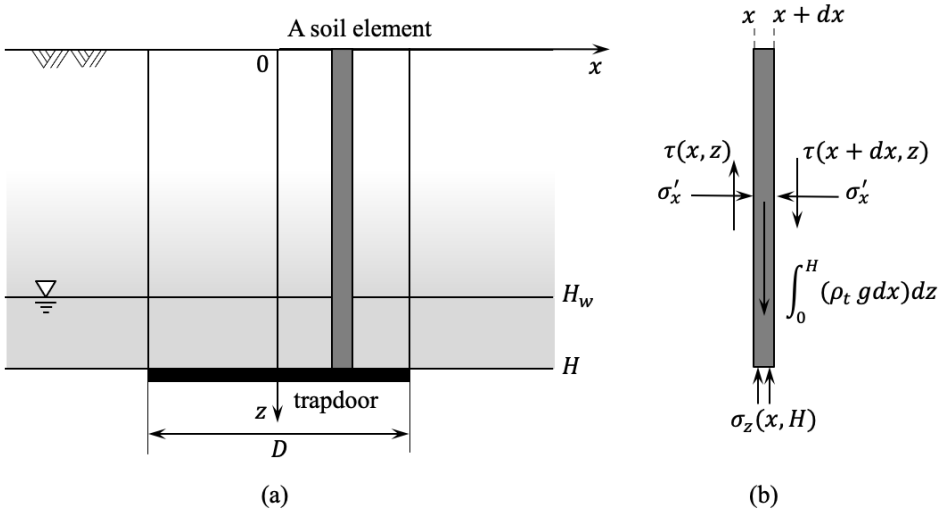

Fig. 5.1 Schematic diagram of (a) active trapdoor model in unsaturated ground; (b) stress distribution on a soil element.

To evaluate the distribution of loosening earth pressure on a trapdoor in unsaturated ground, the schematic view of active trapdoor model is adopted as shown in Fig. 5.1 (a). A trapdoor is located at depth of H, the depth of the groundwater level from the ground surface is defined as H_w. The vertical axis z is along the center line of the trapdoor from the ground surface as the origin. Horizontal axis x is the distance to the origin, which is in the

range of [-*D*/2, *D*/2]. Two vertical failure surfaces are assumed to be developed from the edges of the trapdoor to the ground surface. A small soil element is taken out, on which the stress distribution is shown in Fig. 5.1 (b), herein, the shear stress $\tau(x, z)$ and loosening earth pressure $\sigma_z(x, z)$ vary in both vertical and horizontal direction. By applying the limit equilibrium theory in vertical direction, the first equilibrium equation based on vertical force acting on the soil element above the trapdoor is given as below.

$$-\sigma_z(x,H)dx - \int_0^H \tau(x,z)\,dz + \int_0^H \tau(x+dx,z)\,dz + \int_0^H (\rho_t g dx)\,dz = 0 \tag{5.1}$$

where $\sigma_z(x,H)$ is the loosening earth pressure acting on a trapdoor; $\tau(x,z)$ is shear stress in ground above the trapdoor. By applying Taylor's expansion, the equilibrium equation (5.1) can be written as

$$\sigma_z(x,H) = \int_0^H (\rho_t g)\,dz + \int_0^H \frac{\partial \tau(x,z)}{\partial x}\,dz \tag{5.2}$$

The equation (5.2) is difficult to calculate directly, hence, a significant assumption made by Tamura (2001) should be introduced herein, in which the horizontal distribution of loosening earth pressure at any depth of z should have the same shape except the magnitude $g(z)$ which depends on the depth of *z*. Obviously, $g(z)$ is equal to zero at the ground surface ($z = 0$). Based on the assumption, the loosening earth pressure at any depth of z can be written as

$$\sigma_z(x,z) = f(x)g(z) \tag{5.3}$$

For the shear stress in unsaturated ground, Bishop's effective stress and Mohr-Coulomb failure criteria are still able to evaluate it. Hence, by applying equations (4.8) to (4.10), the shear stress can be written as

$$\tau(x,z) = K_h[\sigma_z(x,z) - u_a + S_r(z)s(z)]tan\phi \tag{5.4}$$

Then, substituting equations (5.3) and (5.4) into equation (5.2) has

$$f(x)g(H) = \int_0^H (\rho_t g)\,dz + \{\int_0^H K_h g(z) tan\phi\,dz\} f(x)' \tag{5.5}$$

where $f(x)'$ is the first derivative of $f(x)$.

For simplifying the calculation of equation (5.5), herein, two definitions are made as

$$\alpha = g(H) \tag{5.6 a}$$

$$\beta = K_h\{\int_0^H g(z)\,dz\}tan\phi \tag{5.6 b}$$

Therefore, equation (5.5) could be simplified as

$$\alpha f(x) = \int_0^H (\rho_t g)\,dz + \beta f(x)' \tag{5.7}$$

By solving the first-order linear differential equation (5.5) yields

$$f(x) = \frac{1}{\alpha}\int_0^H (\rho_t g)\, dz + Ce^{\frac{\alpha}{\beta}x} \tag{5.8}$$

where C is a constant parameter, which could be calculated by initial condition of function $f(x)$.

As the actual loosening earth pressure $\sigma_z(x,z)$ at any depth of z across a trapdoor is assumed in this section, the total load applied on the trapdoor can be calculated by integral of actual loosening earth pressure $\sigma_z(x,z)$ along the width of trapdoor. Hence, the average loosening pressure acting on the trapdoor at any depth can be calculated by dividing total load applied on the trapdoor by area of trapdoor ($1 \times D$), which could be also predicted by the proposed theory shown in the previous section 4.1. Therefore, the second equilibrium equation is written as

$$\frac{2}{D}\int_0^{D/2} \sigma_z(x,z)\, dx = \sigma_z(z) \tag{5.9}$$

Then the first assumption of equation (5.3) is applied to equation (5.9), equation (5.9) reduces to

$$\frac{2}{D}\int_0^{D/2} f(x)g(z)\, dx = \sigma_z(z) \tag{5.10}$$

Herein, another two important assumptions are made as shown below.

$$\frac{2}{D}\int_0^{D/2} f(x)\, dx = 1 \tag{5.11 a}$$

$$g(z) = \sigma_z(z) \tag{5.11 b}$$

Based on the second assumption of equation (5.11 a), the constant parameter of C in equation (5.8) can be determined, substituting equation (5.8) into equation (5.11 a) yields

$$C = D\frac{\int_0^H (\rho_t g)\, dz - \alpha}{2\beta(1 - e^{\frac{\alpha D}{2\beta}})} \tag{5.12}$$

Afterward, substituting equation (5.12) into equation (5.8) to determine the function $f(x)$ of the actual loosening earth pressure yields

$$f(x) = \frac{1}{\alpha}\int_0^H (\rho_t g)\, dz + D\frac{\int_0^H (\rho_t g)\, dz - \alpha}{2\beta(1 - e^{\frac{\alpha D}{2\beta}})}e^{\frac{\alpha}{\beta}x} \tag{5.13}$$

For the second item $g(H)$, it can be evaluated by applying equation (5.11 b). Eventually, the distribution of loosening earth pressure across a trapdoor at depth of *H* could be evaluated by applying equations (5.11 b) and (4.13) to equation (5.3), which is written as

$$\sigma_z(x,H) = f(x)g(H) = \int_0^H (\rho_t g)\, dz + D\alpha\frac{\int_0^H (\rho_t g)\, dz - \alpha}{2\beta(1 - e^{\frac{\alpha D}{2\beta}})}e^{\frac{\alpha}{\beta}x} \tag{5.14}$$

Herein, x is in the range of [0, *D*/2]. For the actual loosening earth pressure acting on another half side of the trapdoor ($x\epsilon[-D/2, 0]$), the magnitude of it is the same as that predicted by equation (5.14) because the actual loosening pressure across the trapdoor is symmetric due to the experiment result (e.g., Evans, 1984; Kikumoto, 2004).

According to equation (5.6 a) and equation (5.11 b), α is written as

$$\alpha = g(H) = \sigma_z(H) \tag{5.15}$$

For the calculation of β, a simple and explicit numerical scheme with incremental depth Δz and equation (5.11 b) are applied to equation (5.6 b), which is shown as below.

$$\beta = K_h\{\int_0^H g(z)\,dz\}tan\phi \approx K_h tan\phi \sum_{i=0}^{i=n} \sigma_z(i \cdot \Delta z)\Delta z \tag{5.16}$$

where n ($n = \frac{H}{\Delta z} - 1$) is a constant parameter. Δz is better to set to a quite small value so that the more precision of β could be obtained.

Overall, the actual loosening earth pressure across a trapdoor in unsaturated ground could be predicted by using equations (5.14), (5.15) and (5.16). For the theory I, the first left and right derivative of equation (5.14) at the center point of trapdoor are not identical, which means the curve of actual loosening pressure at center position of trapdoor is not smooth. However, the experimental result (e.g., Evans, 1984; Kikumoto, 2014) have shown that the actual loosening pressure acting on a trapdoor is smooth everywhere. Hence, the theory proposed in this paragraph has a limitation, but the theory I is simple to predict the distribution of loosening earth pressure across a trapdoor. The theory I will be applied to predict the distribution of loosening earth pressure and compared with that observed in trapdoor test.

5.1.2 A theory II for stress redistribution

As shown in Fig. 5.2 (a), an active trapdoor problem in unsaturated ground is used in this paragraph. The trapdoor is located at depth of *H*, the depth of groundwater level from the ground surface is defined as H_w. Horizontal axis *b* is the distance to the end of a trapdoor, depth of *z* is taken downward from the ground surface. Two vertical sliding surfaces developed from the edges of the trapdoor are assumed herein. For the prediction of stress redistribution $\sigma_z(b, H)$ around the trapdoor, a soil element in stationary zone is taken out, stresses acting on the soil element is shown in Fig. 5.2 (b). According to the limit equilibrium theory, the first equilibrium equation on vertical stress is written as

$$-\sigma_z(b,H)db + \int_0^H \tau(b,z)\,dz - \int_0^H \tau(b+db,z)\,dz + \int_0^H (\rho_t g db)\,dz = 0 \tag{5.17}$$

where $\sigma_z(b,H)$ is the stress redistribution around the trapdoor; $\tau(b,z)$ is shear stress in stationary ground. By applying Taylor's expansion, the equilibrium equation (5.17) reduces to equation (5.18), which is written as

$$\sigma_z(b,H) = \int_0^H (\rho_t g)\,dz - \int_0^H \frac{\partial \tau(b,z)}{\partial b}\,dz \tag{5.18}$$

For the shear stress in equation (5.18), it could be evaluated based on Mohr-Coulomb failure criteria and Bishop's effective stress (1959). By applying equations (4.8) to (4.10), the shear stress can be written as

$$\tau(b,z) = K_s[\sigma_z(b,z) - u_a + S_r(z)s(z)]tan\phi \tag{5.19}$$

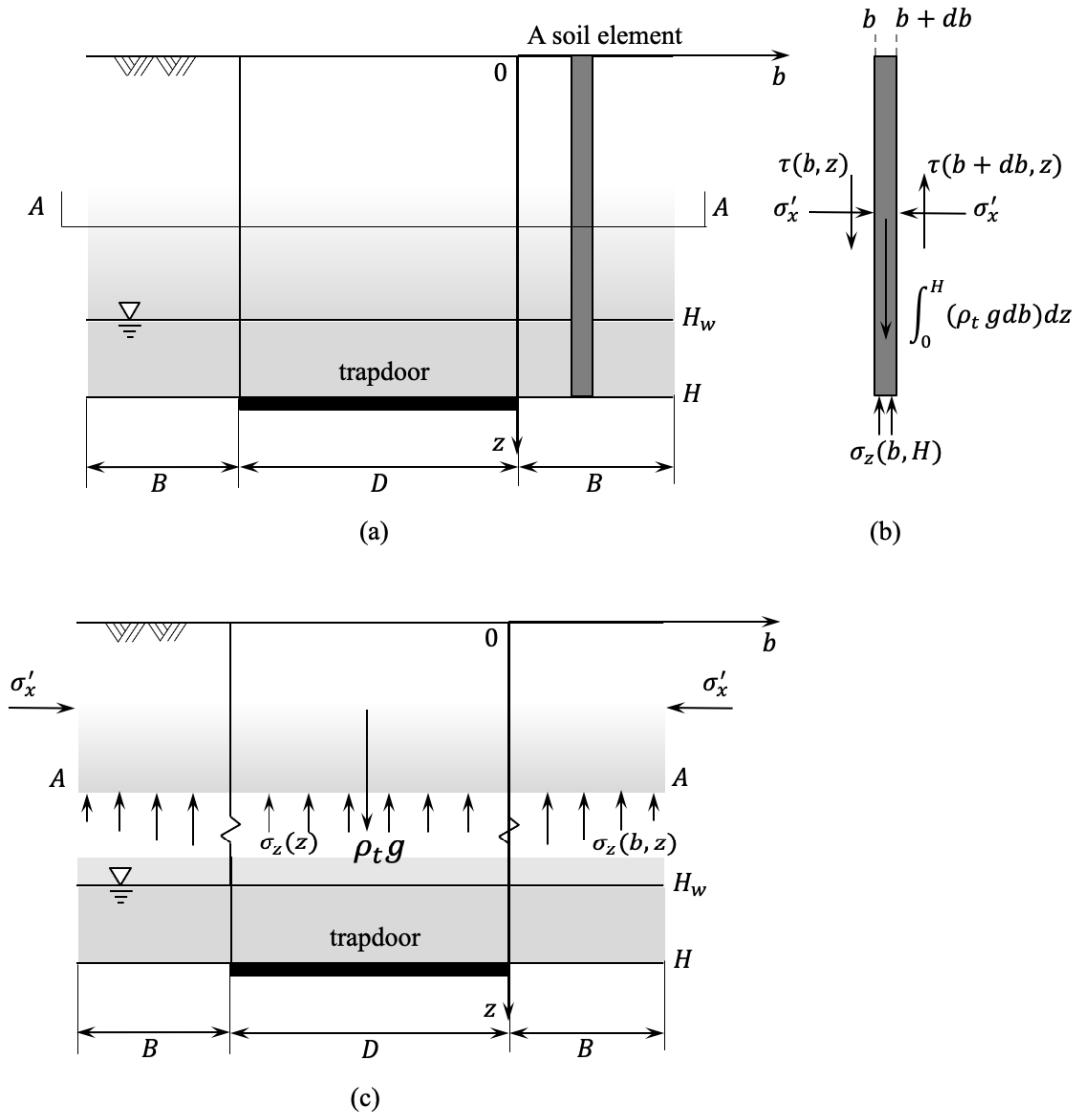

Fig. 5.2 Schematic diagram of (a) trapdoor problem in unsaturated ground; (b) stress distribution on a soil element; (c) section A-A.

Where K_s is the coefficient of lateral earth pressure in the stationary ground. By applying the definition of derivative and equation (5.19) to equation (5.18) yields

$$\sigma_z(b,H) = \int_0^H (\rho_t g)\, dz - \int_0^H \{K_s \sigma_z(b,z) tan\phi\}\, dz \tag{5.20}$$

Equation (5.20) is still not able to do integral directly, hence, a significant assumption (Kikumoto et al., 2004) is adopted to simplify equation (5.20). The principle of the assumption is that the stress redistribution around a trapdoor has the same shape at any depth of z except the magnitude $g(z)$. Meanwhile, the function $g(z)$ should

satisfy one condition that $g(z)$ should be zero at the ground surface ($z = 0$). By using the assumption (Kikumoto et al., 2004), the stress redistribution at any depth z around a trapdoor is written as

$$\sigma_z(b,z) = f(b)g(z) \tag{5.21}$$

Then, by applying equations (5.21) to equation (5.20) has

$$f(b)g(H) = \int_0^H (\rho_t g)\, dz - \{\int_0^H K_s g(z) tan\phi\, dz\} f'(b) \tag{5.22}$$

where $f'(b)$ is the first derivative of $f(b)$.

For simplifying the calculation of equation (5.22), herein, two definitions are made as

$$\alpha = g(H) \tag{5.23 a}$$

$$\beta = K_s\{\int_0^H g(z)\, dz\} tan\phi \tag{5.23 b}$$

Therefore, equation (5.22) could be written as

$$\alpha f(b) = \int_0^H (\rho_t g)\, dz - \beta f'(b) \tag{5.24}$$

By solving the first-order linear differential equation (5.24) yields

$$f(b) = \frac{1}{\alpha}\int_0^H (\rho_t g)\, dz - Ce^{-\frac{\alpha}{\beta}b} \tag{5.25}$$

where C is a constant parameter, which could be calculated by initial condition of function $f(b)$.

To determine the constant parameter C, the second equilibrium equation is needed. Therefore, the ground above an arbitrary depth of z is considered here, the stresses acting on the ground is shown in Fig. 5.2 (c). Herein, shear stress at the boundary is considered to be zero as the distance to the end of trapdoor B is infinite. According to the balance of vertical stress, the second equilibrium equation is written as

$$(D + 2B)\int_0^z (\rho_t g)\, dz = \sigma_z(z)D + 2\int_0^B \sigma_z(b,z)\, db \tag{5.26}$$

By applying the first assumption, equation (5.26) reduces to equation (5.27) as shown below.

$$2\left\{\int_0^B f(b)\, db\right\} g(z) = (D + 2B)\int_0^z (\rho_t g)\, dz - \sigma_z(z)D \tag{5.27}$$

Herein, based on equation (5.27), another important assumption is made as shown below.

$$2\int_0^B f(b)\, db = 1 \tag{5.28a}$$

$$g(z) = (D + 2B)\int_0^z (\rho_t g)\, dr - \sigma_z(z)D \tag{5.28 b}$$

Based on the assumption of equation (5.28 a), the constant parameter C could be evaluated. By substituting equation (5.25) into equation (5.28 a) has

$$C = \frac{2B\int_0^H(\rho_t g)\,dz - \alpha}{2\beta(1-e^{-\frac{\alpha}{\beta}B})} \tag{5.29}$$

Substituting equation (5.29) into equation (5.25) yielded

$$f(b) = \frac{1}{\alpha}\int_0^H(\rho_t g)\,dz - \frac{2B\int_0^H(\rho_t g)\,dz - \alpha}{2\beta(1-e^{-\frac{\alpha}{\beta}B})}e^{-\frac{\alpha}{\beta}b} \tag{5.30}$$

Finally, the stress redistribution around a trapdoor at depth of H could be evaluated by substituting equations (5.21), (5.28 b) and (5.30), which is written as

$$\sigma_z(b,H) = \int_0^H(\rho_t g)\,dz - \alpha\frac{2B\int_0^H(\rho_t g)\,dz - \alpha}{2\beta(1-e^{-\frac{\alpha}{\beta}B})}e^{-\frac{\alpha}{\beta}b} \tag{5.31}$$

Herein, b is in the range of zero to B.

According to equation (5.23 a) and equation (5.28 b), α is calculated as

$$\alpha = g(H) = (D+2B)\int_0^H(\rho_t g)\,dz - \sigma_z(H)D \tag{5.32}$$

For the calculation of β, substituting equation (5.28 b) into equation (5.23 b) has

$$\beta = K_s tan\phi\int_0^H\{(D+2B)\int_0^z(\rho_t g)\,dr - \sigma_z(z)D\}\,dz \tag{5.33}$$

As the second equilibrium equation is established based on an assumption that B is infinite, the equation (5.31) could continue to be simplified. Herein, two limitations are calculated as following.

$$\begin{aligned}\lim_{B\to+\infty}(-\frac{\alpha}{\beta}) &= \lim_{B\to+\infty} -\frac{(D+2B)\int_0^H(\rho_t g)\,dz - \sigma_z(H)D}{K_s tan\phi\int_0^H\{(D+2B)\int_0^z(\rho_t g)\,dr - \sigma_z(z)D\}\,dz}\\ &= -\frac{\int_0^H(\rho_t g)\,dz}{K_s tan\phi\int_0^H[\int_0^z(\rho_t g)\,dr]\,dz}\\ &= -\frac{\int_0^H(\rho_t g)\,dz}{K_s tan\phi\int_0^H[\rho_t g(H-z)]\,dz}\end{aligned} \tag{5.34}$$

$$\lim_{B\to+\infty}(1-e^{-\frac{\alpha}{\beta}B}) = 1 \tag{5.35}$$

Substituting equations (5.32), (5.34) and (5.35) into equation (5.31) has

$$\sigma_z(b,H) = \int_0^H(\rho_t g)\,dz + \frac{[\int_0^H(\rho_t g)\,dz - \sigma_z(H)]D\int_0^H(\rho_t g)\,dz}{2K_s tan\phi\int_0^H[\rho_t g(H-z)]\,dz}e^{-\frac{\int_0^H(\rho_t g)dz}{K_s tan\phi\int_0^H[\rho_t g(H-z)]dz}b} \tag{5.36}$$

In this paragraph, a simple theory II was proposed to predict the stress redistribution around a trapdoor by using equation (5.36). Meanwhile, as a point is far from the end of trapdoor which means *b* is infinite, the earth pressure predicted by equation (5.36) at that point equals to overburden pressure, which is coincide with the expected result. Obviously, the stress redistribution in stationary zone is symmetric, so the magnitude of earth pressure at left side of the trapdoor is the same as that evaluated by equation (5.36) at right side.

5.2 Distribution of earth pressure predicted by theory I and II

To applied theories to predict distribution of loosening earth pressure and stress redistribution, a parameter K_s should be determined. As overburden ratio was 2.0, width of trapdoor was 10 cm, the observed distribution of earth pressure in saturated ground (H_w = 0 .0 cm) compared with that predicted by the theories under various Ks was shown in Fig. 5.3. Obviously, K_s was better to be 0.8 to capture the observed distribution of earth pressure, and this value for K_s was also adopted for prediction in unsaturated ground.

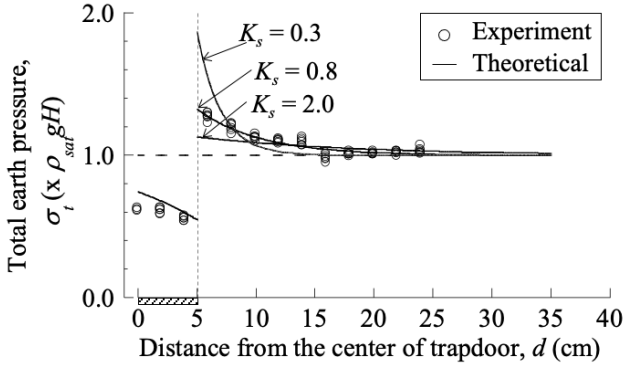

Fig. 5.3 Distribution of earth pressure of trapdoor test in saturated ground for various value of K_s.

Since the distribution of earth pressure in saturated and unsaturated ground were explored in chapter 3, herein, the observed distribution of earth pressure was compared with that predicted by Theory I and II, as shown in Figs. 5.4~5.7. It was shown that the theory I and II could perfectly capture the experiment result in saturated ground. In unsaturated ground, as overburden height was no larger than 20 cm, the theory I and II could capture the stress redistribution observed in trapdoor test. However, as overburden height was 40 cm, the predicted stress redistribution was not consistent with that observed in experiment, the probable reason was that the experiment result was affected by friction as we mentioned in chapter 3. The theory I could capture the distribution of loosening earth pressure across a trapdoor as the ratio of the depth of groundwater level to overburden height was no larger than 0.5. As the ratio of the depth of groundwater level to overburden height was larger than 0.5, the predicted loosening earth pressure had negative pressure, which meant the theory I still had some limitations, the shear stress in the ground above the trapdoor was overestimated as suction was large. The theory I should be improved further in future.

The comparison of the distribution of earth pressure in saturated ground

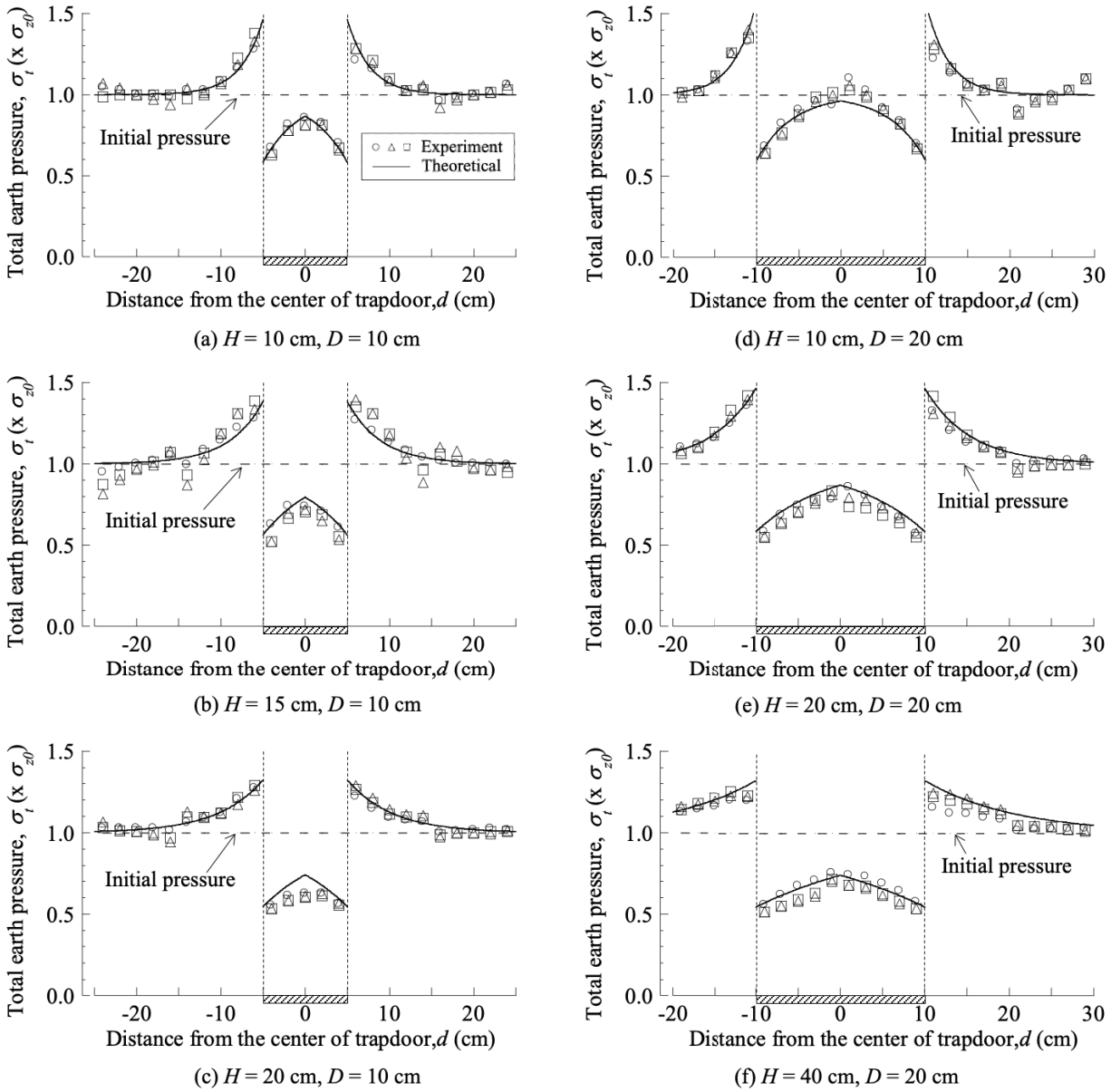

Fig. 5.4 Distribution of the observed and the predicted earth pressure for trapdoor test in saturated ground (a) H/D = 1.0, D = 10 cm, H_w = 0 cm; (b) H/D = 1.5, D = 10 cm, H_w = 0 cm; (c) H/D = 2.0, D = 10 cm, H_w = 0 cm; (d) H/D = 0.5, D = 20 cm, H_w = 0 cm; (e) H/D = 1.0, D = 20 cm, H_w = 0 cm; (f) H/D = 2.0, D = 20 cm, H_w = 0 cm.

The comparison of the distribution of earth pressure in unsaturated ground

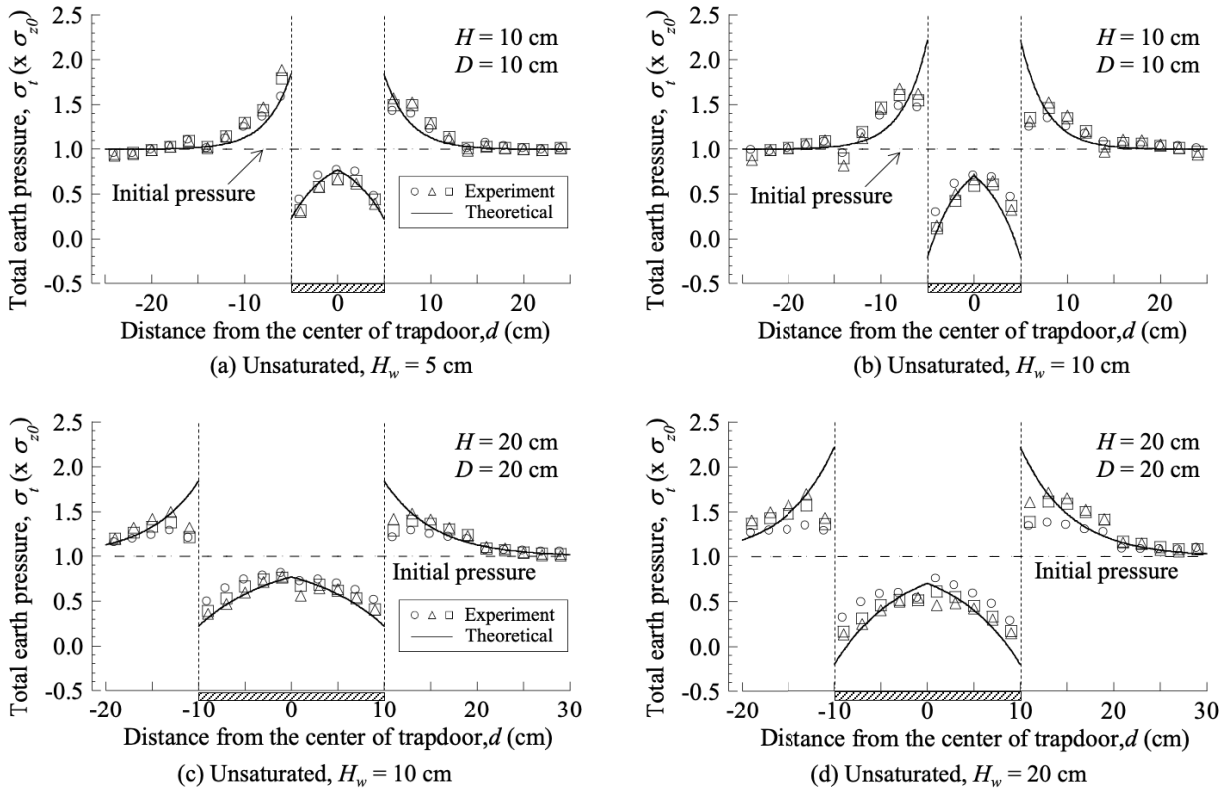

Fig. 5.5 Distribution of the observed and the predicted earth pressure for trapdoor test in unsaturated ground (a) H/D = 1.0, D = 10 cm, H_w = 5 cm; (b) H/D = 1.0, D = 10 cm, H_w = 10 cm; (c) H/D = 1.0, D = 20 cm, H_w = 10 cm; (d) H/D = 1.0, D = 20 cm, H_w = 20 cm.

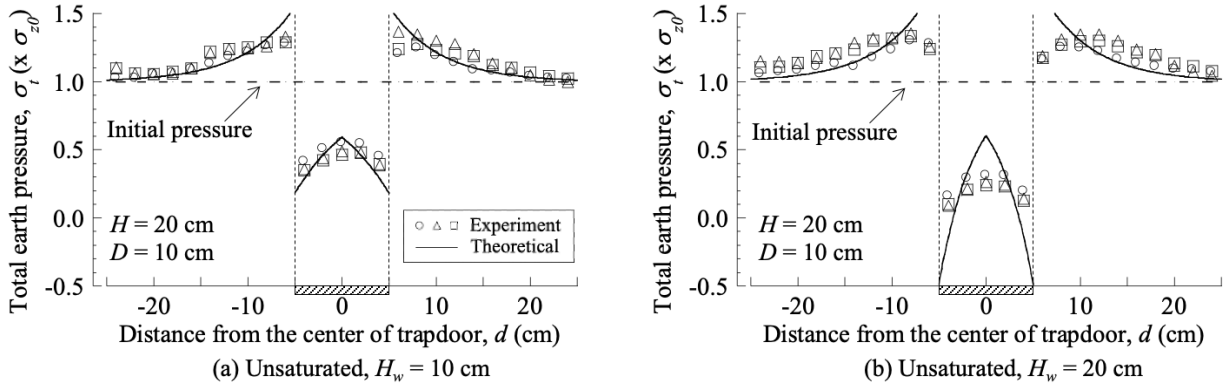

Fig. 5.6 Distribution of the observed and the predicted earth pressure for trapdoor test in unsaturated ground (a) H/D = 2.0, D = 10 cm, H_w = 10 cm; (b) H/D = 2.0, D = 10 cm, H_w = 20 cm.

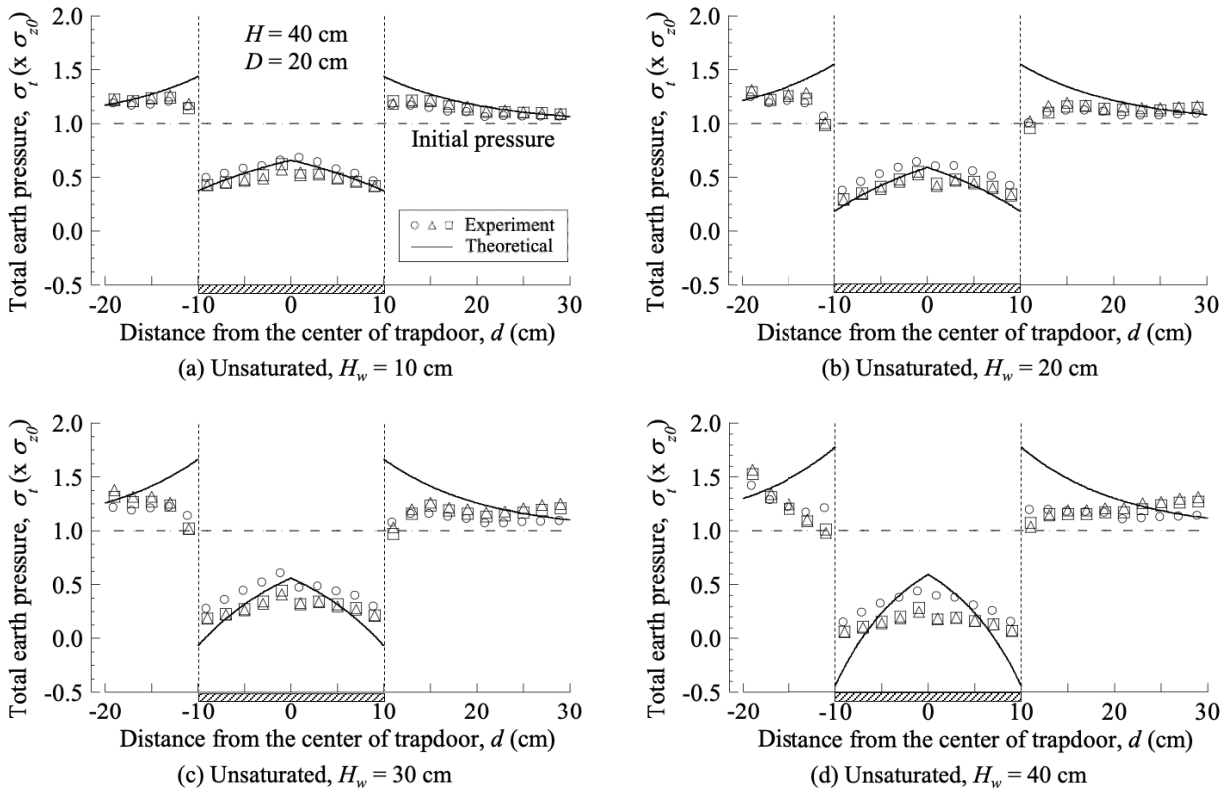

Fig. 5.7 Distribution of the observed and the predicted earth pressure for trapdoor test in unsaturated ground (a) H/D = 2.0, D = 20 cm, H_w = 10 cm; (b) H/D = 2.0, D = 20 cm, H_w = 20 cm; (c) H/D = 2.0, D = 20 cm, H_w = 30 cm; (d) H/D = 2.0, D = 20 cm, H_w = 40 cm.

5.3 Summary

Based on the proposed theory in chapter 4 and the previous contribution (Tamura, 2001, Kikumoto et al., 2004) for predicting the distribution of earth pressure after trapdoor being lowered in dry ground, the theory I and II were developed to predict the distribution of earth pressure in unsaturated ground. For the distribution of earth pressure, the comparison of experiment result and theoretical prediction was also investigated. The conclusion was that the theory I and II could predict the distribution of earth pressure after trapdoor being lowered. However, the theory I for predicting the distribution of loosening earth pressure across a trapdoor had some limitations, especially the depth of groundwater level was larger than 0.5 H, because the shear strength was overestimated. The theory I should be improved further in future.

CHAPTER 6 EFFECT OF THE GROUNDWATER LEVEL RAISE ON LOOSENING EARTH PRESSURE AFTER TRAPDOOR TEST

As we mentioned in chapter 1, the Ushikagi tunnel was collapsed as the groundwater level increased due to agriculture irrigation. It was shown that the changing in the groundwater level affected the stability of a tunnel. To investigate the stability of a tunnel due to the raise of the groundwater level, some tests were carried out in this chapter. Trapdoor test in unsaturated ground was carried out to simulate tunnel excavation, then trapdoor was fixed, the groundwater level was gradually raised to ground surface to explore the changing in distribution of earth pressure and average loosening earth pressure acting on the trapdoor. Furthermore, for the same depth of groundwater level, loosening earth pressure due to the raise of groundwater level was compared with that due to trapdoor being lowered.

6.1 Evolution of loosening earth pressure due to the raise of groundwater level

In this section, a series of tests were conducted to explore the effect of raise of groundwater level on loosening earth pressure. The width of trapdoor was 10 cm, overburden height was 10, 15 and 20 cm respectively, initially, the depth of groundwater level was 1.0 H. Firstly, trapdoor test was carried out by lowering trapdoor until the displacement of trapdoor of 5.0 mm, which was denoted as state 0 as shown as in Fig. 6.1. Then trapdoor was fixed, and the groundwater level was gradually raised to the middle of ground (H_w = 0.5 H), which was denoted as state 1. As the groundwater level attained to groundwater surface (H_w = 0.0 H), it was denoted as state 2.

As shown in Fig. 6.1, overburden height was 20 cm, the depth of groundwater level was 1.0 H. The effect of the groundwater level raise on the distribution of loosening earth pressure was shown in Fig. 6.1 (a). The shape of the distribution of loosening earth pressure was identical, the magnitude of loosening earth pressure became larger, which was less than initial pressure. However, the earth pressure at the stationary zone was smaller, because the soil arching effect became weaker as the depth of groundwater level was smaller. Moreover, to consider the changing in average loosening earth pressure, the relationship of loosening earth pressure and the depth of groundwater level was shown in Fig. 6.1 (b). It was shown that the average loosening earth pressure was larger as the groundwater level was raised to ground surface, during which the mass of water flowed in the ground was also larger. Therefore, one additional test was carried out herein.

The additional test was shown in Fig. 6.2, overburden height was also 20 cm, width of trapdoor was 10 cm, the depth of groundwater level was 1.0 H. Trapdoor was moved upwards until the displacement of trapdoor of 6.0 mm, which was denoted as state 0. Then trapdoor was fixed, the groundwater level was raised to 0.5 H and 1.0 H, which was denoted as state 1 and state 2 respectively. The distribution of loosening earth pressure due to the raise of groundwater level was shown in Fig. 6.2 (a). The shape of the distribution of loosening earth pressure was similar, and the magnitude of loosening earth pressure was smaller, which was larger than initial pressure. Since the reduction of loosening earth pressure became smaller, the earth pressure at stationary zone was also

smaller, soil arching effect was also weaker as the groundwater level gradually moved upwards. Meanwhile, the average loosening earth pressure was smaller as the groundwater level was raised to ground surface, as shown in Fig. 6.2 (b). In the additional test, the mass of water flowed in the ground was also larger, however, the average loosening earth pressure was still smaller, which meant the changing in loosening earth pressure was not due to the increasing of the mass of water.

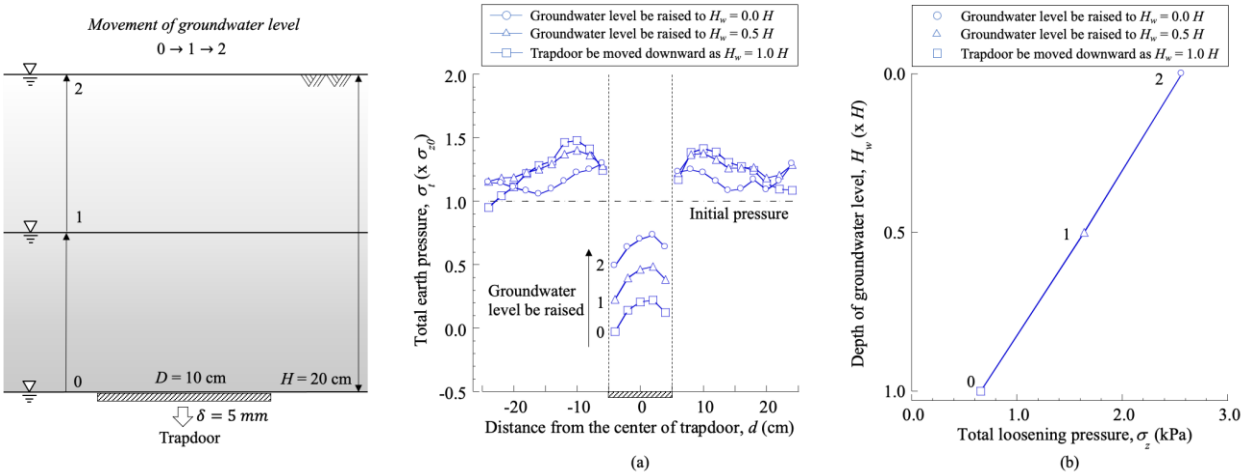

Fig. 6.1 The effect of the groundwater level raise on (a) the distribution of earth pressure (H = 20 cm, D = 10 cm); (b) total loosening earth pressure (H = 20 cm, D = 10 cm).

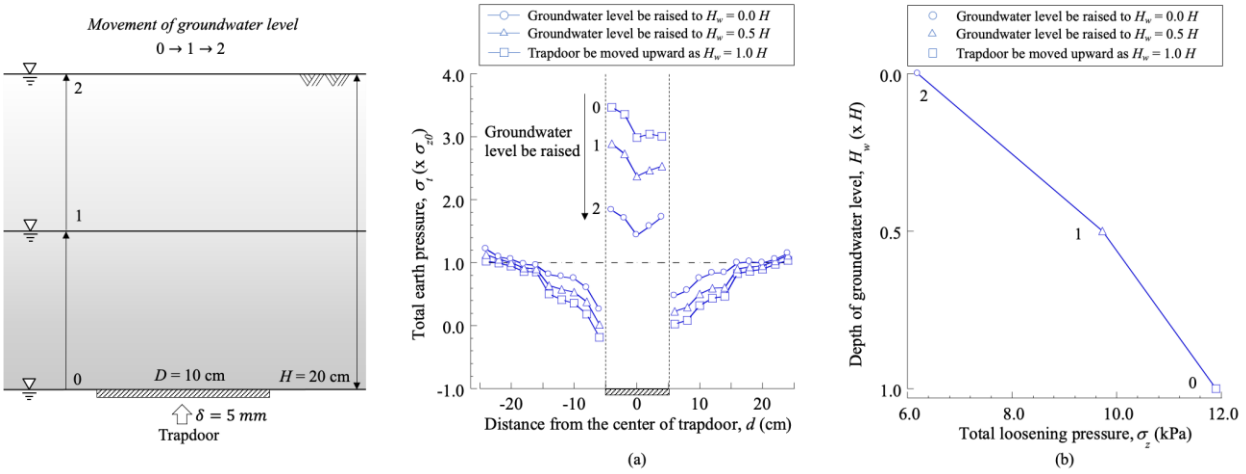

Fig. 6.2 The effect of the groundwater level raise on (a) the distribution of earth pressure (H = 20 cm, D = 10 cm); (b) total loosening earth pressure (H = 20 cm, D = 10 cm).

The comparison of test shown in Fig 6.1 and the additional test shown in Fig. 6.2 was revealed that the effect of the increasing of the mass of water due to groundwater level raise on loosening earth pressure could be ignored. As the groundwater level was raised, shear bands were always existed, the suction was smaller which caused smaller confining pressure and shear stress, hence, the soil arching effect was weaker, the transfer of the weight

of soil above a trapdoor to stationary zone was smaller, that was why loosening earth pressure became larger. And loosening earth pressure was always maximum value as the depth of groundwater level was raised. As width of trapdoor was 10 cm, overburden ratio was 1.0 and 1.5 respectively, the similar tests were also carried out, which was shown in Figs. 6.3 and 6.4, the same tendency of the changing in loosening earth pressure due to the raise of groundwater level was observed.

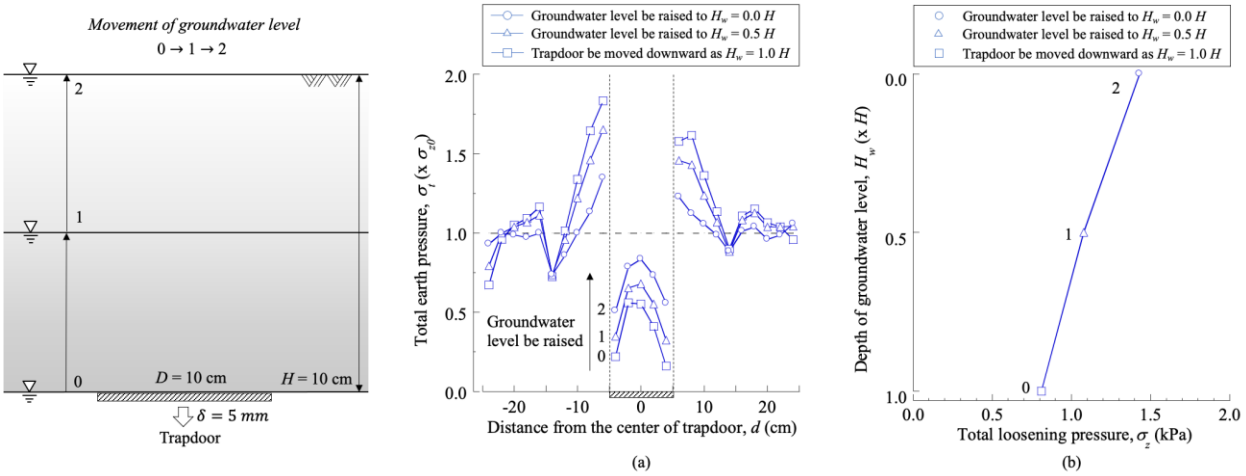

Fig. 6.3 The effect of the groundwater level raise on (a) the distribution of earth pressure (H = 10 cm, D = 10 cm); (b) total loosening earth pressure (H = 10 cm, D = 10 cm).

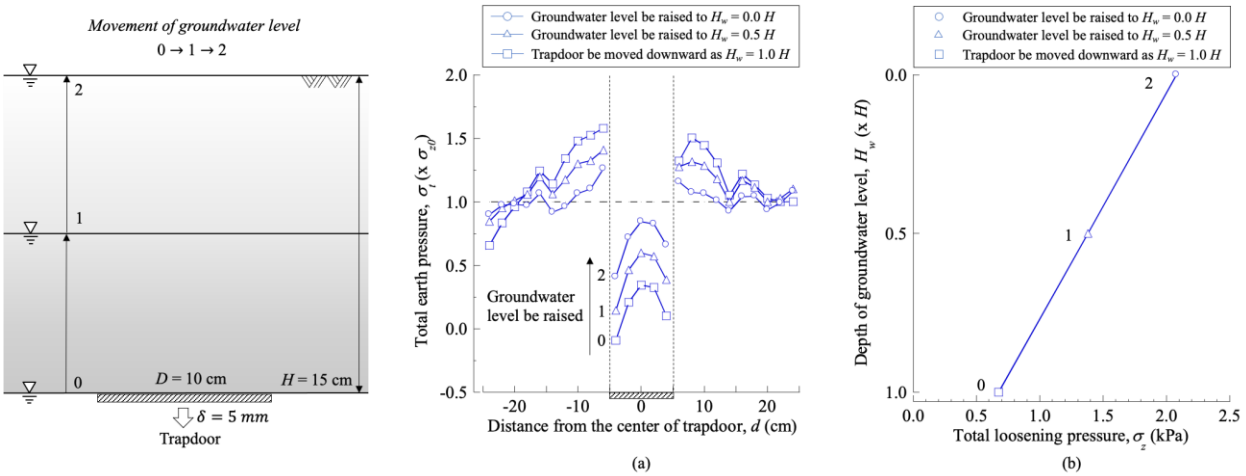

Fig. 6.4 The effect of the groundwater level raise on (a) the distribution of earth pressure (H = 15 cm, D = 10 cm); (b) total loosening earth pressure (H = 15 cm, D = 10 cm).

6.2 Comparison of loosening earth pressures with different path

In previous paragraph, the changing in loosening earth pressure due to the raise of groundwater level was investigated. Herein, when the depth of groundwater level was identical, the relationship of loosening earth pressure due to the raise of groundwater level and loosening earth pressure due to trapdoor being lowered was explored. As the groundwater level was raised to 0.5 *H*, for example, loosening earth pressure was compared with that due to trapdoor being lowered with the depth of groundwater level of 0.5 *H*. Meanwhile, the loosening earth pressure due to the raise of groundwater level was also compared with that predicted by the proposed theory shown in chapter 4. The comparison was summarized in Fig. 6.5. It was revealed that the total loosening earth pressure was larger as the groundwater level was raised to ground surface, which caused the problem of tunnel stability. Moreover, the total loosening earth pressure due to the raise of groundwater level was identical with that due to trapdoor being lowered when the depth of groundwater level was identical, and it was also consistent with that predicted by the proposed theory, which meant the proposed theory could consider the behavior of unsaturated soil. The proposed theory could be utilized to predict the evolution of loosening earth pressure due to the movement of groundwater level in practice project to avoid the problem of tunnel stability, for example, heavy rain in a short period, or agriculture irrigation. For the effective loosening earth pressure, the difference of it with different depth of groundwater level was similar.

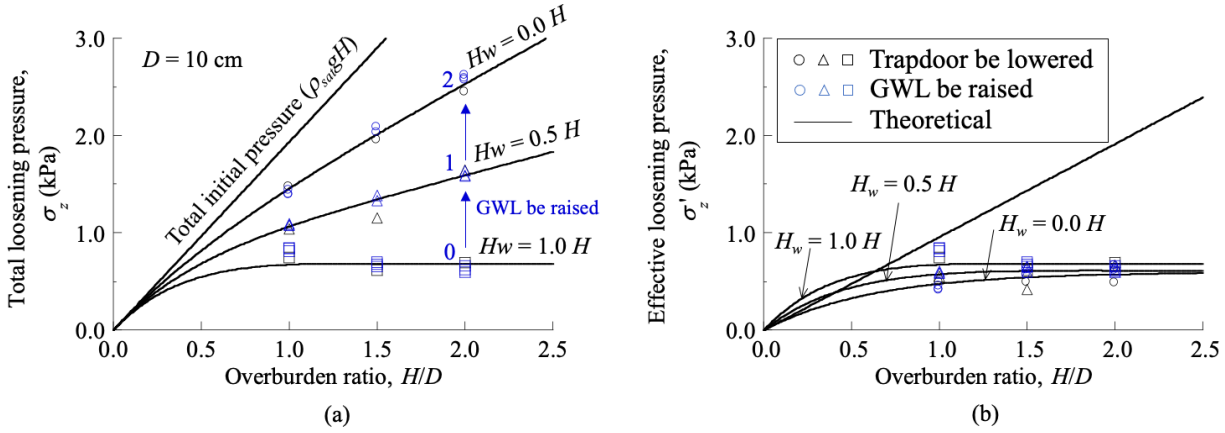

Fig. 6.5 The comparison of loosening earth pressure due to the groundwater level raise with that observed by trapdoor being lowered and that predicted by the proposed theory (a) total loosening earth pressure (*D* = 10 cm); (b) effective loosening earth pressure (*D* = 10 cm).

6.3 Summary

In this chapter, the evolution of loosening earth pressure was investigated as the groundwater level was raised. Meanwhile, when the depth of groundwater level was identical, the loosening earth pressure due to the raise of groundwater level was compared with that observed after trapdoor being lowered and that predicted by the proposed theory. The conclusions were summarized as below:

(1) Loosening earth pressure was larger as the groundwater level was raised to ground surface, because the confining pressure and shear stress was smaller due to the smaller suction, the soil arch effect was significant smaller. The larger loosening earth pressure was easy to cause the problem of tunnel stability.

(2) Loosening earth pressure due to the raise of groundwater level was identical with that observed by trapdoor being lowered and that predicted by the proposed theory when the depth of groundwater level was identical. The proposed theory could be utilized to evaluate the changing in loosening earth pressure due to the movement of groundwater level in practice project in future.

CHAPTER 7 CONCLUSIONS

In this study, soil mechanism of a shallow tunnel excavation in unsaturated ground was explored. Tunnel excavation was simulated by trapdoor test. Therefore, trapdoor test in saturated and unsaturated ground was conducted to explore soil mechanics, failure mechanism and surface settlement. Then a theory was also proposed to evaluate loosening earth pressure in unsaturated ground. Furthermore, the distribution of earth pressure was evaluated theoretically by theory I and II based on the proposed theory. Finally, some tests were carried out to investigate the changing in loosening earth pressure due to the raise of groundwater level. According to the findings in this dissertation, the future research was discussed.

7.1 Conclusions

The key conclusions of this dissertation are shown as following.

- Trapdoor test was carried out in saturated and unsaturated ground. It was shown that the loosening earth pressure gradually decreases from the center to the end of trapdoor, however, at stationary zone, earth pressure at the end of trapdoor is larger than initial pressure, and gradually decreases to initial pressure when the distance to the end of trapdoor is larger. Meanwhile, loosening earth pressure rapidly decreases to minimum pressure as the displacement of trapdoor is 1.0 mm. Moreover, the depth of groundwater level affects total and effective loosening earth pressure. As the depth of groundwater level is deeper, total loosening earth pressure is smaller, however, the corresponding effective loosening earth pressure has a contrary tendency.
- The develop of shear bands is affected by displacement of trapdoor, overburden ratio and the depth of groundwater level. Shear bands in saturated ground is more oblique as overburden ratio is larger. The open of shear bands in unsaturated ground is smaller as the depth of groundwater level is deeper. Multiple shear bands were observed in saturated and unsaturated ground. The first shear bands were emerged as the displacement of trapdoor was 1.0 mm, then the other shear bands inside the first shear bands were observed as the displacement of trapdoor continued to be larger. The maximum surface settlement was smaller as the depth of groundwater level was deeper, this was because the larger suction caused larger confining pressure and shear stress.
- The vertical distribution of total and effective loosening earth pressure in unsaturated ground predicted by the proposed theory is totally different with that in saturated ground. The effect of depth of groundwater level and types of soils on loosening earth pressure, and scale effect were discussed. Total loosening earth pressure is smaller as the depth of groundwater level is deeper, however, the corresponding effective loosening pressure has contrary tendency. Differences in effective loosening earth pressure were demonstrated for different types of unsaturated ground (sandy, loamy and silty clay grounds). In unsaturated

ground with high water retention (such as clay soils), higher effective confining pressure and higher shear resistance along the slip surfaces can be expected.

- Scale effect in unsaturated ground is not observed in the experiment, however, the proposed theory identifies that scale effect should be considered. Contrarily, there is no scale effect in saturated ground, which is verified by experimental result and predicted result. Furthermore, the observed loosening earth pressure is consistent with that predicted by the proposed theory, which means the proposed theory is a valid model to predict loosening earth pressure in practice project.
- Theories for evaluating the distribution of earth pressure are effective to capture the observed distribution of earth pressure, of which one limitation is that the distribution of loosening earth pressure has some negative pressure.
- Loosening earth pressure due to the raise of groundwater level is consistent with that due to trapdoor being lowered as the depth of groundwater level are identical. Meanwhile, the changing in loosening earth pressure due to the raise of groundwater level can be predicted by the proposed theory, which means the proposed theory can consider behavior of unsaturated soils.

7.2 Future research

Mechanism of shallow tunnel excavation in unsaturated ground is explored through trapdoor test in this dissertation. According to the discussion and conclusions in this study, future research activities are summarized as following.

- The theories for evaluating the distribution of earth pressure would be improved further to eliminate its limitation.
- Loosening earth pressure in saturated ground is obtained initially by trapdoor test, then the depth of groundwater level is gradually decreased to explore the changing in loosening earth pressure. Meanwhile, loosening earth pressure due to the decrease of groundwater level is compared with that due to trapdoor being lower and that predicted by the proposed theory as the depth of groundwater level is identical.
- Since an unsaturated soil model haves been proposed (Kikumoto et al., 2010), I intend to apply the model to do some simulation to explore soil mechanics of trapdoor test.

REFERENCES

Adachi, T., Kimura, M. and Kishida, K. (2003), Experimental study on the distribution of earth pressure and surface settlement through three-dimensional trapdoor tests, *Tunnelling and Underground Space Technology*, 18: 171-183.

Ahmadi, A. and Ehsan Seyedi Hosseininia, E. S. (2018), An experimental investigation on stable arch formation in cohesionless granular materials using developed trapdoor test, *Powder Technology*, 330: 137-146.

Atkinson, J. H. and Potts, D. M. (1977), Stability of a shallow circular tunnel in cohesionless soil, *Geotechnique*, 27, NO. 2: 203-215.

Aubeny, C. and Lytton, R. (2003), *Estimating strength versus location and time in high-plasticity clays*, Texas A&M University, Texas, United States.

Bao, C. G., Gong, B. and Zhan, L. (1998), Properties of unsaturated soils and slope stability of expansive soils, *Proceedings of the 2nd international conference on unsaturated soils Beijing*, China: 71-98.

Bierbaumer, A. (1913), *Die dimensionerung des tunnelmauerwerks*, Engelmann, Leipzig, Germany.

Bishop, A. W. (1959), The principle of effective stress, *Teknisk Ukeblad*, 39: 859–863.

Bishop, A.W. and Blight, E. (1963), Some aspects of effective stress in saturation and partly saturated soils, *Geotechnique*, 13 (3): 177-197.

Bishop, A.W. and Donald, I.B., (1961), The experimental study of partially saturated soils in the triaxial apparatus. *Proc. 5 th ICSMFE*, Paris, 1: 13-21.

Borja RI. (2006), On the mechanical energy and effective stress in saturated and unsaturated continua, *International Journal of Solids and Structures*, 43: 1764–1786.

Britton, E. J. and Naughton, P. J. (2011), The Arching Phenomena Observed in Experimental Trap Door Model Tests, *Geo-Frontiers* (ASCE): 788-797.

Brooks, R. H. and Corey, A. T. (1964), *Hydraulic properties of porous medium*, Colorado State University, Fort Collins, Hydrology Paper NO. 3.

Burdine, N. T. (1953), Relative permeability calculations from pore size distribution data, *Journal of Petroleum Technology*, 5: 71-78.

Chen, K. H. and Peng, F. L. (2018), An improved method to calculate the vertical earth pressure for deep shield tunnel in Shanghai soil clay, *Tunneling and Underground Space Technology*, 75: 43–66.

Chevalier, B. and Otani, J. (2011), Arching observation in three-dimensional trapdoor problem with X-ray CT and discrete element method, *Soils and Foundations*, 51 (3): 459-469.

Chevalier, B., Combe, G. and Villard, P. (2012), Experimental and discrete element modeling studies of the trapdoor problem: influence of the macro-mechanical frictional parameters, *Acta Geotechnica*, 7: 15-39.

Costa, Y. D., Zornberg, J. G., Bueno, B. S. and Costa, C. L. (2009), Failure Mechanisms in Sand over a Deep Active Trapdoor, *J. Geotech. Geoenviron. Eng.*, 135 (11):1741-1753.

Dang, H. K. and Meguid, M. (2008), 3D simulation of the trap door problem using the Discrete Element Method, *Proceedings of the 61st Canadian Geotechnical Conference*, 1, Edmonton, Alberta, Canada.

Daniels, K. E., Kollmer, J. and Puckett, J. G. (2017), Photoelastic force measurements in granular materials, *Review of Scientific Instruments*, 88, 051808.

Davis, E. H. (1968), theories of plasticity and the failure of soil masses, *Soil Mechanics: selected topics*, Butterworths, London: 341-380.

Dewoolkar, M. M., Santichaianant, K., and Ko, H. Y. (2007), Centrifuge modeling of granular soil response over active circular trapdoors, *Soils and Foundations*, 47 (5): 931-945.

Engesser, Fr. (1882), Ueber den Erdduck gegen innere Stützwande (Tunnelwande), *Deusche Bauzeitung*, 16: 91-93 (In German).

Feld, J. (1948), Early History and Bibliography of Soil Mechanics, *Proceedings of Second International Conference on Soil Mechanics and Foundation Engineering*, Rotterdam, Vol. 1: 1-7.

Fredlund, D. G. and Pham, H. Q. (2006), A volume-mass constitutive model for unsaturated soils in terms of two independent stress state variables, *Proceeding of 4th International Conference on Unsaturated Soils*, ASCE, Carefree, Arizona: 105-134.

Fredlund, D. G. and Rahardjo, H. (1993), *Soil Mechanics for Unsaturated Soils*, Wiley-Interscience.

Fredlund, D. G. and Rahardjo, H. (1993a), *Soil mechanics for unsaturated soils*, John Wiley & Sons, New York.

Fredlund, D. G. and Rahardjo, H. (1993b), An overview of unsaturated soil behaviour, *Proceedings of the American Society of Civil Engineers Specialty Series on Unsaturated soil Properties*, Dallas, Tex., USA: 1-31.

Fredlund, D. G. and Xing, A. (1994), Equations for the soil-water characteristic curve, *Can. Geotech. J*., 31, 521-532.

Fredlund, D. G. and Xing, A. (1994), Equations for the soil-water characteristic curve, *Can. Geotech. J.*, 31: 521-532.

Fredlund, D. G., Morgenstern N.R. and Widger R.A. (1978), The shear stress of unsaturated soils, *Can. Geotech. J*., 15, 313–321.

Fredlund, D. G., Sheng, D. and Zhao, J. (2011), Estimation of soil suction from the soil-water characteristic curve, *Can. Geotech. J.*, 48: 186-198.

Fredlund, D. G., Xing, A., Fredlund, M. D. and Barbour, S. L. (1995), The relationship of the unsaturated soil shear strength to the soil-water characteristic curve, *Can. Geotech. J*., 32, 440-448.

Fredlund, M. D., Wilson, G. W. and Fredlund, D. G. (2002), Use of grain-size distribution for estimation of the soil-water characteristic curve, *Can. Geotech. J.*, 39 (5): 1103-1117.

Gan, J. K. M., Fredlund, D. G. and Rahardjo, H. (1988), Determination of the shear strength parameters of an unsaturated soil using the direct shear test, *Can. Geotech. J*., 25, 500–510.

Gardner, W. R. (1958), Some steady state solutions of the unsaturated moisture flow equation with application to evaporation from a water table, *Soil Science*, 84 (4): 228-232.

Garven, E. A. and Vanapalli, S. K. (2006), Evaluation of empirical procedures for predicting the shear strength of unsaturated soils, *Proceedings of the 4th International Conference on Unsaturated Soils*, Carefree, Arizona, United States: 2570-2581.

Guan, G. S., Rahardjo, H. and Choon, L. E. (2010), Shear strength equations for unsaturated soil under drying and wetting, *J. Geotech. Geoenviron. Eng*., 136 (4): 594-606.

Guo, P. J. andShunhua Zhou, S. H. (2013), Arch in granular materials as a free surface problem, *Int. J. Numer. Anal. Meth. Geomech.*, 37: 1048-1065.

Hains, W. B. (1930), Studies in the physical properties of soil. V. The hysteresis effect in capillary properties, and the modes of moisture distribution associated therewith, *The Journal of Agricultural Science*, 20:97–116.

Handy, R. L. (1985), The arch in soil arching, J. Geotech. Engrg., 111 (3): 302-318.

Harris, G. W. (1974), A Sandbox Model Used to Examine the Stress Distribution Around a Simulated Longwall Coal-Face, *International Journal of Rock Mechanics, Mining Science and Geomechanical Abstracts*, Pergamon Press, 11: 325-335.

Hodnett, M. G. and Tomasella, J. (2002), Marked differences between van Genuchten soil water-retention parameters for temperate and tropical soils: a new water-retention pedo-transfer functions developed for tropical soils, Geoderma, 108: 155–180.

Hong, W. P., Lee, J. H. and Lee, K. W. (2007), Load transfer by soil arching in pile-supported embankments, *Soils and Foundations*, 47 (5): 833-843.

Iglesia, G. R., Einstein, H. H. and Whitman, R. V. (2014), Investigation of soil arching with centrifuge tests, *J. Geotech. Geoenviron. Eng.*, 140 (2): 04013005.

Jacobsz, S. (2016), Trapdoor experiments studying cavity propagation, *Proceedings of the 1st Southern African Geotechnical Conference*, Sun City, South Africa, Vol. 1: 159-165.

Jaky, J. (1948), Pressure in silos, *Proceeding of Second International Conference on Soil Mechanics and Foundation Engineering*, Rotterdam, 1: 103-107.

Jennings, J. E. B. and Burland, J. B. (1962), Limitations to the use of effective stresses in partly saturated soils, *Geotechnique*, 12: 125-144.

Jiang, M. J., Du, W. and Xi, B. (2018), Distinct element analysis of Trapdoor test for cemented soils, *Proceeding of GeoShanghai 2018 International Conference: Fundamentals of Soil Behaviours*: 718-726.

Khalili, N. and Khabbaz, M. H. (1998), A unique relationship for χ for the determination of the shear strength of unsaturated soils, *Geotechnique*, 48 (5): 681-687.

Khalili, N., Geiser, F. and Blight, G. E. (2004), Effective stress in unsaturated soils: Review with new evidence, *Int. J. Geomech*., 4: 115-126.

Kikumoto, M. (2004), *Study on earth pressure mechanics around a tunnel*, Ph.D. thesis, Kyoto university (In Japanese).

Kikumoto, M. and Kishida, K. (2003), Mechanical behavior on the Sandy ground through the 3-D Trapdoor Experiment, *Proc. of the 12th Asian Regional conf. on Soil Mechanics and Geotechnical Engineering*, Singapore, Singapore, 1, 863–866.

Kikumoto, M., Kimura, M., Kishida, K. and Adachi, T. (2003), 3d trapdoor tests and its simulation on mechanical behavior of ground during tunneling, *J. JSCE*, 750/III-65, 145–158 (in Japanese).

Kikumoto, M., Kimura, M., Kishida, K. and Tamura, T. (2004), Estimation of the distribution of earth pressure around a tunnel, *Journal of Tunnel Engineering*, JSCE, 14: 27-34.

Kikumoto, M., Kyokawa, H., Nakai, T. and Shahin, H. M. (2010), A simple elasto–plastic model for unsaturated soils and interpretations of collapse and compaction behaviours, *Proceedings of the 5th International Conference on Unsaturated Soils*, Alonso E, Gens A (eds.), 849–855.

Kim, W. S. and Borden, R. H. (2011), Influence of soil type and stress state on predicting shear strength of unsaturated soils using the soil-water characteristic curve, *Can. Geothech. J.*, 48: 1886-1900.

Kohgo, Y., Nakano, M. and Miyazaki, T. (1993), Theoretical aspects of constitutive modelling for unsaturated soils, *Soils and Foundations*, 33 (4): 49-63.

Komolvilas, V. and Kikumoto, M. (2017), Simulation of liquefaction of unsaturated soil using critical state soil model, *Int. J. Numer. Anal. Meth. Geomech*., 41: 1217–1246.

Kong, X. X., Liu, Q. S., Zhang, Q. B., Wu Y. X. and Zhao, J. (2018), A method to estimate the pressure arch formation above underground excavation in rock mass, *Tunneling and Underground Space Technology*, 71: 382-390.

Koutsabeloulis, N. C. and Griffiths, D. V. (1989), Numerical modelling of the trap door problem, *Geotechnique*, 39 (1): 77-89.

Krynine, D. P. (1945), Discussion of 'stability and stiffness of cellular cofferdams,' by Karl Terzaghi, Trans. Am. Soc. Civ. Eng., 110: 1175-1178.

Ladanyi, B. and Hoyaux, B. (1969), A study of the trap-door problem in a granular mass, *Can. Geotech. J*., 6 (1): 1-14.

Lamborn, M. J. (1986), *A micromechanical approach to modelling partly saturated soils*, M. Sc. Thesis, Texas A & M University, Texas, United States.

Lee, I. M., Sung, S. G. and Cho, G. C. (2005), Effect of stress state on the unsaturated shear strength of a weathered granite, *Can. Geotech. J*., 42: 624-631.

Leong, E. C. (2019), Soil-water characteristic curve – Determination, estimation and application, *Proceeding of 7th Asia-Pacific Conference on Unsaturated Soils*, 7 (2): 21-30.

Leontovich, V. (1959), *Frames and arches: Condensed solutions for structure analysis*, McGraw Hill, New York.

Liang, L. J. and Xu, C. J. (2019), Numerical and theoretical research on stress distribution in the loosening zone of the trapdoor problem, *Int. J. Numer. Anal. Methods Geomech*., 43 (7): 1426-1447.

Liang, L. J., Xu, C. J., Chen, Q. Z. and Chen, Q. S. (2020), Experimental and Theoretical Investigations on Evolution of Soil-Arching Effect in 2D Trapdoor Problem, *Int. J. Geomech*., 20 (6): 06020007.

Lu, N. and Likos, W. J. (2006), Suction Stress Characteristic Curve for Unsaturated Soil, J. *Geotech. Geoenviron. Engrg.*, 132 (2): 131–142.

Mahdi, A. N., Han, J., Jawad, S., Abdulrasool, G. and Xu, C. (2017), Investigation of stability of soil arching under surface loading using trapdoor model tests, *Proceedings of the 19th International Conference on Soil Mechanics and Geotechnical Engineering*, Seoul, Korea.

Marston, A. and Anderson, A. O. (1913), *The theory of loads on pipes in ditches and tests of cement and clay drain tile and sewer pipe*, Bulletin 31, Iowa Engineering Experiment Station, Iowa State College, Ames, IA.

McKee, C. R. and Bumb, A. C. (1984), The importance of unsaturated flow parameters in designing a monitoring system for hazardous wastes and environmental emergencies*, Proceeding of Hazardous Materials Control Research Institute National Conference*, Huston, Tex.: 50-58.

McKee, C. R. and Bumb, A. C. (1987), Flow-testing coalbed methane production wells in the presence of water and gas, *Society of Petroleum Engineers (SPE) Formation Evaluation*, Richardson, Tex.: 599-608.

McNulty, J. W. (1965), *An experiment study of arching in sand*, Technical Report No. I-674, US. Waterways Experiment Station, Vicksburg.

Möller, T. (2020), *Sinkhole formation: can a comparison with tunneling illuminate the process?*, Ph. D. Thesis*,* University of Cambridge, UK.

Mualem, Y. (1976), A new model for predicting hydraulic conductivity of unsaturated porous media, *Water Resources Research*, 12 (3): 513-522.

Murayama, S. and Matsuoka, H. (1971), Earth pressure on tunnels in sandy ground, *Proc. of JSCE*, 187: 95–108 (in Japanese).

Nakai, T., Xu, L. M. and Yamazaki, H. (1997), 3D and 2D model tests and numerical analyses of settlements and earth pressures due to tunnel excavation, *Soils and Foundations*, 37 (3): 31-42.

Nakamura, K. and Kikumoto, M. (2014), Modeling water-NAPL-air three -phase capillary behavior in soils, *Soils and Foundations*, 54 (6), 1225–1235.

Ng, C. W. W. and Menzies, B. (2007), Advanced Unsaturated Soil Mechanics and Engineering, Taylor & Francis.

Öberg, A. and Sällfors, G. (1997), Determination of shear strength parameters of unsaturated silts and sands based on the water retention curve, *Geotech. Testing J.*, 20 (1): 40–48.

Oberg, A. L. and Sallfors, G. (1997), Determination of shear strength parameters of unsaturated silts and sands based on water retention curve, *Geotechnical Testing Journal*, 20: 40-48.

Palmeira, E. M. and Gomes, R. C. (1996), Comparisons of predicted and observed failure mechanisms in model reinforced soil walls, *Geosynthetics International*, Vol. 3, No. 3: 329–347.

Park, K. H. and Jung, Y. H. (2020), Quantitative detection of contact force chains in a model particle assembly using digital RGB photoelastic measurements, *KSCE J. Civ. Eng*., 24 (1): 63-72.

Park, K. H., Baek, S. H. and Jung, Y. H. (2020), Investigation of arch structure of granular assembly in the trapdoor test using digital RGB photoelastic analysis, *Powder Technology*, 366: 560-570.

Pereira, J. H. F. and Fredlund, D. G. (2000), Volume change behavior of collapsible compacted gneiss soil, *J. Geomech. Geoenviron. Eng.*, 126 (10): 907-916.

Potts, D. M., Dounias, G. T. and Vaughan, P. R. (1987), Finite element analysis of the direct shear box test, *Geotechnique*, 37, No. 1: 11–23.

Pufahl, D., Fredlund, D. G. and Rahardjo, H. (1983), Lateral earth pressures in expansive clay soil, *Can. Geotech. J.*, 20: 228–241.

Rassam, D. W. and Cook, F. J. (2002), Predicting the shear strength envelope of unsaturated soil, *Geotechnical Testing Journal*, 28: 215-220.

Rui, R., Ye, Y. Q. et. al. (2020), Experimental and Theoretical Investigations on Active Earth Pressure Distributions behind Rigid Retaining Walls with Narrow Backfill under a Translational Mode, *Int. J. Geomech*., 20 (10): 04020178.

Rui, R., Zhai, Y. X., Han, J. van Eekelen, S. J. M. and Chen, C. (2019b), Deformations in trapdoor tests and piled embankments, *Geosynthetics International*, 27 (2): 219-235.

Sadrekarimi, J. and Abbasnejad, A. (2010), Arching effect in fine sand due to base yielding, *Can. Geotech. J.*, 47: 366-374.

Sahoo, J. P. and Ganesh, R. (2018), Active earth pressure on retaining walls with unsaturated soil backfill, *Proc. Ground Improvement and Earth Structures*, 1–19.

Schnellmann, R. (2015), Uncertainties in the estimation of unsaturated shear strength from soil-water characteristic curve, Ph. D. Thesis, Nanyang Technological University, Singapore.

Schrefler, B. A. (1984), *The finite element method in soil consolidation (with applications to surface subsidence)*, Ph.D. Thesis, Swansea Univ., UK.

Shahin, H. M., Nakai, T., Zhang, F., Kikumoto, M. and Nakahara, E. (2011), Behavior of ground and response of existing foundation due to tunneling, *Soils and Foundations*, 51 (3): 395-409.

Sivakumar, V. (1993), *A critical state framework for unsaturated soil*, Ph.D. Thesis, Univ. of Sheffield, UK.

Sloan, S. W., Assadi, A. and Purushothaman, N. (1990), Undrained stability of a trapdoor, *Geotechnique*, 40 (1): 45-62.

Song, J. H., Chen, K. F., Li, P., Zhang, Y. H. and Sun, C. M. (2018), Soil arching in unsaturated soil with different water table, *Granular Matter*, 20 (4): 1-11.

Stone, K. J. L. and Wood, D. M. (1992), Effects of dilatancy and particle size observed in model test on sand, *Soils and Foundations*, 32 (4), 43–57.

Tamura, T. (2001), Active and passive earth pressure on the trap door, *Proc. of Int. Conf. on modern Tunneling Science and Technology (IS-KYOTO2001)*: 1989-1992.

Tanaka, T. and Sakai, T. (1987), A Trap-door Problem in Granular Materials: Model tests and finite element analyses, *Irrigation Engineering and Rural Planning*, NO. 11: 8-15.

Tanaka, T. and Sakai, T. (1993), Progressive failure and scale effect of trap-door problems with granular materials, *Soils and Foundations*, 33 (1): 11-22.

Tarantino, A. and Tombolato, S. (2005), Coupling of hydraulic and mechanical behavior in unsaturated compacted clay, *Géotechnique*, 55(4), 307–317.

Tekinsoy, M. A., Kayadelen, C., Keskin, M. S. and Söylemez, M. (2004), An equation for predicting shear strength envelope with respect to matric suction, *Computers and Geotechnics*, 31: 589-593.

Terzaghi, K. (1936), Stress distribution in dry and saturated sand above a yielding trapdoor, *Proceedings of the 1st International Conference on Soil Mechanics and Foundation Engineering*, Cambridge, Mass.: 307–311.

Terzaghi, K. (1936), The shearing resistance of saturated soils and the angle between the planes of shear, *Proceedings of the 1st International Conference on Soil Mechanics and Foundation Engineering*, Harvard University Press, Cambridge, Mass: 54-56.

Terzaghi, K. (1943), Theoretical soil mechanics, *John Wiley & Sons*, New York: 66–76.

Tien, H. J. (1996), *A Literature Study of the Arching Effect*, Master Thesis, Massachusetts Institute of Technology, USA.

Unno, T., Kazama, M., Uzuoka, R. and Sento, N. (2008), Liquefaction of unsaturated sand considering the pore air pressure and volume compressibility of the soil particle skeleton, *Soils and Foundations*, 48 (1), 87–99.

Vahedifard, F., Leshchinsky, D., Mortezaei, K. and Lu, N. (2016), Effective stress-based limit-equilibrium analysis for homogeneous unsaturated slopes, *Int. J. Geomech*., 16(6): D4016003.

van Genuchten, M. Th. (1980), A closed-form equation for predicting the hydraulic conductivity of unsaturated soils, *Soil Sci. Soc. Am. J.*, 44: 892–898.

Vanapalli, S. K. and Fredlund, D. G. (2000), Comparison of different procedures to predict unsaturated soil shear strength, Proceeding of Session of Geo- Denver 2000 – Advanced in Unsaturated Geotechnics, Denver, CO, United States, 287: 195-209.

Vardoulakis, I., Graf, B. and Gudehus, G. (1981), Trap-Door Problem With Dry Sand: A Statical Approach Based Upon Model Test Kinematics, *Int. J. Numer. Anal. Meth. Geomech*., 5: 57-78.

Vo, T and Russel, A.R. (2016), Bearing capacity of strip footing on unsaturated soils by the slip line theory, *Computers and Geotechnics*, vol. 74: 122-131.

Wu, Y., Yamamoto, H., and Yao, Y. (2013), Numerical study on bearing behavior of pile considering sand particle crushing, *Geomechanics and Engineering*, 5 (3), 241–261.

Xu, C. J., Liang, L. J., Chen, Q. Z., Luo, W. J. and Chen, Y. F. (2019), Experimental study of soil arching effect under seepage condition, *Acta Geotechnica*, 14: 2031-2044.

Zarnani, S., EI-Emam, M. M. and Bathurst, R. J. (2011), Comparison of numerical and analytical solutions for reinforced soil wall shaking table tests, *Geomechanics and Engineering*, Vol. 3, No. 4: 291–321.

Zhang, H. F., Zhang, P., Zhou, W., Dong, S. and Ma, B. S. (2016), A new model to predict soil pressure acting on deep burial jacked pipes, *Tunneling and Underground Space Technology*, 60: 183–196.

ACKNOWLEDGEMENTS

Firstly, I would like to express my sincerely gratitude to Prof. Mamoru KIKUMOTO, my academic advisor, for the opportunity to study in his group in Yokohama National University, for his instruction and for his support on my research activity and living in Japan. My supervisor, KIKUMOTO sensei, is a knowledgeable, amiable and strict supervisor. I was deeply impressed by his lectures, his attitude to research activity and his novel ideas on research, and I learned a lot from him. His constructive advice and encouragement helped me complete my research and this thesis. What I have learned from him is a huge wealth in my future life.

To Professor Kimitoshi HAYANO and Associate Professor Ying CUI, I also would like to express my sincerely appreciation for their assistance and guidance during mu study in YNU. I would like to extend my sincere appreciation to all committee members: Professor Takayuki SUZUKI, Professor Koichi MAEKAWA, Professor Kimitoshi HAYANO, Professor Mamoru KIKUMOTO and Associate Professor Ying CUI for their comments and suggestions to improve the quality of my thesis.

Furthermore, I would like to give special thanks to the financial support from the Ministry of Education, Culture and Sport, Science and Technology, Japan during my Ph. D study in Yokohama National University.

I would like to give my special thanks to Dr. Bank san, Dr. Vu san and Dr. Putra san for their guidance and assistance on my research, and for explanation of basic knowledge and sharing their experience on research. My special thanks to Dr. Chortham san, Doctoral student Florince san, Doctoral student Pranav san, Doctoral student Nghia san, Doctoral student Ali san, master student Liu san and some other Japanese students for their assistance on my research and my living, we shear our experiences each other, we discuss knowledge and research activity each other, we encourage each other. I will always remember you all in my life.

Finally, I would like to give my thanks to my parents, my younger brother, my wife, and my daughter for their encouragement and support. Especially to my wife, Ting, I appreciate her understanding, support, dedication and love during these 5 years. I owe her a lot and I love her forever.